University of Stavanger

FACULTY OF SCIENCE AND TECHNOLOGY

MASTER'S THESIS

Study program/specialization: Petroleum Engineering / Drilling Technology	Spring semester, 2023 Open
Author: Oruj Alimardanli	. . . . Oruj Alimardanli . . . . . . (Signature of Author)
Faculty supervisor: Mesfin Belayneh	
Title of Master's thesis in English: **Effect of Saw dust on the Bentonite and KCL based drilling fluids: Experimental and Simulation studies.**	
Credits (ECTS): 30	
Keywords: • Drilling fluid • Rheology • Viscoelasticity • Saw dust • Polymer Replacement	Number of pages: 114 + Supplemental material/other: 31 Stavanger, 15.06.2023

Acknowledgement

I would like to express my deepest gratitude to the wonderful people around me who assisted and motivated me to complete this master's thesis. Their encouragement and support have been invaluable to me.

I am extremely grateful to my supervisor - Mesfin Belayneh for his guidance and expertise. His patience and belief in me have been inspiring. Moreover, his assistance and knowledge have been very crucial in my investigation.

I would also like to express my gratitude to my lab mentors - Sivert Bakken Drangeid and Kim Andre Nesse Vorland. I value the time and consideration in the laboratory and the feedback they provided.

I would like to thank a lot to my family and friends for always being there for me. Their affection and confidence in my abilities have always been my inspiration. I appreciate their sacrifices and unwavering support.

Finally, I would like to extend my gratitude to everyone who has contributed in any way they could to this thesis.

.

Abstract

Designing drilling fluids properly plays an extremely important role in effective and reliable drilling operations. Oil Based Muds (OBM) are significantly used for drilling operations as they provide better lubrication, stability in shale operations, fast penetration rates etc. However, there are economic and ecological hinders to use OBMs in the drilling operations. Water Based Muds (WBM) are extensively used for drilling purposes, being relatively cheaper than OBMs, versatile and eco-friendly.

However, bentonite and KCL based WBMs have flocculation and sagging issues at room and higher temperatures in the absence of proper polymers, other chemicals, or additives. That's why, WBMs are being systematically utilized with the addition of several groundbreaking additives, including polymers and other chemicals, to obtain solid performance in more cost-effective ways. Polymers, on the other hand are also expensive additives to use in drilling fluids even performing adequately in WBMs. The substitution of polymers with performance-effective, eco-friendly and cost-effective additives is a hot topic being discussed in oil companies nowadays.

The focus of this thesis is to analyze the effect of saw dust (SD), <71 μm and 125-150 μm of particle sizes in both bentonite and KCL based WBMs as a whole and replacement additive. The main objective is to design a thermally stable WBM by replacing polymers with the abovementioned sized saw dust with the concentration of 1, 3 and 5 g. The fluids are characterized by fluid loss, viscosity, pH values and viscoelastic amplitude sweep properties and their values.

Results obtained from experimental and simulation studies show that ~0.0029 wt% concentrations of <71 μm SD and 125-150 μm SD and ~0.009 wt% 125-150 μm SD are the best concentrations for replacement, whole and whole bentonite fluids respectively. Fluid loss reduction percentages for those fluids are 7%, 7% and 14% respectively, while KCL based replacement fluids show strong bonds with the addition of saw dust particles.

Table of content

List of figures

List of tables

List of symbols

A	Constant in Robertson-Stiff model relative to k, []
B	Constant in Robertson-Stiff model relative to n, []
C	Constant in Robertson-Stiff model, correction factor, [1/s]
d	Diameter of the pipe, [m]
D	Hydraulic flow size, [m]
f	Friction factor, []
G’	Storage modulus, [Pa]
G’’	Loss modulus, [Pa]
k	Consistency index, [lbs/100ft2/s]
L	Length of the flow line, [m]
n	Flow behavior index, []
$P_{annulus}$	Pressure drop in annulus, [bar]
Pp	Pump pressure, [Pa]
ΔP_{fs}	Pressure loses in the surface flow lines, [Pa]
ΔP_{fdp}	Pressure losses in the drill pipe, [Pa]
ΔP_{fdc}	Pressure losses in the drill collar, [Pa]
ΔP_{b}	Pressure losses in the nozzles of the drill bit, [Pa]
ΔP_{fadc}	Pressure losses in the annular spacing between the well and the drill collar, [Pa]
ΔP_{fadp}	Pressure losses in the annular spacing between the wellbore and the drill pipe, [Pa]
τ	Shear stress [lbm/100 sqft]
γ	Shear rate [1/s]
ρ	Density [kg/m^3]
u_m	Average Velocity [m/s]
ε	Surface roughness coefficient []
ω	Angular frequency [rad/s]

List of abbreviations

API	American Petroleum Institute
BHP	Bottom Hole Pressure
BHA	Bottom Hole Assembly
cP	Centipoise
ECD	Equivalent circulating density
FL	Filtrate Loss
FLR	Filtrate Loss Reduction
gpm	Gallons per minute
ID	Inside diameter
LCM	Lost Circulation Material
LSYS	Lower shear yield stress
LVE	Linear viscoelastic
MW	Mud weight
OBM	Oil-based mud
OD	Outside diameter
Pac	Polyanionic cellulose
pH	Potential of Hydrogen
ppg	Pounds per gallon
PV	Plastic viscosity
RPM	Rotation per minute
SBM	Synthetic-based mud
SD	Saw Dust
SG	Specific gravity
SS	Shear Stress
TVD	True vertical depth
UiS	University of Stavanger
WBM	Water-based mud
XG	Xanthan Gum
YP	Yield point
YS	Yield stress

1 Introduction

This MSc thesis presents the eco-friendly and cost-effective additives effect on the KCL and Bentonite based drilling fluids. The study primarily deals with the drilling fluid formulation and their properties characterization. Moreover, the drilling fluids modelling and drilling fluids performance and simulation studies are also presented.

The experimental characterization methods include viscosity of the drilling fluids were measured at 22^{o}C, 50^{o}C and 80^{o}C, viscoelasticity, filtrate loss, pH and loss circulation performance studies. The simulation study deals with the hydraulic performance of the drilling fluids at measured 80^{o}C.

1.1 Background

Drilling fluid is an integral part of drilling and well constructure works. To ensure safe drilling operations, drilling fluid must be designed according to the formation pressure, wellbore conditions to achieve a solid performance with well performing available additives. Among many others, the primary function of drilling fluid is to transport cutting from bottom to surface, to control well pressure, to lubricate and cool the well and drill bit. Moreover, cutting transfer functionality directly depends on rheological behavior of drilling fluid. [1]

Demand for drilling fluids with improved characteristics and thermal stability is rising as the petroleum sector starts to explore deep-water, arctic, geothermal, and extended-reach reserves. This is because these drilling operations frequently experience more severe circumstances and a limited operational window. Because of its numerous advantageous qualities, including improved lubricity, temperature endurance, and shale inhibition, oil-based drilling fluids (OBM) are now used more frequently when drilling such difficult wells. However, these fluids are expensive and have environmental risks [2]. Due to OBMs' success, more and more attention is being paid to the development of water-based drilling fluids.

The cutting lifting and hydraulic performance of drilling fluids highly determined by its density and viscosity properties. However, the rheological and the physical properties of drilling fluids are affected by temperature, pressure and chemical ingredients.

Properly designed drilling fluid such as thermal stable, density stable, and good filter cake properties that mitigate filtrate loss and creates a thin filter cake are the key successful drilling operation. The thermal stable rheological and density properties allow for a precise well control and hence mitigate well bore instability issues, barite sagging as well as will have good cutting transport performances. The thin and impermeable mud cake controls filtrate loss and hence mitigate both differential sticking and formation damage issue. Moreover, the good quality of mud cake increases the wellbore strength.

In the recent years, the application of nanotechnology in in drilling fluids have shown good performance such as improving rheological properties [3], [4], filtrate loss and mud cake reduction [5], [6], improve the lubricity [7], [8] and wellbore strengthening [9]. However, the nanoparticles are industrial products, which are expensive and has issues on health and environmental negative impacts. Studies also have shown than polymers improve the fluids the drilling fluid properties. However, an elevated temperature degrades the polymers and as a result, reduces the drilling fluid viscosity [10].

Therefore, it is important to design a drilling fluid that has thermal stabile and good filtrate control performances. In this thesis, the performance of eco-friendly additives, saw dust, on the properties of Bentonite and KCL based drilling fluids will be evaluated.

1.2 Problem formulation

The main consideration for the drilling fluid design is that drilling fluids must be cost effective, has good performance, and environmentally friendly. Water Based Muds (WBM) are relatively more eco-friendly and economically feasible drilling fluids compared to OBMs. However, the properties of the drilling fluid may be affected due to several reasons, such as flocculation of bentonite particles, polymer precipitation and degradation etc. Due to the cost effective and environment friendly, it is important to

formulate WBM having improved performances that can tolerate temperature and also less formation damage properties.

Davoodi et al (2018) [11] have studies the impact of pistachio on the bentonite-based drilling fluid. In this study, they used the idea of polymer replacement by the pistachio and see of the additive improve the drilling fluid property. Their study has shown that pistachio decreased the filtrate loss significantly. However, the author of this thesis evaluated the availability additives to be used for practical operation for instance in the North Sea. For this, this thesis work was designed to investigates the impact of cheap eco-friendly additives, which is saw dust. The issues therefore addressed are:

- The performance of saw dust sizes on the whole bentonite-based drilling fluid.
- The performance of saw dust in KCL based drilling fluid.
- The performance of saw dust replacement with polymers in KCL and Bentonite based drilling fluid with the objective of cost saving.
- The bridging performance of drilling fluid with and without saw dust systems with the objective of self-healing effect.

1.3 Objective

The primary objective of this thesis work is to answer the research issues addressed in section §1.2. To achieve the goal, the activities are experimental, modelling and performance simulation studies.

1.4 Research methods

The research methods implemented in this thesis are outlined into four parts. The scope of the project is displayed in Figure 1.1.

- The first part deals with the literature study including drilling fluids, rheological properties measured at 22^{o}C, 50^{o}C and 80^{o}C and theories to characterize drilling fluids (rheology, viscoelasticity, lost circulation) and theories for hydraulics simulation studies

- The second part deals with experimental works including fluid formulation and characterization through measurement.
- The third part presents the rheological parameter determination through modelling of the measurement.
- The last part presents the hydraulics simulation study of the drilling fluids measured in the experimental parts.

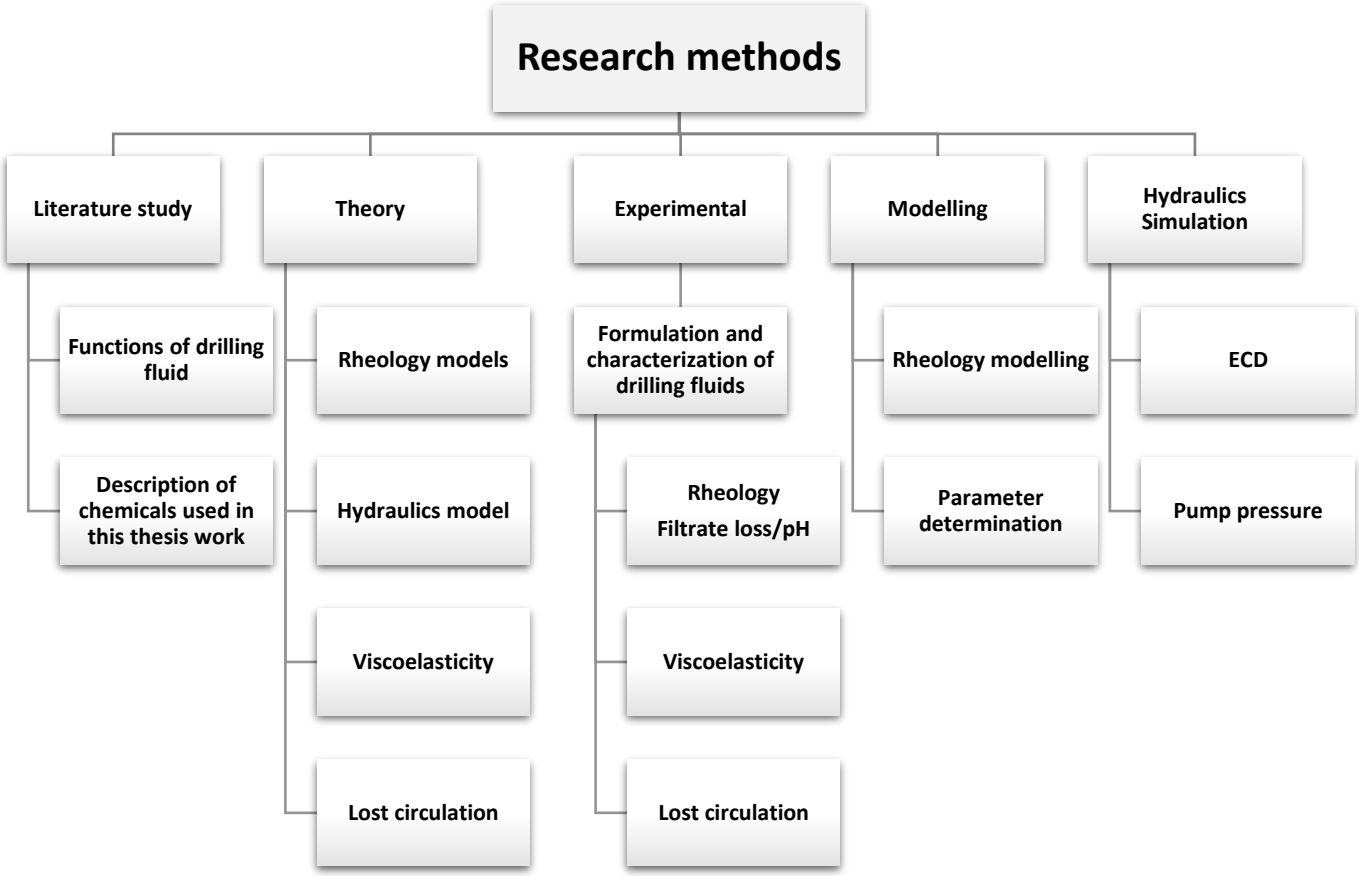

Figure 1.1 Research methods employed in this thesis

2 Theory and Literature study

Chapter two presents the literature review on the drilling fluids and the theories used for modeling and simulation of the drilling fluids.

2.1 Drilling fluid

2.1.1 Functions of drilling fluid

Drilling fluid, also referred to as drilling mud, is essential to the drilling procedure. Being a specially formulated fluid, it is circulated through the wellbore during drilling operations. Drilling fluids perform various functions and have specific properties to ensure drilling efficiency, wellbore stability, and drilled formation protection.

Cooling and lubrication: Drilling fluids assist in cooling and lubricating the drill bit and the drilling assembly. The heat generated by drilling is dissipated, therefore friction is reduced and the wear on the drilling equipment is minimized.

Cuttings removal: Rock fragments, drill cuttings, and other debris are transported to the surface by the drilling fluids. The fluids generate a hydrodynamic pressure which transports debris out of the wellbore, preventing clogging and ensuring that the drill bit has a clear pathway.

Formation pressure control: Drilling fluids exert hydrostatic pressure on the wellbore to counteract formation pressure. This pressure control helps to prevent wellbore instability and blowouts.

Wellbore stability: A filter cake is created by the drilling fluids on the wellbore wall, which stabilizes the wellbore and prevents fluid invasion into the formation. In addition, they prevent the wellbore walls from collapsing by providing support.

Formation evaluation: Transport formation cuttings are transported to the surface by drilling fluids, which provides valuable information about the composition and properties

of the drilled formations. This data assists in assessing the potential of hydrocarbon reservoirs. [12]

2.1.2 Properties of Drilling Fluids

Drilling fluids provides both viscosity and physical properties, where their properties are affected by temperature and pressure.

Mud Weight (Density): Being the density of the drilling fluid, mud weight is usually expressed in pounds per gallon (ppg) or kilograms per cubic meter (kg/m^3). To control formation pressures and prevent wellbore instability, the mud weight is regulated. It is affected by the inclusion of barite and other weighting agents.

Viscosity and Fluid Loss Control: Controlling fluid loss is about preventing the invasion of drilling fluid filtrate into the formation. Several additives, including polyanionic cellulose (PAC) and other fluid loss control agents, are utilized to form a filter cake and reduce fluid loss. [13]

2.1.3 Types of Drilling Fluids

The typical drilling fluids are water based, oil based, synthetic based and pneumatic drilling fluids.

Water-Based Mud (WBM): The most commonly used drilling fluids are water-based muds (WBM). They consist of a continuous phase of water with various additives and particulates dispersed throughout. WBM is adaptable, economical, and environmentally friendly. It can be formulated with a variety of additives to attain the specific properties necessary for drilling in various formations. [14] [15]

Oil-Based Mud (OBM): Oil, typically diesel or mineral oil, is the continuous phase of oil-based muds. OBM provides superior lubricity, greater temperature stability, and less formation damage than WBM. In challenging drilling environments with high

temperatures, reactive formations, or when drilling through hydrocarbon-bearing formations, OBM is frequently used. [14]

Synthetic-Based Mud (SBM): The continuous phase of synthetic-based muds is synthetic hydrocarbon-based fluids. Combining the benefits of WBM and OBM, SBM offers enhanced stability, lubricity, and environmental acceptability. They are mostly used in environmentally sensitive areas and offshore drilling. [14]

Pneumatic Drilling Fluid: Also referred to air or gas drilling fluids, pneumatic drilling fluids use compressed air or gas as the drilling fluid. Specific applications, for which pneumatic drilling fluids are used, include drilling through unconsolidated or highly permeable formations. These fluids minimize fluid invasion and decrease formation damage. [14]

Each kind of drilling fluid has advantages and disadvantages, and the selection is based on criteria such as wellbore conditions, formation characteristics, and environmental factors. Various additives, such as viscosifiers, weight materials, filtration control agents, and shale inhibitors, can be added to the drilling fluid to tailor its properties to the drilling operation and meet the specific requirements.

2.2 Rheological Properties

2.2.1 Plastic Viscosity

Plastic viscosity (PV) quantifies the resistance to flow of a fluid under laminar conditions. It indicates the friction that occurs within the fluid. A greater PV demonstrates a fluid with greater viscosity, while a lesser PV indicates a fluid with a more fluid-like behavior. PV is determined in drilling fluid rheology by quantifying the difference in viscosity between the shear rate at 600 revolutions per minute (RPM) and 300 RPM. Typically, the unit of measurement is centipoise (cP) or pound per 100 square feet (lb/100 ft^2). [16]

A fluid with a higher plastic viscosity value is more viscous and needs higher shear stress to initiate flow. It denotes a fluid that is thicker and more resistant, exhibiting slower flow

rates and greater frictional drag. A lower plastic viscosity value, on the other hand, shows a more fluid-like behavior, allowing the fluid to flow easily.

2.2.2 Yield Point

The yield point (YP) is the minimum shear stress necessary for fluid flow initiation. It indicates the ability of the fluid to withstand static stress prior to flow exhibition. The yield point is crucial for suspending cuttings and maintaining hole cleaning efficiency.

YP is calculated by plotting shear stress against shear rate and identifying the point at which the graph deviates from linearity, indicating the onset of fluid flow. It is measured in units of force per unit area, such as Pascal (Pa) or pound-force per square inch (psi). [16]

A fluid with a higher yield point needs a greater shear stress to initiate flow. This property is essential for preventing sagging and keeping solid particulates suspended in the drilling fluid. A greater yield point improves hole cleansing, cuttings transport, and wellbore stability.

Plastic viscosity and yield point are interrelated and provide valuable information regarding the flow behavior and deformation resistance of drilling fluids. The apparent viscosity, which is the ratio of yield point to plastic viscosity, is frequently used to evaluate the fluid's overall flow characteristics and pumpability.

Drilling fluid engineers may tailor the fluid's rheological properties to meet the drilling operation's particular demands by manipulating the fluid's plastic viscosity and yield point. Balancing these properties contributes to the overall success and efficiency of the drilling process by ensuring effective cuttings removal, appropriate hole cleaning, and stable wellbore conditions.

2.2.3 Lower Shear Yield Stress

Lower Shear Yield Stress (LSYS) is a rheological property describing a fluid's behavior at low shear rates. It is the minimum shear stress necessary to initiate fluid flow from a

static state. When the fluid experiences low shear rates, such as during static conditions or when subjected to extremely low flow rates, the LSYS is especially useful.
Lower shear yield stress is significant in drilling fluid engineering because it affects the fluid's ability to keep solid particles suspended and prevent settling. During drilling operations, the drilling fluid should effectively suspend drill cuttings and other solids in order to guarantee efficient hole cleaning and prevent debris accumulation in the wellbore.

When drilling fluid is at rest or subjected to very low shear rates, the fluid particles tend to settle due to gravitational forces. The LSYS indicates the fluid's resistance to settling and ability to maintain particle suspension in these conditions. [16]. It shows the minimum shear stress required to initiate flow and prevent particles from settling.

By measuring the LSYS, drilling fluid engineers can assess the fluid's ability of suspension and modify the fluid's composition or additives to improve its performance. Increasing the LSYS can improve the fluid's ability to suspend solids, minimize settling, and sustain effective hole cleaning.

2.2.4 Gel Strength

Gel strength is a measurement of a drilling fluid's capacity to suspend solids and prevent settling. It is related to the formation of a gel-like structure due to the interaction of colloidal particles within a fluid. After a period of static condition, gel strength is measured by determining the shear stress at low shear rates (typically 3 or 10 s^{-1}). Typically, gel strength is determined with a rotational viscometer or rheometer, which applies a controlled shear stress to the fluid and measures the resultant torque or rotational resistance. Low shear rates, typically between 3 and 6 RPM, are used to simulate static or near-static conditions. [17]

Greater gel strength values show gel structures with greater resistance to flow and deformation. A drilling fluid with a high gel strength can effectively suspend and transport solid particles, thereby minimizing settling and preserving hole cleaning.

Moreover, it helps to prevent fluid loss into permeable formations, assuring wellbore stability and minimizing formation damage. [17]

Several variables can affect the gel strength of a drilling fluid, including the type and concentration of gelling agents or viscosifiers used in the formulation, the temperature, the shear history, and the presence of solids and contaminants. Drilling fluid engineers are able to tailor the gel's strength to the particular needs of the drilling operation and formation conditions by adjusting these variables.

2.3 Relationship between Shear Stress and Shear Rate

The relationship between shear stress and shear rate is specified by the fluid's flow behavior or rheological properties. Flow behavior of different fluids vary, as do their responses to shear stress and shear rate. [18]

The linear shear stress and shear rate characterize Newtonian fluids, such as oil and water. The viscosity of the fluid corresponds to the proportionality constant.

Fluids that are not Newtonian, such as drilling fluids, typically exhibit complex flow behaviors. Their response to shear stress and shear rate may be nonlinear, as well as having time-dependent, or shear-thinning/thickening properties. For non-Newtonian fluids, the relationship between shear stress and shear rate is typically described by empirical models or fluid-specific rheological equations. [18]

To optimize the design and performance of drilling fluids, it is essential to comprehend the relationship between shear stress and shear rate. It helps to select suitable viscosifiers, additives, and fluid formulations to attain the rheological properties and flow characteristics needed for efficient drilling operations. To quantify the relationship between shear stress and shear rate and to characterize the flow behavior of drilling fluids, rheological measurements including viscosity and yield stress are performed.

Drilling fluids' rheological properties, shear stress, and shear rate are interdependent and influenced by variables such as fluid composition, solids content, temperature, pressure,

and additives. Understanding and regulating these parameters is crucial for optimizing the drilling process. Effective cuttings removal, wellbore stability, and overall drilling performance are guaranteed by proper rheological properties. Rheological measurements are performed with specialized instruments such as viscometers and rheometers, which apply a controlled shear stress or shear rate to the fluid and measure its response.

2.3.1 Shear Stress

In a fluid, shear stress is the force per unit area that operates parallel to a plane. It represents the fluid's resistance when subjected to deformation or flow. Shear stress is determined in force per unit area units, such as Pascals or pound-force per square inch. When a shear force is applied to a fluid, the particles of the fluid deform and flow. The shear stress at a particular point within a fluid is proportional to the applied force and can be calculated by dividing the force by the area over which it is applied. Shear stress is a measure of the fluid's internal friction or resistance. [18]

2.3.2 Shear Rate

Shear rate is the rate at which adjacent layers of fluid move relative to one another. Shear rate is defined as the velocity gradient between the fluid layers. It determines the intensity of shear forces a fluid experience. Typically, it is measured in reciprocal seconds (s^{-1}). Greater shear rates show more rapid deformation and greater shear stresses within the fluid. On the other hand, slower deformation and lower shear stresses correspond to lower shear rates. [18]. Shear rate is an essential criterion for describing the flow behavior and viscosity of a fluid

2.4 Fluid rheology models

Fluid rheology is the study of how fluids flow and deform under the influence of applied forces. It is a crucial aspect of drilling fluid engineering as it determines the behavior and performance of the fluid during drilling operations. Several rheological properties are used to characterize drilling fluids, including plastic viscosity, yield point, lower shear yield point, gel strength, shear stress, and shear rate.

The rheological parameters of the drilling fluids determine the hydraulics and cutting transport phenomenon in the wellbore. In general shear stress-shear rate behaviors of the Newtonian and non-Newtonian fluids. Since drilling fluids have non-Newtonian behavior, different non-Newtonian models will be reviewed and used for the characterization.

Table 2.1 is one the dataset that has been measured in chapter 5 was used to describe the behaviors of the models to be presented in this section.

Table 2.1: Saw Dust Blended Bentonite drilling fluid

RPM	Dial Reading
600	36.0
300	24.0
200	19.5
100	14.0
60	12.0
30	9.5
6	8.0
3	7.5

2.4.1 Bingham model

The Bingham Plastic model is described by the yield stress and plastic viscosity. According to the model, the shear stress varies linear with the shear rate. The model is API model and reads [19] [20]:

$$\tau = YS + PV * \gamma \tag{2.1}$$

Where, PV is Plastic viscosity, and YS is Bingham yield stress. The parameters are determined from the measured dial readings data as:

$$PV\ [cP] = \theta_{600} - \theta_{300} \tag{2.2}$$

$$YS\left[\frac{lbf}{100sqft}\right] = \theta_{300} - \mu_p = 2 * \theta_{300} - \theta_{600} \tag{2.3}$$

Figure 2.1 shows the Bingham model generated by curve fitting. As shown in the figure, as the shear rate increases, the viscosity is constant. However, the drilling fluids behaves as shear thinning behavior, where the viscosity decreases as the shear rate increases.

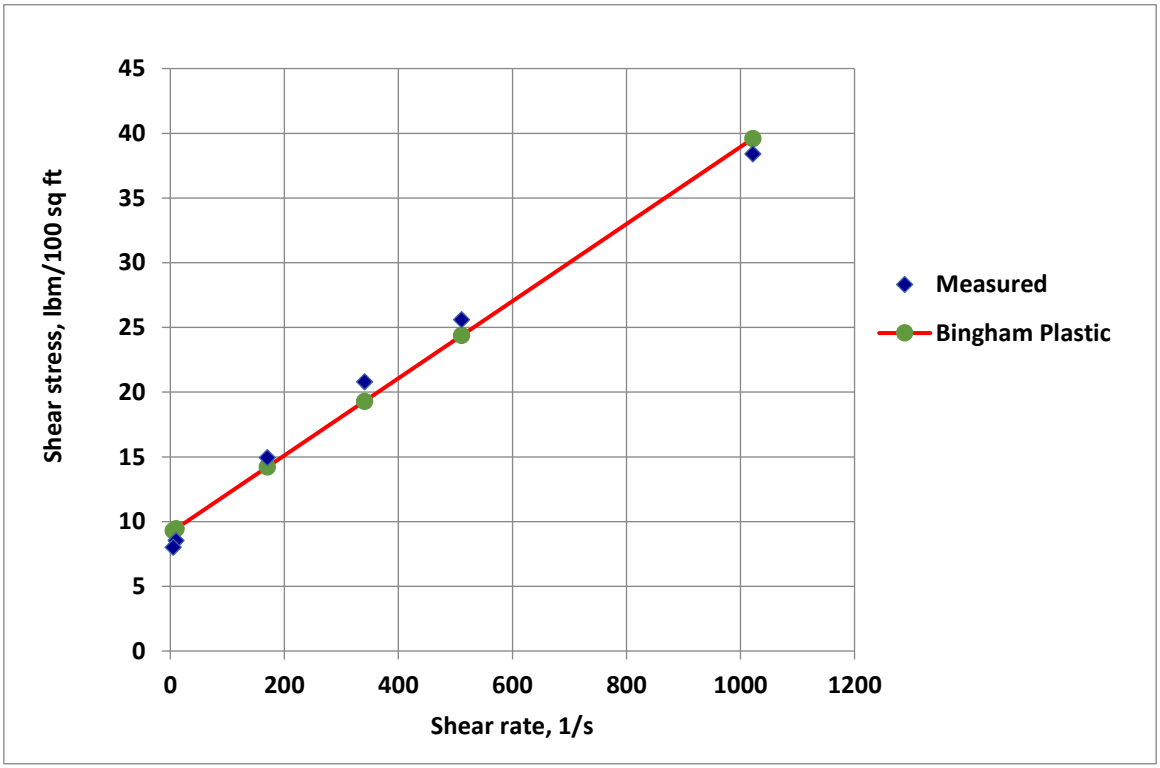

Figure 2.1: Comparison between Bingham plastic model and measurement

2.4.2 Power Law model

Unlike the Bingham model, the Power law model is also another API model, which describes shear thinning fluids. However, the model does not determine the yield stress at very low shear rate. The model is given as [19] [20]:

$$\tau = K(\dot{\gamma})^n \tag{2.4}$$

Where n is the power law index and k [$lbs^n/100ft^2$] is the consistency index.

- When the n =1, the fluid is Newtonian,
- When n < 1, Pseudo plastic behavior (shear thinning),
- When n > 1, Dilatant behavior (shear thickening).

Figure 2.2 is generated by curve fitting method. However, the flow and consistency index parameters can also be determined from the measured dial reading data [19] [20]:

$$n = 3.32 \log\left(\frac{\theta_{600}}{\theta_{300}}\right) \tag{2.5}$$

$$K = \frac{\theta_{300}}{511^n} = \frac{\theta_{600}}{1022^n} \tag{2.6}$$

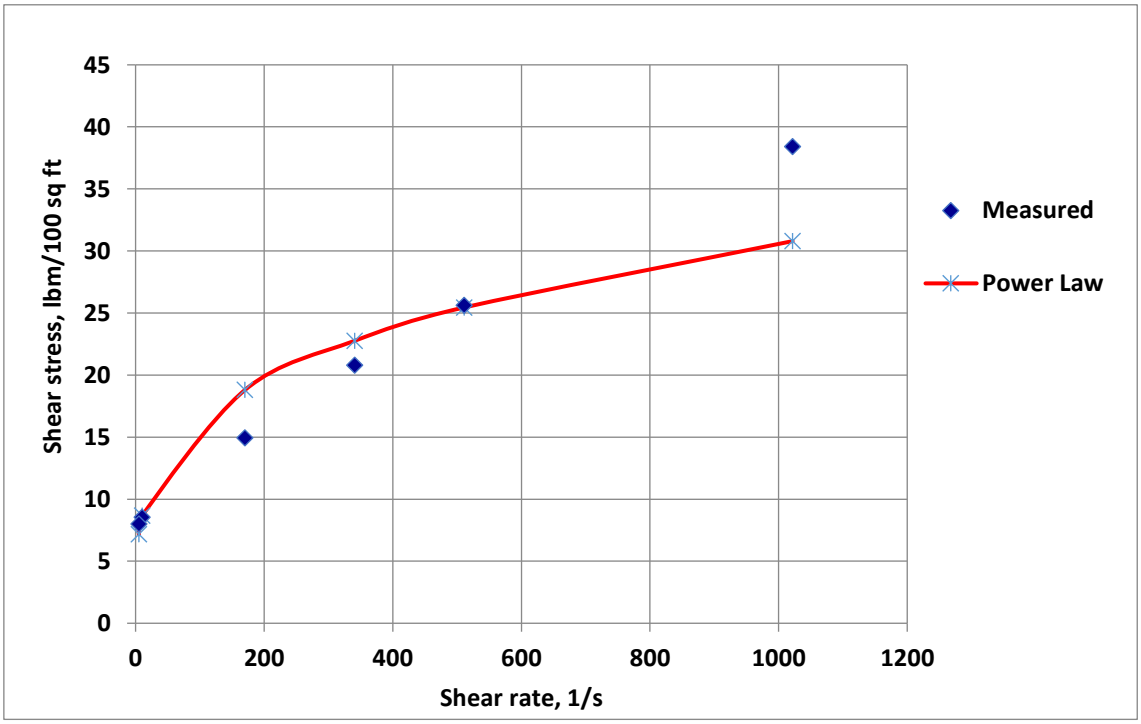

Figure 2.2: Comparison between Power law model and measurement

Even though the shear thinning behavior described by the Power law model, non-Newtonian fluids requires a certain external pressure to set the fluid in motion. This fact is not described by the Power law model.

2.4.3 Herschel-Bulkley model

Herschel-Bulkley model is utilized to improve the weakness of the Power law model. The Herschel-Bulkley model presents a yield Power law, by including yield stress to the Power law model. The model is therefore described by three parameters, such as yield stress, shear thinning and consistency index. The Herschel-Bulkley model reads [19]:

$$\tau = \tau_0 + K\dot{\gamma}^n \tag{2.7}$$

Where

- τ_y is Herschel-Bulkley yield stress (YS),
- n is flow index,
- K is consistency index.

Both the consistency index and flow index values are determined from the curve fitting between the model and the measured viscometer data. For this, firstly the yield stress should be estimated by using equation 2.7 [19]:

$$\tau_0 = \frac{\tau^{*2} - \tau_{min} - \tau_{max}}{2\tau^{*} - \tau_{min} - \tau_{max}} \quad (2.8)$$

Where the τ^* is calculated by interpolation from the corresponding value of the geometrical mean of the shear strain:

$$\gamma^* = \sqrt{\gamma_{min}\gamma_{max}} \quad (2.9)$$

Where γ_{min} and γ_{max} are the maximum and minimum shear rates, and the γ^* value is calculated as 72.28s^{-1}.

As shown in Figure 2.3, the model describes the drilling fluid better than the Power law model reducing the error deviation from the measurement:

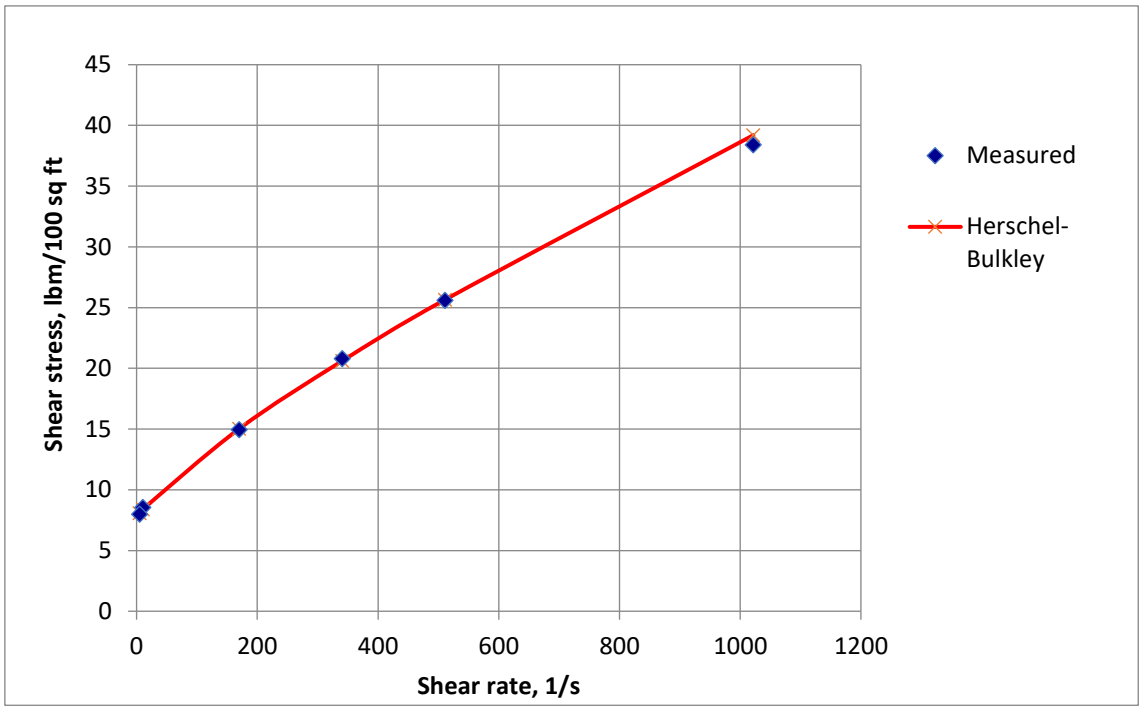

Figure 2.3: Comparison between Herschel-Bulkley model and measurement

2.4.4 Unified model

The Unified model is also a modified Power law model like the Herschel-Buckley model. Here, the difference is that the yield stress is determined from the 3 and 6 RPM dial readings. The Unified model reads [19]:

$$\tau = \tau_{yl} + k * \gamma^n \tag{2.10}$$

The lower shear yield point (τ_{yL}) (LSYS) is estimated according to Zamora and Power as [19]:

$$\tau_{yL} = (2 * \theta_3 - \theta_6) * 1.066 \tag{2.11}$$

Here the consistency index (k) and flow index (n) parameters are also be determined from the curve fitting. Figure 2.4 is the comparison between the model and the measurement., which shows very good agreement.

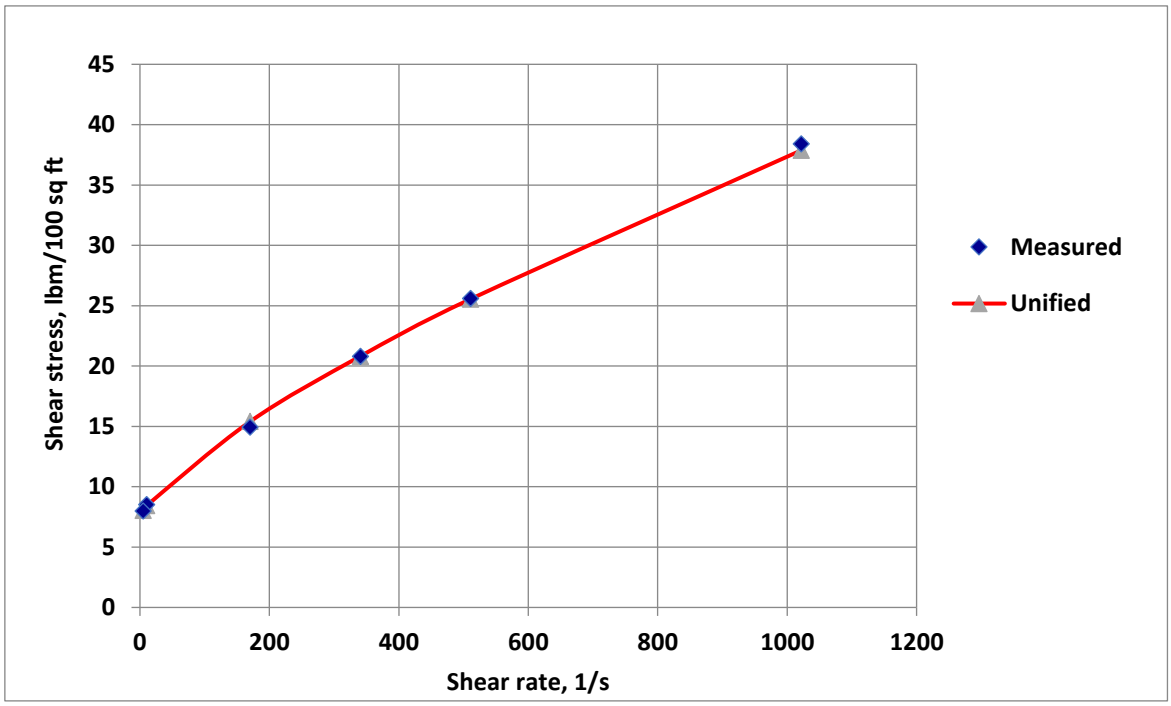

Figure 2.4: Comparison between Unified model and measurement

2.4.5 Robertson-Stiff model

It is reported that the Robertson-Stiff model describes the rheology of drilling fluid and cement slurry well. The model is like a power law model with the terms that includes shear strain correction factor, C, and the model reads [19]:

$$\tau = A(\dot{\gamma} + C)^B \tag{2.12}$$

The Robertson-Stiff parameters A and B are like the *K* and n in the Power Law model. The shear rate correction is estimated from the maximum and minimum shear rate as [19]:

$$C = \frac{\gamma_{min} \cdot \gamma_{max} - \gamma^{*2}}{2\gamma^{*} - \gamma_{min} - \gamma_{max}} \tag{2.13}$$

Where γ^{*} is estimated by interpolation from the corresponding geometric mean of shear stress as [19]:

$$\tau^{*} = \sqrt{\tau_{min} \times \tau_{max}} \tag{2.14}$$

The Robertson-Stiff yield stress is determined for the zero-shear stress and given by AC^{B}.

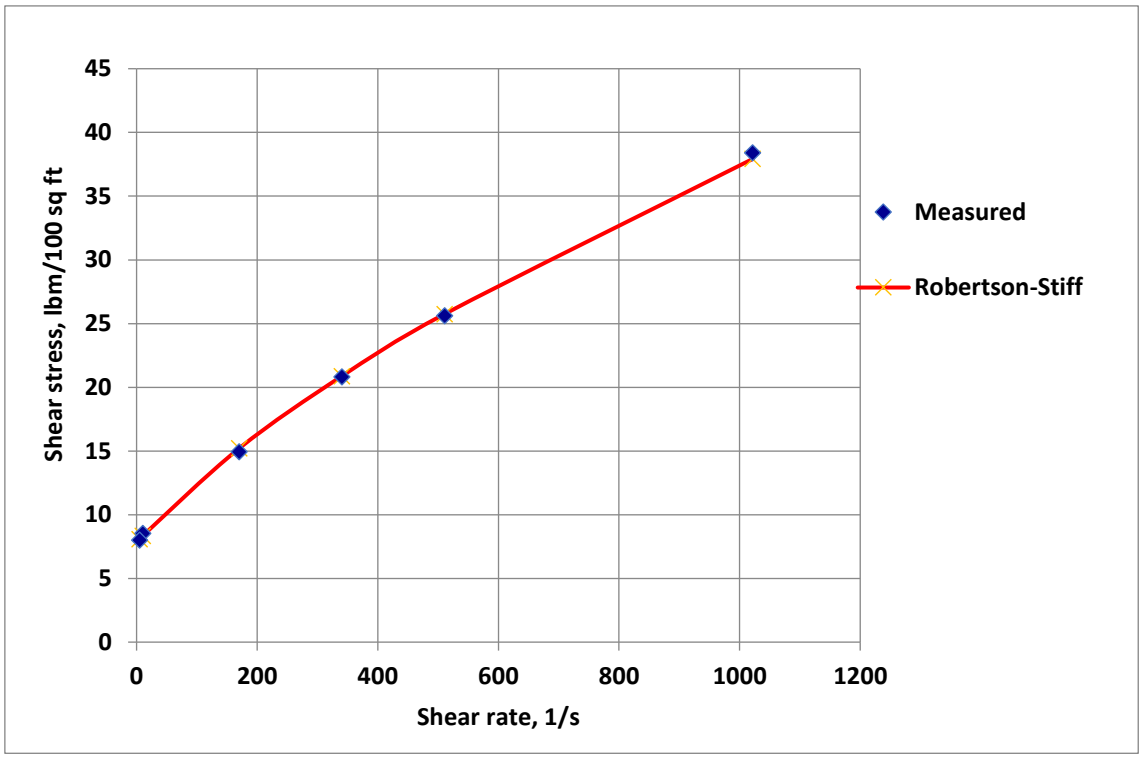

Figure 2.5: Comparison between Robertson and Stiff model and measurement

2.5 Hydraulics model

The performance of the drilling fluids to be formulated in this thesis are evaluated by calculating the hydraulics such as ECD and Pump pressure. The rheological and the physical properties of the drilling fluids along with the circulation medial control the well pressure and the cutting lifting performances. Under static condition, the bottom hole pressures determined from the density of the drilling fluid and the vertical depth as [21]:

$$BHP = 0.0981*MW * Depth \quad (2.15)$$

Where

- BHP is Bottom Hole Pressure (bar),
- MW is Mud weight (sg),
- Depth is True Vertical Depth (TVD) (m).

2.5.1 ECD

During drilling operation, rig pump will be activated. Hence drilling fluid will circulate through the well. When drilling flows, the dynamic friction in the annuls will be generated is against the flow direction. Consequently, the friction will provide an additional pressure in the wellbore annulus. The bottom hole pressure during dynamic circulation is the therefore the sum of the hydrostatic pressure and the friction pressure loss. The Equivalent Circulating Density (ECD) calculated from the total pressure as [20] [21]:

$$ECD(sg) = MW + \frac{\Delta P_{annulus}}{0.0981 * TVD} \tag{2.16}$$

Where

- $\Delta P_{annulus}$ is Pressure drop in annulus (bar),
- MW is Static Mud Weight (sg),
- TVD is True Vertical Depth (m).

Where annular pressure loss is calculated from the Darcy formula as [20] [21]:

$$\Delta P = \frac{f \rho u_m^2 L}{2D} \tag{2.17}$$

Where

- f is friction factor,
- L is length of the flow line,
- ρ is density of fluid,
- u_m is the average velocity,
- D is hydraulic flow size.

The friction factor *f* calculated as [22]:

$$\frac{1}{\sqrt{f}} = -1.8 log_{10}\left\{\frac{6.6}{R_e} + \left(\frac{\varepsilon}{3.71}\right)^{1.11}\right\} \tag{2.18}$$

Where

- ε is surface roughness coefficient (ε = k/d),

- k is surface roughness,
- d is diameter of the pipe.

2.5.2 Pump pressure

When fluid flows through the circulation system, pressure losses. The pump therefore should be strong enough to overcome these friction losses in order to maintain the circulation. Figure 2.6 shows the circulation system, and the pressure losses depends on the geometry of the circulation system [23].

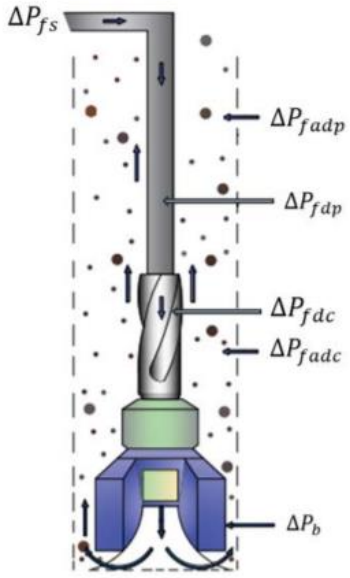

Figure 2.6: Frictional pressure loss in circulation [23]

The pump pressure is therefore determined by the sum of the pressure losses across the flow lines as [23]:

$$P_p = \Delta P_{fs} + \Delta P_{fdp} + \Delta P_{fdc} + \Delta P_b + \Delta P_{fadc} + \Delta P_{fadp} \quad (2.19)$$

Where

- ΔP_{fs} is pressure loses in the surface flow lines,
- ΔP_{fdp} is pressure losses in the drill pipe,
- ΔP_{fdc} is pressure losses in the drill collar,
- ΔP_b is pressure losses in the nozzles of the drill bit,

- ΔP_{fadc} is pressure losses in the annular spacing between the well and the drill collar,
- ΔP_{fadp} is pressure losses in the annular spacing between the wellbore and the drill pipe.

In Ochoa [19] paper, several hydraulics models are documented. These are Bingham plastic, Power law, Herschel-Bulkley, Unified, Robertson & Stiff and Casson. Among these, in this thesis, the Unified model prediction was used to evaluate the hydraulic performance of the selected drilling fluid. The reason for the selection of the Unified model is based on the work of Sadigov [24]. He compared several models with the measurement and results showed Unified model prediction is quite well compared with the other hydraulic models. was quite good for most drilling fluids. Table 2.2 summarizes the Unified model across annulus, pipe and the nozzle [19]:

Table 2.2: Unified hydraulics model [19]

Unified model	
Pipe Flow	Annular flow
$\mu_p = R_{600} - R_{300}, [cP] \quad \tau_y = R_{300} - \mu_p, [lbf/100ft^2] \quad \tau_0 = 1.066 \cdot (2 \cdot R_3 - R_6)$	
$n_p = 3.32 \cdot log\left(\frac{2 \cdot \mu_p + \tau_y}{\mu_p + \tau_y}\right)$ $k_p = 1.066\left(\frac{\mu_p + \tau_y}{511^{n_p}}\right)$	$n_a = 3.32 \cdot log\left(\frac{2 \cdot \mu_p + \tau_{y-\tau_y}}{\mu_p + \tau_{y-\tau_y}}\right)$ $k_a = 1.066\left(\frac{\mu_p + \tau_y - \tau_0}{511^{n_a}}\right)$ $k = [lbf \cdot sec^n/100ft^2]$
$G = \left(\frac{(3-\alpha)n+1}{(4-\alpha)n}\right) \cdot \left(1 + \frac{\alpha}{2}\right)$ $\alpha = 1\ for\ pipe$ $\alpha = 1\ for\ annuli$	
$v_p = \frac{24.51 \cdot q}{D_p^2}$	$v_a = \frac{24.51 \cdot q}{D_2^2 - D_1^2}$ $v = [ft/min]$
$\gamma_w = \frac{1.6 \cdot G \cdot v}{D_R} = [sec^{-1}]$	
$\tau_w = \left[\left(\frac{4-\alpha}{3-\alpha}\right)^n \tau_0 + (k \cdot \gamma_w^n)\right] = [lbf/100ft^2]$	
$N_{Re} = \frac{\rho \cdot v_p^2}{19.36 \cdot \tau_w}$	$N_{Re} = \frac{\rho \cdot v_a^2}{19.36 \cdot \tau_w}$
$f_{laminar} = \frac{16}{N_{Re}}$ $f_{transient} = \frac{16 \cdot N_{Re}}{(3470 - 1370 \cdot n_p)^2}$ $f_{turbulent} = \frac{a}{N_{Re}^b}$ $a = \frac{\log(n) + 3.93}{50} \quad b = \frac{1.75 - \log(n)}{7}$	$f_{laminar} = \frac{24}{N_{Re}}$ $f_{transient} = \frac{16 \cdot N_{Re}}{(3470 - 1370 \cdot n_a)^2}$ $f_{turbulent} = \frac{a}{N_{Re}^b}$ $a = \frac{\log(n) + 3.93}{50} \quad b = \frac{1.75 - \log(n)}{7}$
$f_{partial} = (f_{transient}^{-8} + f_{turbulent}^{-8})^{-1/8}$	
$f_p = (f_{partial}^{12} + f_{laminar}^{12})^{1/12}$	$f_a = (f_{partial}^{12} + f_{laminar}^{12})^{1/12}$
$\left(\frac{dp}{dL}\right) = 1.076 \cdot \frac{f_p \cdot v_p^2 \cdot \rho}{10^5 \cdot D_p} = [psi/ft]$ $\Delta p = \left(\frac{dp}{dL}\right) \cdot \Delta L = [\text{psi}]$	$\left(\frac{dp}{dL}\right) = 1.076 \cdot \frac{f_a \cdot v_a^2 \cdot \rho}{10^5 \cdot (D_2 - D_1)} = [psi/ft]$ $\Delta p = \left(\frac{dp}{dL}\right) \cdot \Delta L = [\text{psi}]$
$\Delta p_{Nozzles} = \frac{156 \cdot \rho \cdot q^2}{\left(D_{N1}^2 - D_{N2}^2 - D_{N3}^2\right)^2} = [psi]$	

2.6 Viscoelasticity

Viscoelastic (VE) refers to the materials properties that exhibits both viscous and elastic behavior. The viscoelasticity property describes how the strength of the gel structure of fluids that controls the solid suspension potential of the drilling fluid [25].

Figure 2.7 shows the two parallel plate oscillatory test. The drilling fluid is exposed to the oscillatory dynamic loading [26].

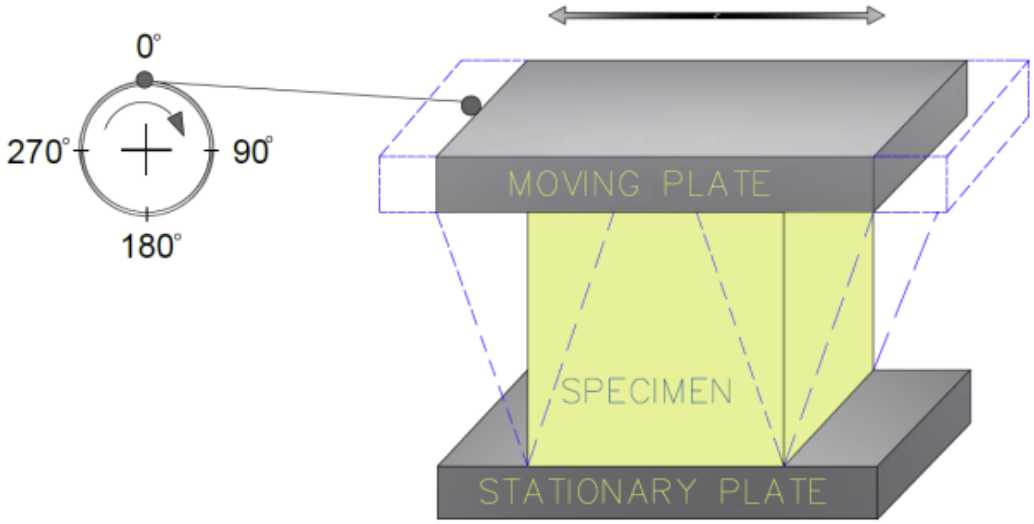

Figure 2.7: Illustration of the Two-Plate-Model for the oscillatory test [26]

During testing, the elastic modulus or storage modulus (G') of the fluid is measured. The viscous modulus refers to the loss modulus (G''), which is the measure of the energy loss during dynamic loading [27].

2.6.1 Dynamic Shear stress - Shear rate

The shear stress and shear rate are described by a sign function as [18]:

$$\gamma(t) = \gamma_o \sin(\omega t) \tag{2.20}$$

$$\tau(t) = \tau_o \sin(\omega t + \delta) \tag{2.21}$$

Expanding and collecting terms, we get:

$$\tau(t) = \tau_o[\sin(\omega t)\cos\delta + \cos(\omega t)\sin(\delta)] \quad (2.22)$$

$$\tau(t) = \gamma_o\left[\left(\frac{\tau_o}{\gamma_o}\cos\delta\right)\sin(\omega t) + \left(\frac{\tau_o}{\gamma_o}\sin\delta\right)\cos(\omega t)\right] \quad (2.23)$$

$$\tau(t) = [G'\sin(\omega t) + G''\cos(\omega t)] \quad (2.24)$$

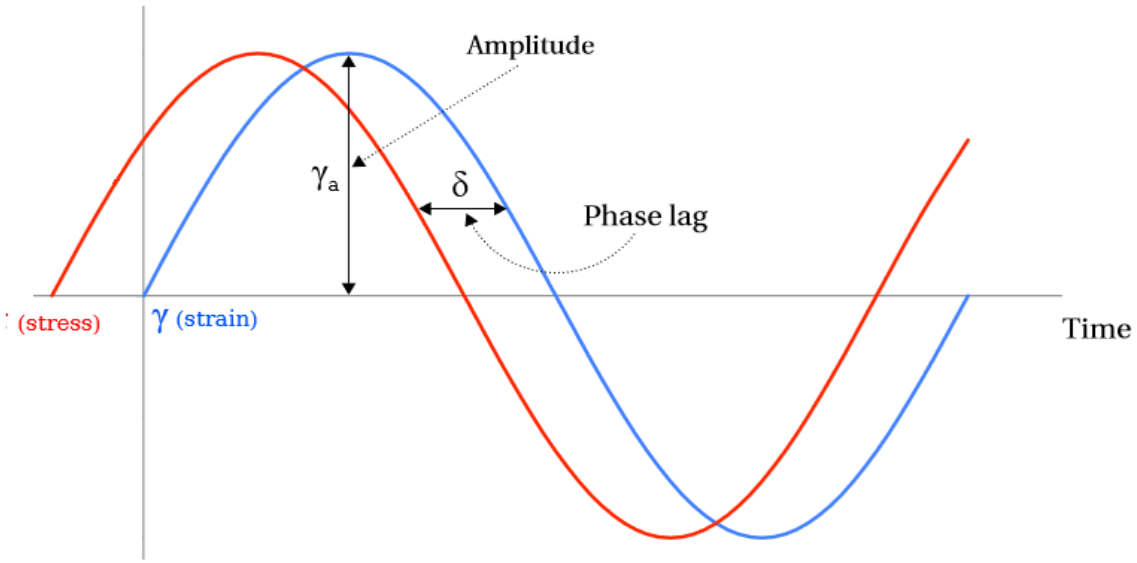

Figure 2.8: Plot of the stress and strain curves against time [28]

From equations 2.23 and 2.24, the storage (G') and loss (G'') moduli can be given as:

$$G' = \frac{\tau_o}{\gamma_o}\cos\delta \quad (2.25)$$

$$G'' = \frac{\tau_o}{\gamma_o}\sin\delta \quad (2.26)$$

$$\tan\delta = \frac{G''}{G'} \quad (2.27)$$

The ratio G''/ G' is the damping factor (or loss factor). As shown in Figure 2.8, the time lag between the sine curve is regarded as the phase shift angle or loss angle (δ).

Table 2.3 shows the behavior of viscoelasticity based on the phase angle and the elastic and viscous moduli. When the damping angle is 0° (perfectly elastic) and 90° (perfectly

viscous). When the angle is (δ = 45°) the material possesses equal portion viscous and elastic properties.

Table 2.3: Viscoelastic behavior with changing angles [26]

Ideally viscous flow behavior	Behavior of viscoelastic liquid	50/50 ratio between viscous and elastic portions	Behavior of viscoelastic gel or solid	Ideally elastic behavior
δ = 90°	90° > δ > 45°	δ = 45°	45° > δ > 0°	δ = 0°
tan δ → ∞	tan δ > 1	tan δ = 1	tan δ < 1	tan δ → 0
G' → 0	G'' > G'	G' = G''	G' > G''	G'' → 0

2.6.2 Amplitude sweep

Amplitude sweeps oscillatory test is conducted by varying amplitudes while keeping the rotation speed (10 rad/s) and temperature (22°C) constant. The test results are illustrated as in Figure 2.9. The linear viscoelastic region (LVER) is determined by drawing the horizontal axis on the storage modulus until it deviates. Afterward, the storage modulus reduces and cross with the loss modulus, where the system behaves equal portion of elastic and viscous. The point where the elastic moduli meet is called flow point [26].

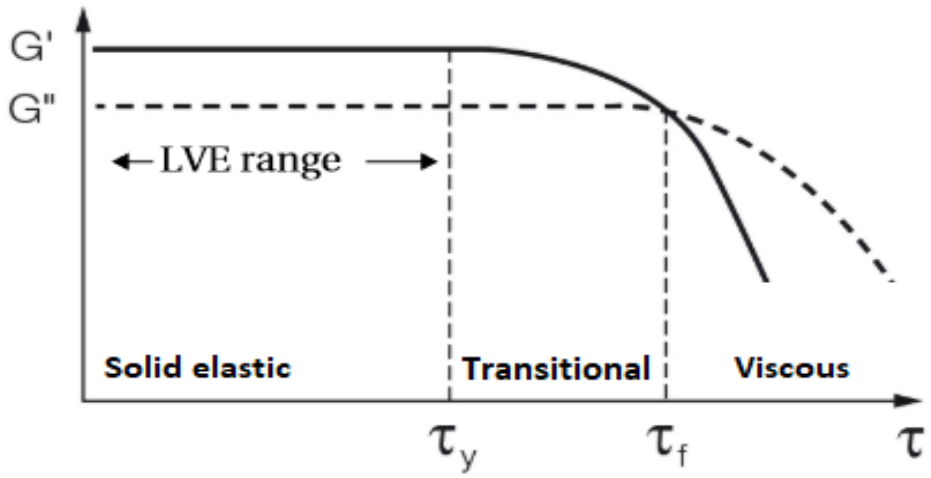

Figure 2.9: Illustration of amplitude sweep test result [26]

In the elastic dominated and in the transition regions, the storage (G') modulus is higher than the loss modulus (G''). In the viscous dominated region, the loss modulus (G'') is greater than the storage modulus (G'). Figure 2.10 illustrate how to determine the shear stress at the flow point and the yield stress based on the shear stress vs phase angle plot

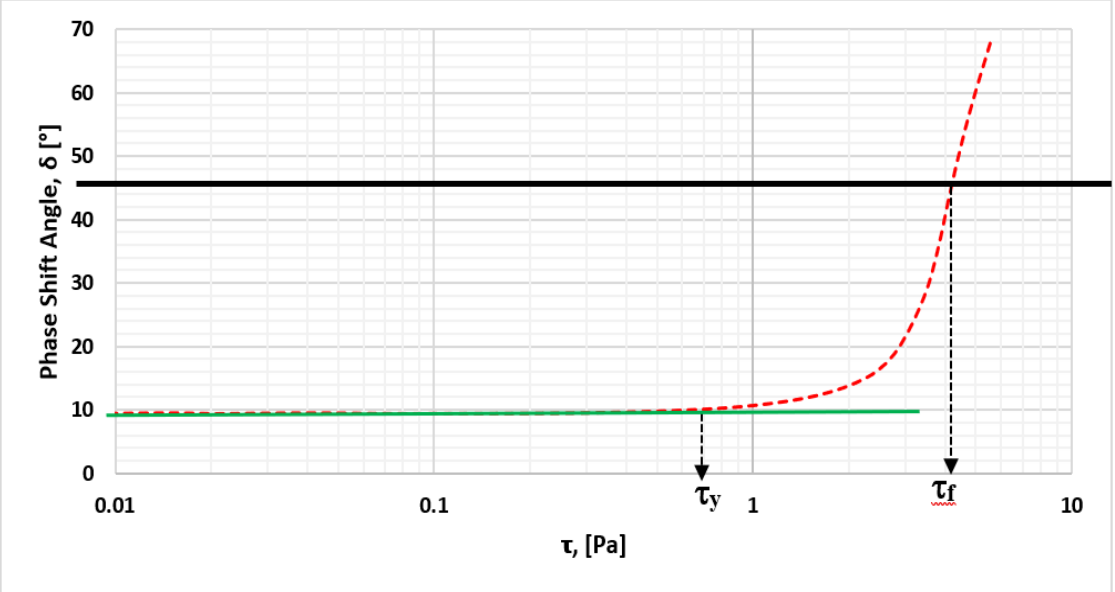

Figure 2.10: Phase shift angle vs. Shear stress for Bentonite fluids

3 Experimental works

Chapter 3 presents the experimental work with regards to drilling fluid design, characterization methods along with the equipment used.

3.1 Materials description

3.1.1 Bentonite

Bentonite is a clay mineral that is frequently introduced as a viscosifier and filtration control agent to water-based drilling fluids. It provides viscosity to the fluid, which helps to suspend drill cuttings and prevents sagging. Sufficient drilling fluid viscosity assists in the suspension of solids (such as barite and drill cutting). Bentonite also creates a filter cake on the wellbore wall to reduce fluid loss. It substantially affects the rheological properties, suspension, and filtration control of the drilling fluid.

Bentonite is also composed of the non-clay minerals [29]. below displays the percentile results of the element analysis. SiO2 and Al2O3 are the predominant concentrations, as demonstrated [30]. Bentonite has a specific gravity of approximately 2,6 sg.

Components	*Composition in %*
Silica, SiO_2	64.32
Alumina, Al_2O_3	20.74
Cumulative water	5.14
Ferric oxide, Fe_2O_3	3.03
Soda, Na_2O	2.59
Magnesia, MgO	2.30
Lime, CaO	0.50
Ferrous Oxide, FeO	0.46
Potash, K_2O	0.39
Sulfuric Anhydride	0.35
Titanium Oxide, TiO_2	0.14
Phosphoric Anhydride	0.01
Other minor constitutes	0.01

Figure 3.1: Bentonite's elements and compostion in % [30]

Figure 3.2 is a structure of Montmorillonite. As shown in the figure, the building blocks of the Montmorillonite mineral are octahedron and tetrahedron structures [29]:

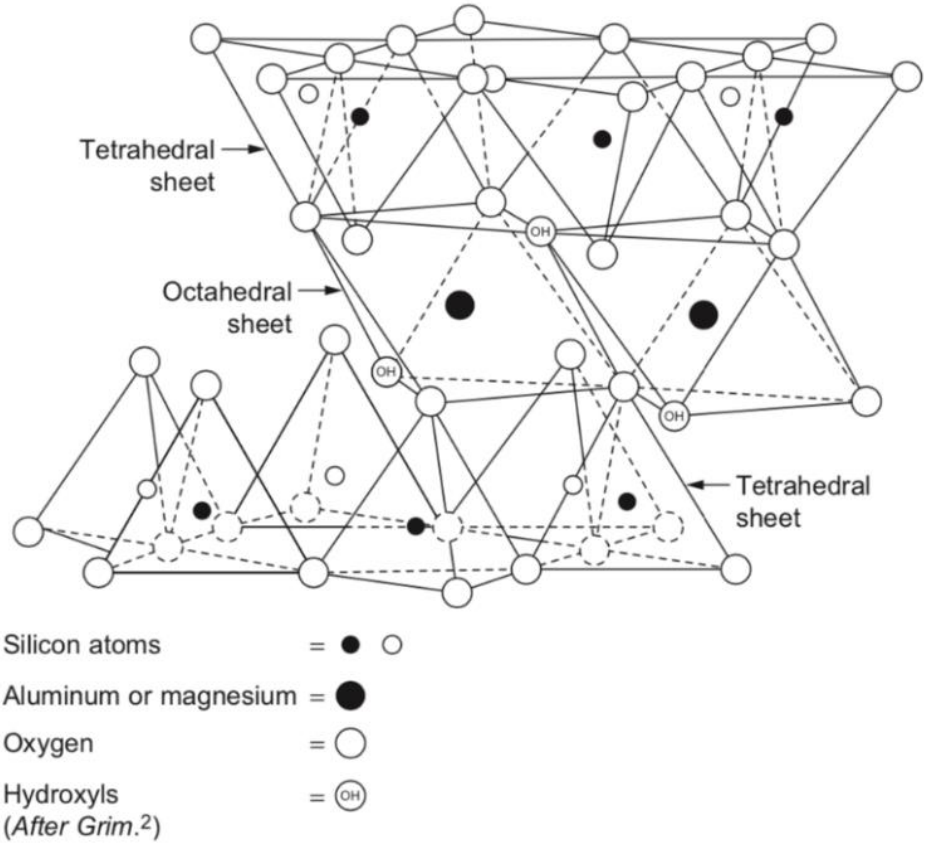

Figure 3.2: Illustrations of Montmorillonite structure [31]

3.1.2 KCL

The chemical compound potassium chloride (KCl) is composed of potassium and chloride ions. It is a crystalline solid with a salty flavor and is commonly used as a substitute for table salt. Due to its unique properties, KCl is utilized in numerous industries and applications. It readily dissolves in water. [32]

Potassium chloride (KCl) is frequently utilized in water-based drilling muds to control shale swelling problems. The mechanism of shale inhibition occurs when positive potassium ions (K+) are attracted to the negatively charged clay surface and then fill the spaces between clay platelets [32]. The potassium ions will then prevent water molecules from being invaded the clay platelets, thereby reducing the likelihood of shale swelling.

KCl is injected into these mud systems to control osmotic pressure and prevent fluid migration into the formation, which could damage the formation and reduce well production.

Adding KCl to WBMs has several benefits. First, it stabilizes the shale, preventing the formation's clay minerals from swelling and dispersing [32]. This reduces the risk of wellbore collapse or formation damage and maintains wellbore stability. In addition, KCl increases the inhibition of clay hydration, reducing water sensitivity of the clays and enhancing the overall performance of the drilling fluid. Maintaining hydrostatic pressure and avoiding difficulties with well control requires regulating the fluid density.

3.1.3 Soda ash (Na_2CO_3)

Frequently, drilling fluids contain soda ash as an alkaline agent. It assists in raising the pH of the fluid, resulting in optimal hardness and pH values. In addition, it may aid in reducing clay swelling. Soda ash has no significant effect on the viscosity, density, or suspension characteristics of the drilling fluid. The chemical formula of soda ash has (Na2CO3) [33]:

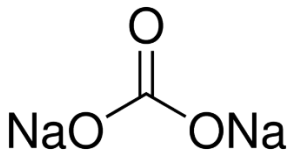

Figure 3.3: Chemical structure of soda ash [33]

3.1.4 Polyanionic Cellulose (PAC)

Figure 3.4 shows chemical structure of Polyanionic Cellulose. PAC is a water-soluble polymer that is frequently added to drilling fluids to prevent fluid loss. By producing a thin, low-permeability filter cake on the wellbore wall, it improves the rheological characteristics and regulates water loss. PAC can make the fluid viscous and enhance its suspension qualities. It is successful in minimizing fluid loss and preserving stable holes.[34]

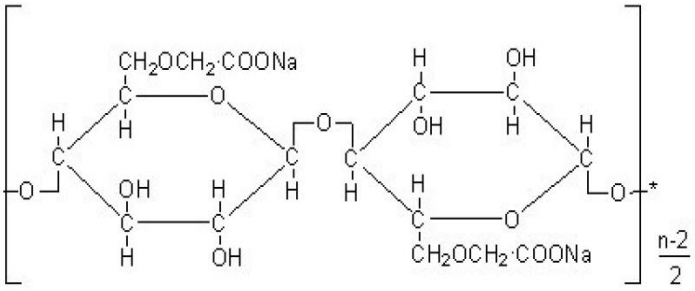

Figure 3.4: Chemical Structure of PAC [34]

3.1.5 Polyanionic Cellulose Polymer (PolyPac)

The polyanionic cellulose polymer (PolyPac) is another type of this material. Comparable to PAC's benefits in terms of fluid loss reduction, viscosity improvement, and suspension characteristics. It facilitates stable and effective drilling fluid performance [35].

3.1.6 Xanthan gum

Xanthan gum (XG) is a water-soluble polymer with a high molecular weight [31]. The viscosifying agent xanthan gum is utilized in drilling fluids. Figure 3.5 depicts the molecular structure of xanthan gum [31]. Five ring structures make up XG, which consists of a two-ring backbone and a three-ring side chain [31].

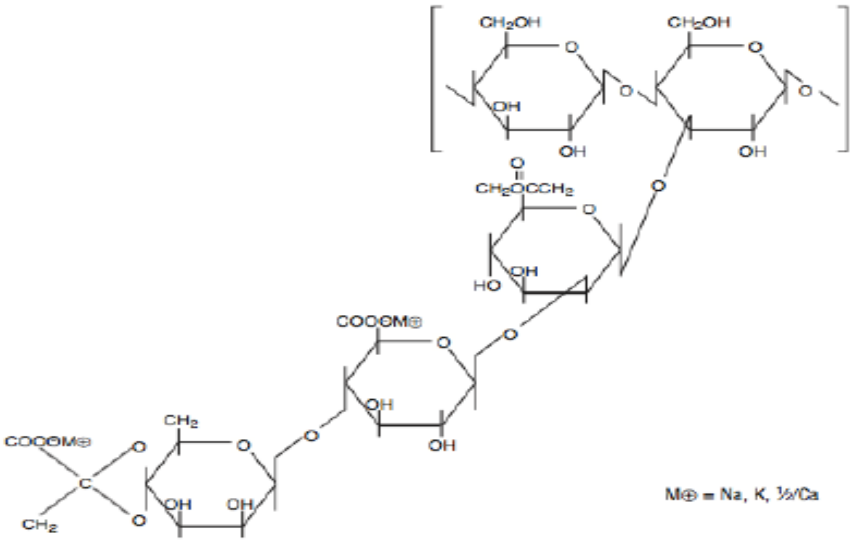

Figure 3.5: Xanthan gum structure [31]

3.1.7 Barite ($BaSO_4$)

Barite, also known as barium sulfate (BaSO4), is a common weighting agent in drilling fluids [36]. It is one of the most employed materials for increasing the density of drilling fluids, which is crucial for regulating formation pressures, preventing blowouts, and maintaining wellbore stability during drilling operations.

Barite is well-suited for its role in drilling fluids due to a number of essential properties [36]:

High Specific Gravity: Barite possesses a high specific gravity spanning between 4.2 and 4.5 g/cm3. This high density enables drilling fluid engineers to achieve the required mud weight or density to balance formation pressures. By introducing barite to the drilling fluid, its density could be increased to generate hydrostatic pressure which prevents unwanted influxes of formation fluids from entering the wellbore [36].

Inertness: Barite is chemically inert and nonreactive with other components of drilling fluids. It has no negative effect on the performance of other additives or the drilling fluid's stability. This inertness guarantees that the drilling fluid does not undergo unintended chemical reactions that could compromise its functionality [36].

Suspension Properties: The platy or flaky structure of barite particles aids in their suspension in the drilling fluid. These particles can be readily dispersed and distributed uniformly throughout the fluid, thereby minimizing settling and ensuring uniform density [36].

Solids Control: By reducing the settlement of cuttings and drilled solids, barite contributes to the maintenance of solids control. The increased density of the drilling fluid allows for the efficient removal of cuttings from the wellbore, thereby preventing clogging and enhancing overall drilling efficiency [36].

Filtration Control: Barite can contribute to the control of fluid loss by forming a thin filter cake on the wellbore walls. This filter cake functions as a physical barrier, minimizing fluid loss while decreasing fluid invasion into permeable formations [36].

3.1.8 Carbopol

Carbopol is a synthetic polymer that is used to modify the rheology of drilling fluids. It is possible to increase the fluid's viscosity and gel strength, thereby improving its suspension qualities. Carbopol increases the effectiveness of hole cleaning and avoids solid particles from sagging [37]. Carbopol is introduced to drilling fluids in order to modify the fluid's rheological properties, especially the viscosity and flow behaviors. It provides resistance to flow and increases the viscosity of the fluid by forming a three-dimensional network structure within the fluid. The introduction of Carbopol could help to attain the desired flow properties and enhance cuttings suspension, thereby preventing settling and enhancing the hole cleaning efficiency [37].

3.1.9 Saw dust

Saw dust refers to the small particles or shavings produced when wood is cut or shaped with saws or other woodworking tools. It is mainly composed of wood fibers and has a fibrous, porous structure.

Sawdust could be added to drilling fluids to alter their properties and performance. Due to its ability to decrease the filtration rate of drilling fluids, it is usually regarded as a potential fluid loss control agent [38]. By adding sawdust into the formulation of the fluid, it is possible to limit fluid loss into the formation, maintain wellbore stability, and minimize formation damage.

Saw dust's effectiveness as a fluid loss control additive is a result of its porous structure that could act as a physical barrier, preventing the passage of fluid through the formation [38]. The fine particles tend to have a larger surface area and superior sealing properties,

which can affect the filtration control effectiveness. However, it is essential to strike a balance in the particle size to prevent excessive clogging and hindered fluid flow.

Furthermore, using sawdust as a drilling fluid additive may be subject to certain restrictions and considerations. The possibility for degradation or disintegration of sawdust particles at high temperatures or in chemically aggressive environments is one factor to consider. Moreover, sawdust may have compatibility issues with particular additives or drilling fluid systems, which must be evaluated during formulation design.

It is worth noting that the use of sawdust as a drilling fluid additive may have certain limitations and considerations. Some factors to consider include the potential for degradation or disintegration of sawdust particles under high temperatures or in chemically aggressive environments. Additionally, sawdust may have specific compatibility issues with certain additives or drilling fluid systems, which need to be evaluated during the formulation design [38].

Overall, saw dust is an appropriate choice for controlling fluid loss in water-based drilling fluids, providing a cost-effective and environmentally friendly solution. However, the particular application and performance of sawdust as a drilling fluid additive can differ based on drilling conditions, formation characteristics, and other fluid components. The optimal concentration and particle size of sawdust in order to achieve the desired fluid loss control and maintaining drilling efficiency must be determined through testing and evaluation.

3.1.10 Quartz

Quartz is one of the most common minerals in the Earth's crust and the most essential silica mineral; it is found in significant quantities in igneous, metamorphic, and sedimentary rocks. The mineral is a common base material in a variety of industrial applications. Due to its chemical composition (SiO2) and unique properties, quartz can be utilized as both a bulk product (such as quartz grains in the glass or foundry industries) and a high-tech material (such as piezo or optical quartz) [39].

Figure 3.6 is the cumulative particle size distribution of the quartz particle. As shown the D50 value lies in the range between 315-355 micrometers [39].

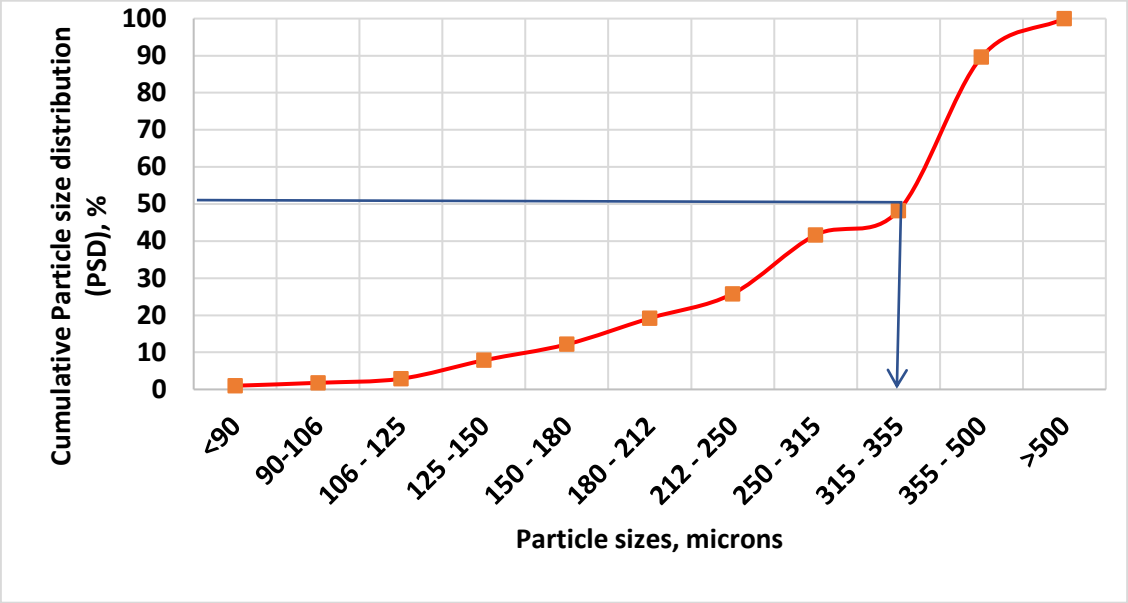

Figure 3.6: Particle Size Distribution of Quartz particles used

Figure 3.7 shows the weight percent of the Quartz particles. As shown in the Figure, about 40% of the Quartz mass is in the range of 355-500 microns.

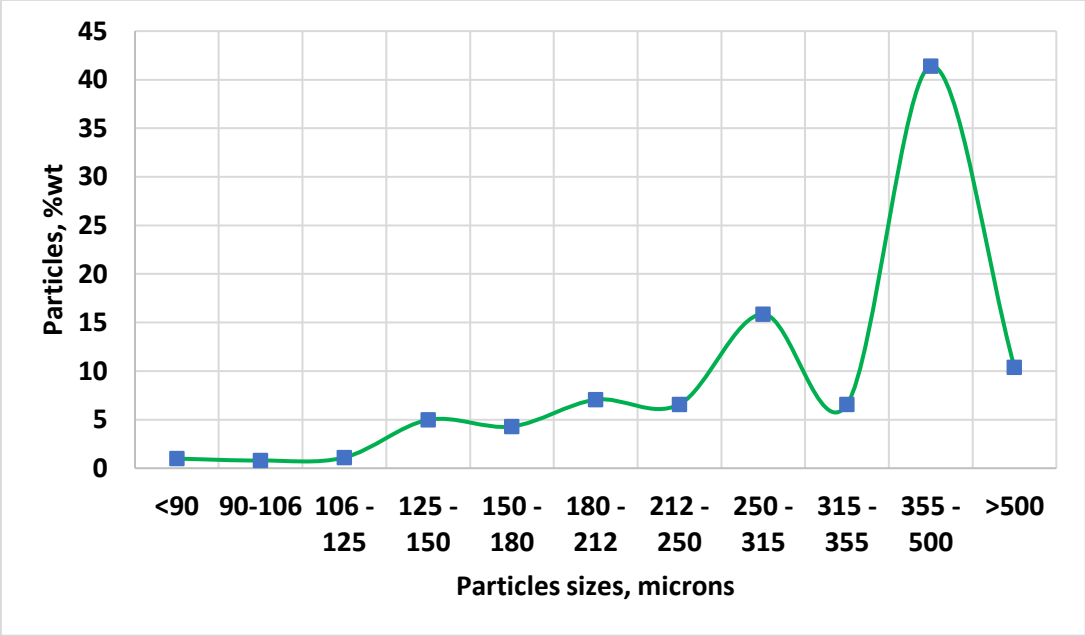

Figure 3.7: Quartz Particle weight Percent

3.2 Experimental setup

For the synthesis and characterization of the drilling fluids, typical equipment is used. The drilling fluids are mixed with a high-speed Hamilton beach mixer. We mixed the drilling fluids systems very well during synthesis and characterization, so the system was free of clumps. The following describes the equipment and the test procedures.

3.2.1 VG viscometer

Before testing the viscosity, the drilling fluids were mixed for 1-2 min in order to have the system good dispersion. Fann-35 viscometer was used for measuring viscosity response of the drilling fluids at shear rates of 600, 300, 200, 100, 60, 30, 6 and 3. The measurements were performed at 22°C, 50°C and 80°C.

The fluids have been heated with heating cup, which can handle up to 50°C. However, for the 80°C testing, a heating plate was used to elevate the temperature of the drilling fluid to 80°C. Figure 3.8 shows the equipment used during testing process.

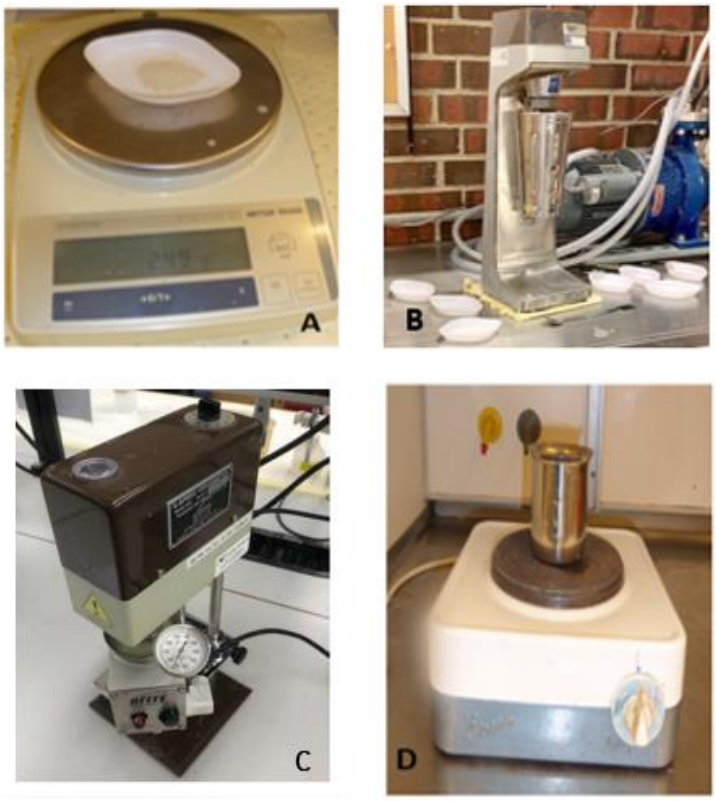

Figure 3.8: (A) Weight balance, (B) Hamilton Beach mixer, (C) Fann-35 viscometer with the heating cup and thermometer and (D) Oven.

3.2.2 Viscoelasticity

Figure 3.9 is an Anton Paar MCR 302. It is utilized to measure the viscoelasticity properties of the drilling fluids. In this thesis, only amplitude sweeps oscillatory test was conducted at room temperature.

The amplitude sweep test was conducted with the angular frequency (ω) of 10 rad/s and the strain interval of 0.005% to 1000%. From the measurement, one can determine the storage, shear, loss and damping factor for the fluid systems.

Figure 3.9: Anton Paar MCR 302 rheometer

3.2.3 pH

Figure 3.10 is Mettler Toledo pH meter used to measure the drilling fluids pH by calibrating the pH meter prior to each test. The pH value (acidity and alkalinity) controls the properties of the drilling fluid. To obtain the fluids in alkaline condition, the desired soda ash was used.

Figure 3.10: Mettler Toledo pH meter

3.2.4 Filtrate loss

Figure 3.11 shows during API filter test rig. During testing 100 psi is applied on the drilling fluid and the filtrate loss is collected after 7.5 minutes.

Figure 3.11: API filter press

3.2.5 Particle Sieve analyzer

Bentonite and KCL based fluids have been tested with two different particle size of saw dust as mentioned earlier. UiS provided industrial saw dust, which is "StopLoss" brand for experimental purposes. To conduct the experiments, firstly sieving procedure of saw dust has been conducted and abovementioned particle sizes of saw dust has been retrieved from the system. Figure 3.12 shows the particle sieve analyzer and Figure 3.13 shows the un-sieved Saw dust. Figure 3.14 and Figure 3.15 show the sieved <71 micron and 125-150 microns saw dust, respectively.

Figure 3.12: Unsieved Saw Dust

Figure 3.13: Particle sieve Analyzer

Figure 3.15: <71 μm sieved Saw dust

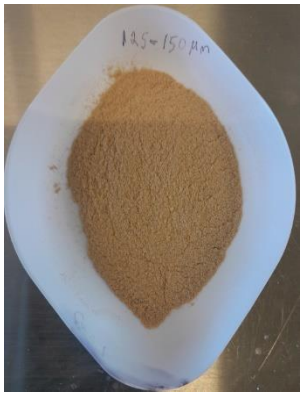

Figure 3.14: 125-150 μm sieved saw dust

3.2.6 Bridging Lost Circulation

The lost circulation performance of the drilling fluids has been evaluated using static bridging Gilson equipment (Figure 3.16). The test was to investigate if the presence of the saw dust able to heal the possible micro fractures in the wellbore. This will be assessed by comparing the saw dust blended drilling fluid with the saw dust free base fluid.

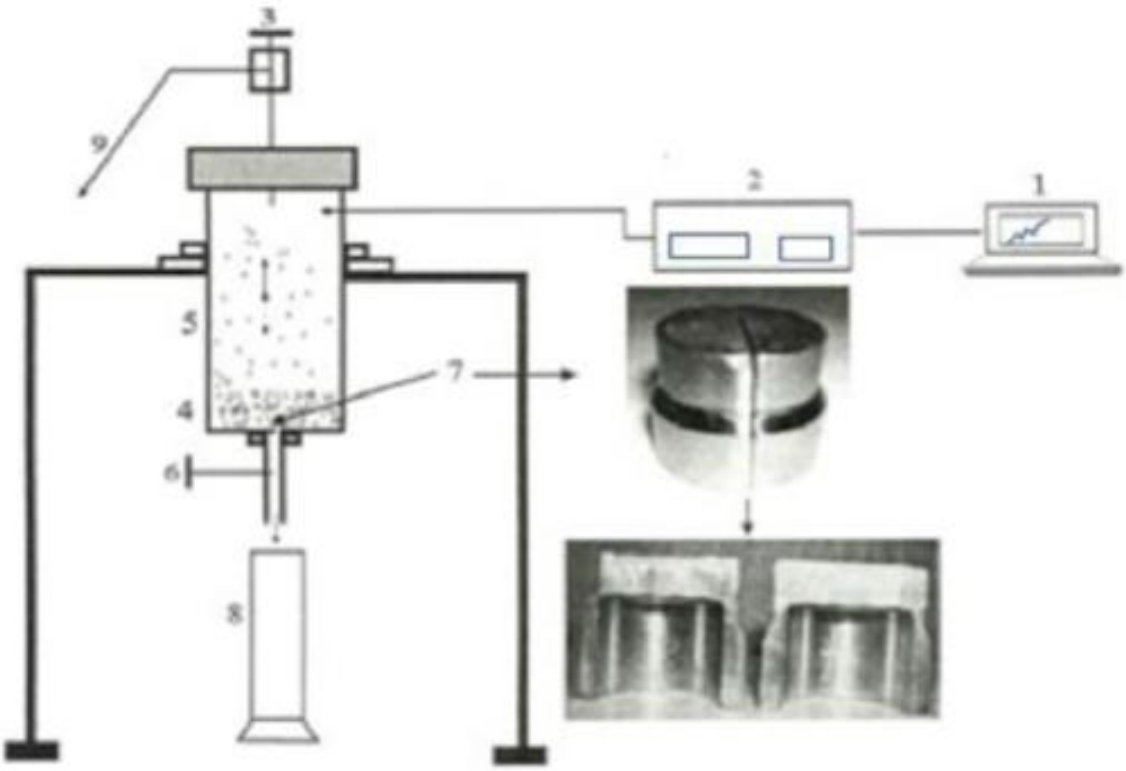

Figure 3.16: Static bridging test Experimental set up

Figure 3.16 shows the lost circulation experiment. As shown the cylindrical drilling fluid holder (5) has a dimension of 35 mm (inner diameter) and 64 mm (outer diameter) and 150 mm long. At the bottom of the cylinder, different slot sizes are placed. The length and the depth of the slots are 10 mm and 24.4 mm, respectively. The slot simulates a fracture around the wellbore.

During testing, the drilling fluid will make a mud cake at (7). The pressure applied by Gilson pump (2) on the mud cake, the bridging performance of the mud cake is logged using PC-control (1). The testing will be conducted until 20 min duration.

3.2.7 Mixing Method and Time Procedure for all used additives

Table 3.1 below provides an information about the mixing method, taken time and addition method for all the additive used in the experiments.

Table 3.1: Method of mixing and taken time for the additives

Additive	**Mixing Method and Time**
1. Water	- mixed with all other chemicals as a drilling fluid basis liquid
2. Soda Ash	- mixed at high speed for 5 minutes
3. KCL	- mixed at high speed for 5 minutes
4. PolyPac + Pac	- mixed at low speed for 5 minutes
5. Sawdust	- mixed at high speed for 5 minutes
6. Bentonite	- mixed at low to high speed for 5 minutes
7. Barite	- mixed at high speed for 10 minutes
8. Carbopol	- mixed in low to high speed for 2.5 minutes
9. Xanthan Gum	- mixed at low to high speed for 5 minutes (ex-situ)
10. Antifoam	- added as droplets at high speed while fluid mixed (ex-situ)

4 Results and Discussion

Chapter 4 presents the results he measured data and the discussion of the results obtained from drilling fluids characterization. In this thesis, the impact of saw dust have been investigated in Bentonite and KCL based drilling fluids.

Two methods were employed for the investigation. The first one is called ‘’**whole drilling fluid**’’ and the second one is called ‘’**Replacement**’’.

- The **whole drilling** fluid means adding saw dust on the base drillings and compare the impacts with the base fluid.
- The **Replacement** drilling fluid means by removing a certain concentration of polymer and replace it by adding saw dust on the base drillings and compare the impacts with the base fluid. the idea here is to reduce the cost of polymer and replace it by cost effective eco-friendly additive.

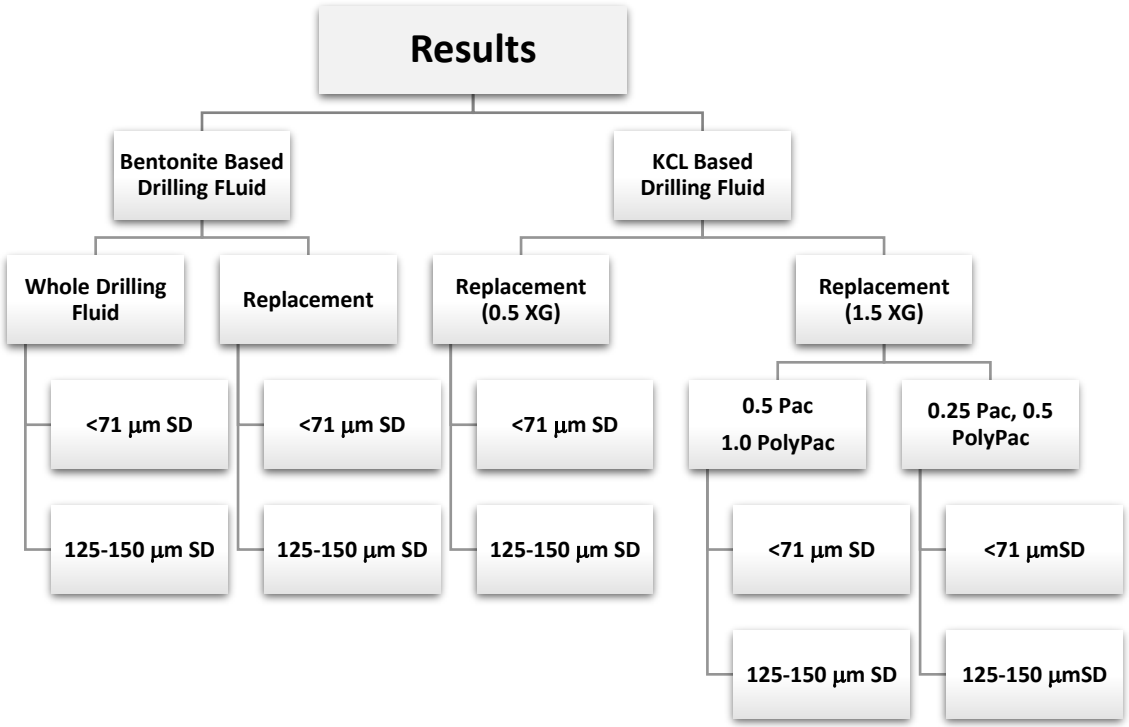

Figure 4.1: Test Results structure for bentonite and KCL based WBM

4.1 Bentonite Drilling Fluid Systems

In this section, viscosity, filtrate loss and pH value results for bentonite-based drilling fluids are shown and impact of saw dust in two different particle sizes are discussed (<71 µm & 125-150 µm). All the experiments have been done according to abovementioned design structures and procedures. Ex-situ additions of certain components are shown in the fluid design tables accordingly.

4.1.1 Effect of Saw Dust in Whole Bentonite Base Drilling Fluid

In this design, fluids are prepared according to the design tables below (Table 4.1, Table 4.2). Basic principle of this fluid design is to study different effects, (such as pH value, viscosity measurements and filtrate loss) of saw dust on whole fluid without replacing any polymer.

Table 4.1: Whole bentonite fluids with three different concentrations of <71 µm SD

Additives	**Base Fluid**	**Fluid 1.1**	**Fluid 1.2**	**Fluid 1.3**
Water	350 ml	350 ml	350 ml	350 ml
Soda ash	3.2 g	3.2 g	3.2 g	3.2 g
Pac	0.5 g	0.5 g	0.5 g	0.5 g
PolyPac	1.0 g	1.0 g	1.0 g	1.0 g
Bentonite	10 g	10 g	10 g	10 g
Barite	150 g	150 g	150 g	150 g
Carbopol	0.08 g	0.08 g	0.08 g	0.08 g
SawDust <71 µm	**-**	**1 g**	**3 g**	**5 g**

Table 4.2: Whole bentonite fluids with three different concentrations of 125-150 µm SD

Additives	**Base Fluid**	**Fluid 2.1**	**Fluid 2.2**	**Fluid 2.3**
Water	350 ml	350 ml	350 ml	350 ml
Soda ash	3.2 g	3.2 g	3.2 g	3.2 g
Pac	0.5 g	0.5 g	0.5 g	0.5 g
PolyPac	1.0 g	1.0 g	1.0 g	1.0 g
Bentonite	10 g	10 g	10 g	10 g
Barite	150 g	150 g	150 g	150 g
Carbopol	0.08 g	0.08 g	0.08 g	0.08 g
SawDust 125-150 µm	**-**	**1 g**	**3 g**	**5 g**

Laboratory test measurements are conducted with the fluids after waiting 24 hours in order to observe existence of sagging issue and to analyze more realistic cases.

4.1.1.1 Impact of <71 μm SD on the viscosity of the base fluid

The impact of <71 μm SD on viscosity of the fluid was investigated by comparing whole reference and whole first batch fluid systems. In figure 4.2 the shear stress responses of the fluid systems in whole and containing 1 g <71 μm SD are plotted as a function of RPM.

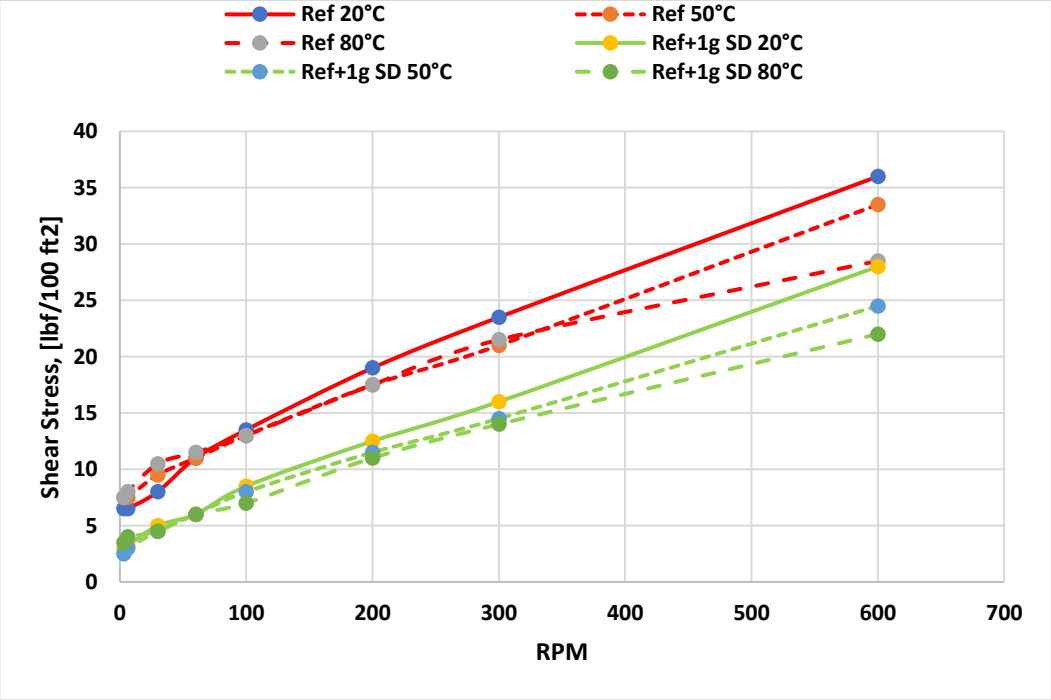

Figure 4.2: Viscometer data at 20°C, 50°C, 80°C for whole reference and 1 g <71 μm SD fluids

It is clearly seen from the Figure 4.2 that the addition of 1 g of sawdust results in a lower shear stress compared to the reference fluid. This indicates that the presence of sawdust particles has influenced the fluid's viscosity, creating stronger bonds between the fluid molecules and making it stronger overall. The reduction in shear stress suggests an increase in the internal friction within the fluid due to the presence of the sawdust particles.

In addition, while examining the shear stress values at 50°C and 80°C, it can be noticed that they represent similar trends. This suggests that the fluid maintains its viscosity consistently within the tested temperature range. The stability implies that it possesses

thermal stability, remaining relatively unchanged as it is subjected to higher temperatures. This desirable characteristic ensures consistent performance even under varying thermal conditions.

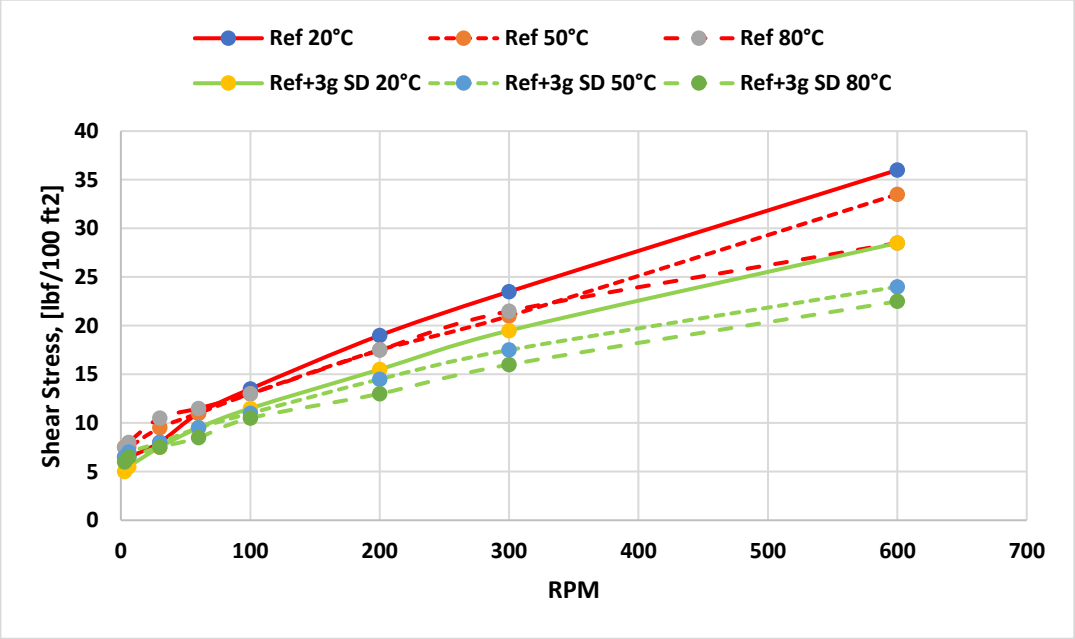

Figure 4.3: Viscometer data at 20°C, 50°C, 80°C for whole reference and 3 g <71 µm SD fluids

Figure 4.3 shows that, addition of 3 g saw dust shows relatively same trend as 1 g. Shear stress values are being lower than reference fluid almost in all RPMs. For 50°C and 80°C shear stress values show the same trends, which means the fluid is thermally stable and do not vary as cooked. This characteristic is particularly valuable in drilling operations where the fluid is exposed to varying thermal conditions. However, at higher speed (around 600 RPM) values there is slightly different behavior of SS compared to case with just 1 g of SD.

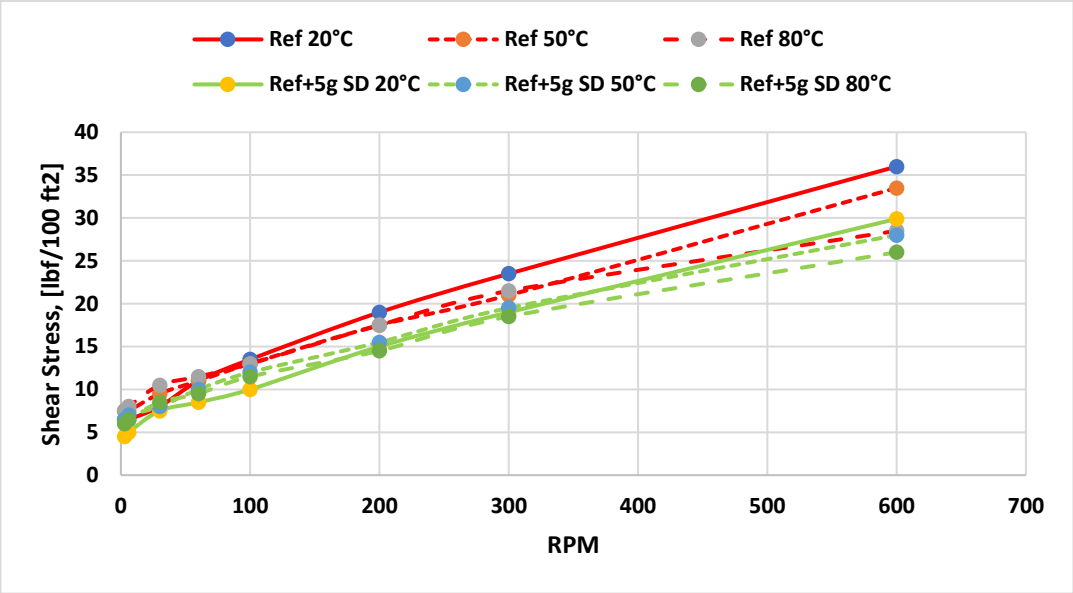

Figure 4.4: Viscometer data at 20°C, 50°C, 80°C for whole reference and 5 g <71 µm SD fluids

It can be clearly seen from the Figure 4.4 that after adding 5 g <71 µm SD to the reference fluid, fluid start to show lower shear stress in all three temperatures (20°C, 50°C, 80°C). It represents the importance of optimum concertation and non-linear dependency of performance versus additive quantity.

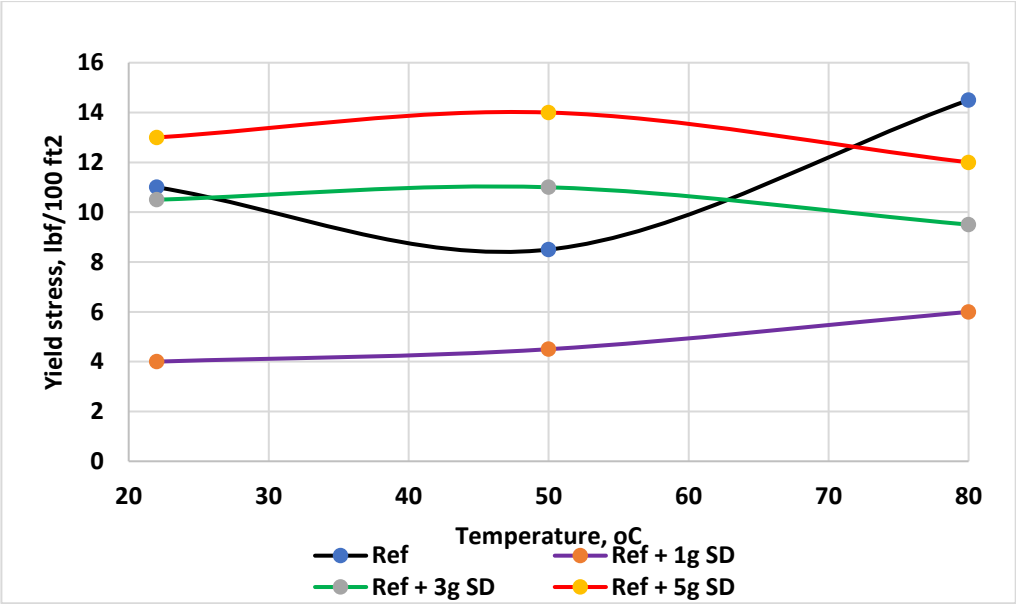

Figure 4.5: Bingham yield stress of whole bentonite reference and <71 µm SD fluids at different temperatures

The obtained Bingham yield stress values of whole bentonite reference fluid and fluid with the abovementioned additive are demonstrated in Figure 4.5. As it is clearly observed from the graph, addition of <71 μm SD in all three concentrations led to have Bingham yield stress values not much different even after cooked. While addition of 1 g concentration showed less yield stress, 3 g and 5 g concentrations showed relatively higher values. Additionally, stress value lines became smoother after adding SD to the system, making fluids thermally more stable rather than whole base reference fluid without SD.

4.1.1.2 Impact of <71 μm SD on the pH and filtrate loss of the base fluid

pH values of the fluids have been measured and luckily enough, the results do not show any abrupt reduction or increase in the values compared to the whole base fluid (Table 4.3).

Table 4.3: pH of whole bentonite reference and first batch fluids

Drilling Fluid	**Base Fluid**	**Fluid 1.1 SD (<71 μm, 1 g)**	**Fluid 1.2 SD (<71 μm, 3 g)**	**Fluid 1.3 SD (<71 μm, 5 g)**
pH	10.57	10.68	10.54	10.41

The filtrate loss experiment was done with the whole bentonite fluid using API filter test rig filter press equipment. After applying 100 psi pressure on the fluids and waiting 7.5 minutes, impact of <71 μm saw dust has been studied. Results showed that, in comparison with reference base fluid, Fluid 1.2 and Fluid 1.3 showed filtrate loss reduction percentages, with 2.9% and 2.0% respectively (Figure 4.6). It undoubtedly proves the capability of saw dust as filtrate loss control additive for water-based mud. These figures would be high in real drilling processes due to circulating flow rather than statically applied pressure in lab analyses.

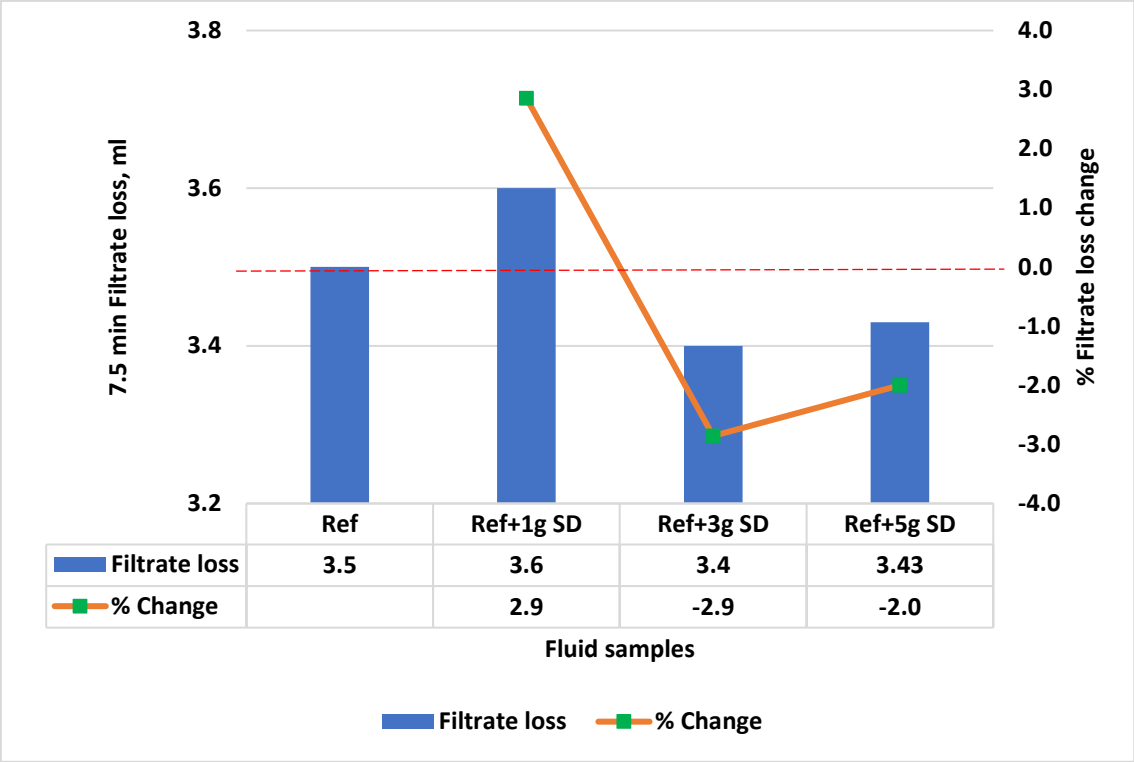

Figure 4.6: Filtrate Loss and Filtrate Loss Change of whole bentonite reference and first batch (<71 μm) fluids

4.1.1.3 Impact of 125-150 μm SD on the viscosity of the base fluid

It is clearly seen from Figure 4.7 that, addition of 1 g saw dust shows less shear stress values compared to reference fluid, which means particles created stronger bonds between molecules and made the fluid stronger. Additionally, for 50°C and 80°C shear stress values show the same trends in lower and mid values, which means the viscosity of the fluid is stable and do not vary as cooked. The stability in shear stress suggests stable internal friction within the fluid due even though the presence of the sawdust particles. This is also good point to mention, as 1 g concentration of lower particle size showed reduction in shear stress values. Particle size of the saw dust do matter, as bigger particle size end up with less internal friction in the fluid.

Overall, fluid maintains its viscosity consistently within the tested temperature range. The stability implies that it possesses thermal stability, remaining relatively unchanged as it

is subjected to higher temperatures. This desirable characteristic ensures consistent performance even under varying thermal conditions.

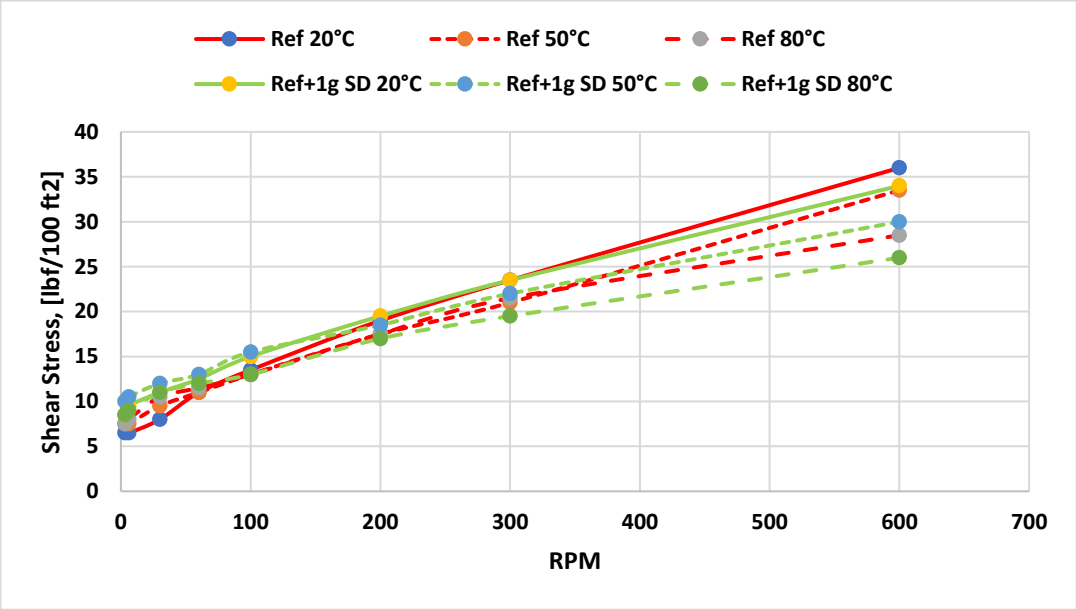

Figure 4.7: Viscometer data at 20°C, 50°C, 80°C for whole reference and 1 g 125-150 µm SD fluids

Figure 4.8 shows addition of 3 g saw dust and it depicts less but closer shear stress values compared to reference fluid, meaning strong particle bonds between molecules and made the fluid stronger. While looking at 20°C, reference fluid and fluid with 3 g saw dust additive almost match up the same shear stress values. This might be because of friction as there is no thermal coefficient playing role. Concentration of 3 g might create homogenous fluid as mixed, making its viscosity not much different than the reference fluid. Additionally, for 50°C and 80°C shear stress values show the same trends in lower and mid values, which means the viscosity of the fluid is stable and do not vary as cooked.

Overall, fluid maintains its viscosity consistently within the tested temperature range. The stability implies that it possesses thermal stability, remaining relatively unchanged as it is subjected to higher temperatures. This desirable characteristic ensures consistent performance even under varying thermal conditions.

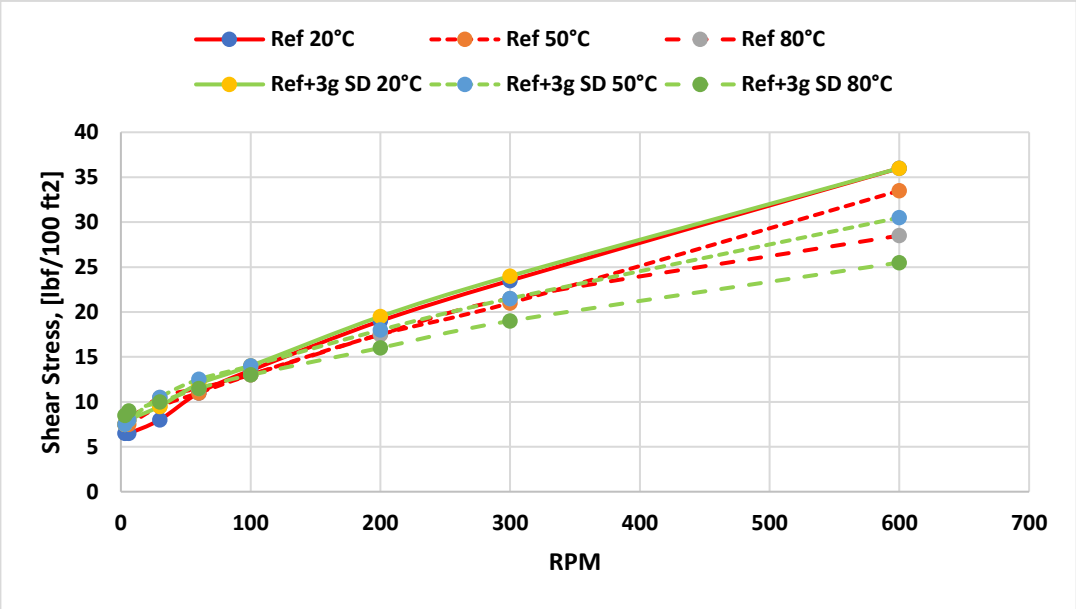

Figure 4.8: Viscometer data at 20°C, 50°C, 80°C for whole reference and 3 g 125-150 µm SD fluids

It can be clearly seen from the Figure 4.9 that after adding 5 g 125-150 µm SD to the reference fluid, fluid start to show lower shear stress in all three temperatures (20°C, 50°C, 80°C) but with similar trends. It represents the importance of optimum concertation and non-linear dependency of performance versus additive quantity.

The inclusion of 5 g of sawdust shows a slightly diminished improvement compared to the previous cases. The shear stress values remain lower than the reference fluid but exhibit a less pronounced reduction. Additionally, it is worth noting that the higher concentration of sawdust particles results in increased filtration loss, indicating a greater potential for fluid loss during the drilling process. This suggests that while the addition of sawdust still affects the fluid's viscosity, the benefits become less prominent, and the trade-off of increased filtration loss should be considered when using a higher concentration of sawdust particles.

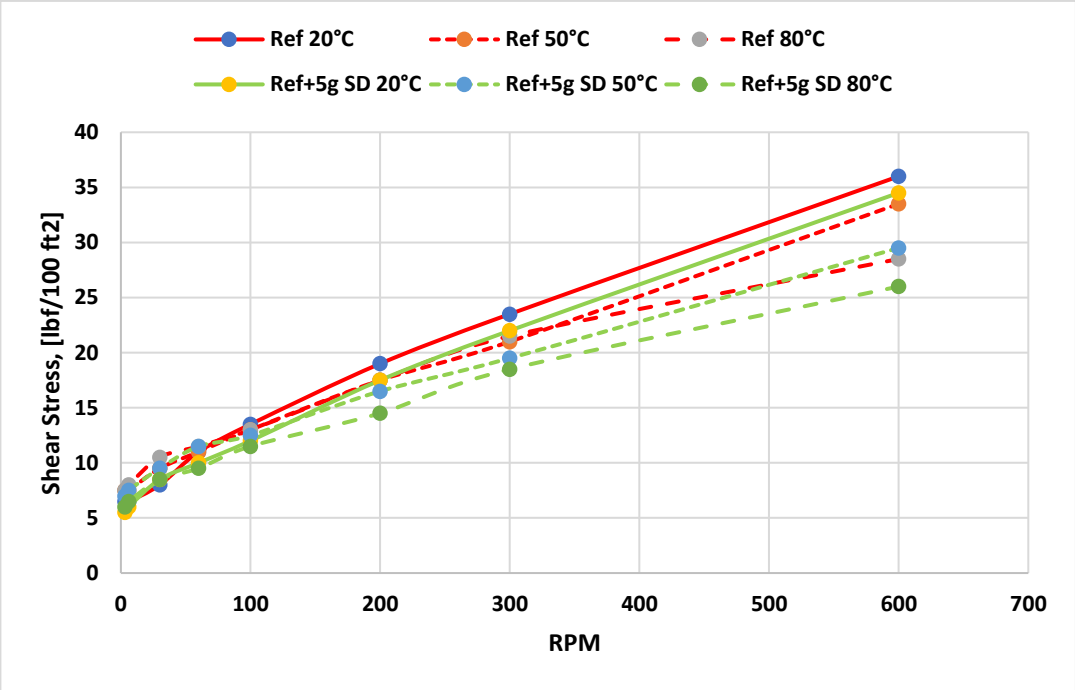

Figure 4.9: Viscometer data at 20°C, 50°C, 80°C for whole reference and 5 g 125-150 µm SD fluids

The obtained Bingham yield stress values of whole bentonite reference fluid and fluid with the abovementioned additive are demonstrated in Figure 4.10. As it is clearly observed from the graph, addition of 125-150 µm SD in all three concentrations led to have Bingham yield stress values not much different even after cooked. While addition of 5 g concentration showed less yield stress, 1 g and 3 g concentrations showed relatively higher values. Additionally, stress value lines became so much smoother after adding SD to the system, making fluids thermally more stable rather than whole base reference fluid without SD. The best concentration is probably 3 g, as it shows almost perfect stability within the temperature range.

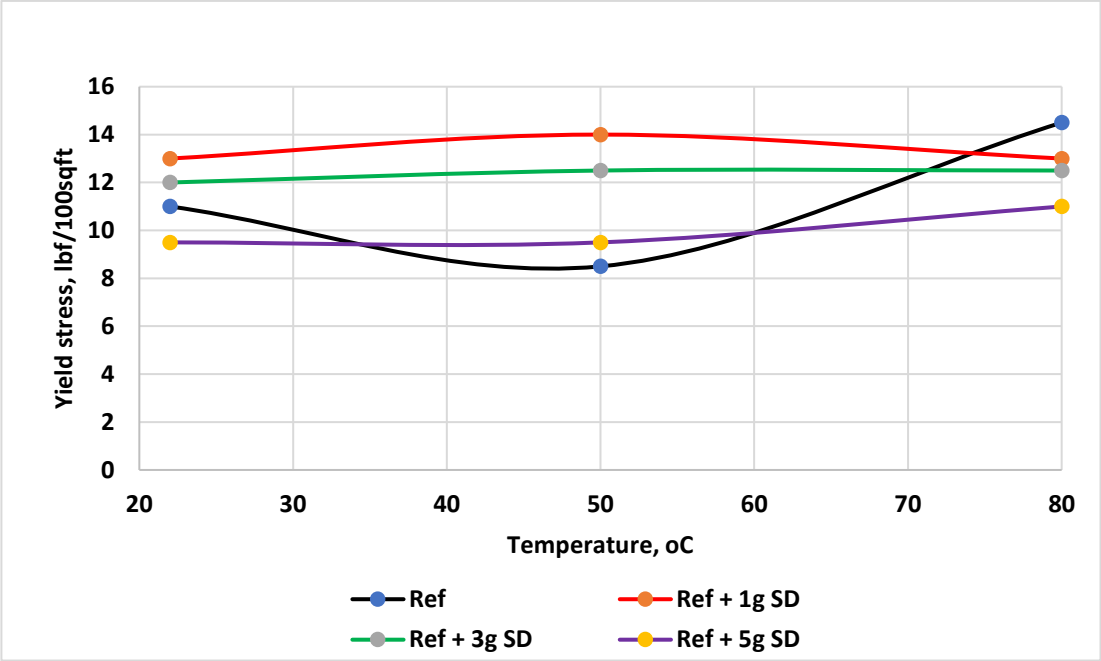

Figure 4.10: Bingham yield stress of whole bentonite reference and 125-150 µm SD fluids at different temperatures

Figure 4.10 illustrates that addition of SD in diverse concentrations stabilizes the dependency of yield stress from temperature remarkably. Meanwhile 5 g of SD shows 18% less yield stress compared to least amount of addition (1 g).

4.1.1.4 Impact of 125-150 µm SD on the pH and filtrate loss of the base fluid

pH values of the fluids have been measured and the results do not show any abrupt reduction or increase in the values compared to the whole base fluid. It's worth noting that the pH values of the fluids containing saw dust were slightly lower compared to the base fluid without saw dust (Table 4.4). This change in pH may be attributed to the introduction of sawdust particles into the fluid system. This decrement of pH value affects mainly 2 points: 1. Clay Swelling Control - Controlling the swelling of clay minerals present in the formation & wellbore stability; 2. Corrosion Control - Controlling Corrosiveness towards metal equipment and casing & well integrity.

Table 4.4: pH of whole bentonite reference and second batch fluids

Drilling Fluid	**Base Fluid**	**Fluid 2.1 SD (125-150 µm, 1 g)**	**Fluid 2.2 SD 125-150 µm, 3 g)**	**Fluid 2.3 SD 125-150 µm, 5 g)**
pH	10.57	10.21	10.05	10.46

The same filtrate loss experiment done with the whole bentonite fluid first batch with 3 different concentrations is also conducted for the second batch of fluids containing 125-150 µm SD using API filter test rig filter press equipment. After applying 100 psi pressure on the fluids and waiting 7.5 minutes, impact of 125-150 µm SD has been studied. Results showed that, compared to reference base fluid and first batch of fluids with <71 µm SD, Fluid 2.1 and Fluid 2.2 showed the best filtrate loss reduction percentages, with 7.1% and 14.3% respectively (Figure 4.11). It surely proves the capability of saw dust as filtrate loss control additive for water-based mud. Also, particle size of 125-150 µm showed homogenous fluid mixture, less sagging and more viscosity.

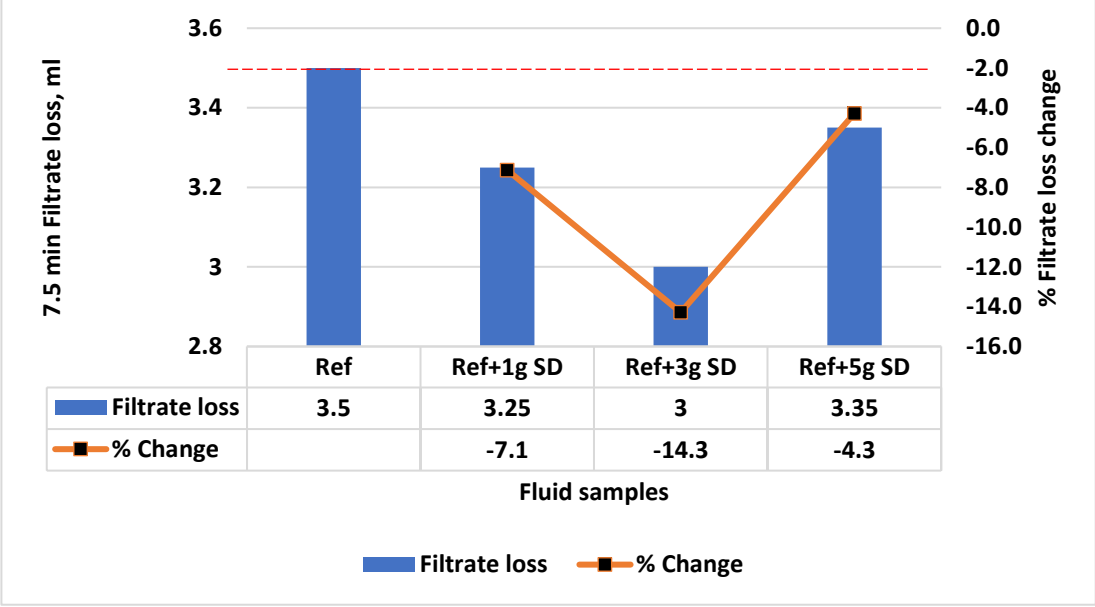

Figure 4.11: FL & FLR of whole bentonite second batch fluids with 125-150 µm SD

Overall, the addition of sawdust, particularly in the particle size range of 125-150 µm, in the specified concentrations, resulted in a notable reduction in filtrate loss, making it a promising additive for controlling fluid loss in the drilling mud system.

4.1.2 Effect of Saw Dust in Polymer Replacement Bentonite Base Fluid

In this design, fluids are prepared according to the design tables below. Basic principle of this fluid design is to study different effects (such as pH value, viscosity measurements and filtrate loss) of replacing Pac & PolyPac with two different particle sizes of saw dust. The idea here is to reduce the cost of polymer and replace it by cost effective eco-friendly additive with satisfactory performance. The main goal of replacing polymers and adding saw dust in not only economic and ecological side, but also to achieve less filtrate loss compared the equivalent fluids in whole system.

Table 4.5: Replacement bentonite fluids with three different concentrations of <71 µm SD

Additives	**Base Fluid**	**Fluid 3.1**	**Fluid 3.2**	**Fluid 3.3**
Water	350 ml	350 ml	350 ml	350 ml
Soda ash	3.2 g	3.2 g	3.2 g	3.2 g
Pac	0.5 g	-	-	-
PolyPac	1.0 g	-		
Bentonite	10 g	10 g	10 g	10 g
Barite	150 g	150 g	150 g	150 g
Carbopol	0.08 g	0.08 g	0.08 g	0.08 g
Antifoam	5 drops	5 drops	5 drops	5 drops
SawDust <71 µm	**-**	**1 g**	**3 g**	**5 g**
Xanthan Gum	0.5 g	0.5 g	0.5 g	0.5 g

Table 4.6: Replacement bentonite fluids with three different concentrations of 125-150 µm SD

Additives	**Base Fluid**	**Fluid 4.1**	**Fluid 4.2**	**Fluid 4.3**
Water	350 ml	350 ml	350 ml	350 ml
Soda ash	3.2 g	3.2 g	3.2 g	3.2 g
Pac	0.5 g	-	-	-
PolyPac	1.0 g	-	-	-
Bentonite	10 g	10 g	10 g	10 g
Barite	150 g	150 g	150 g	150 g
Carbopol	0.08 g	0.08 g	0.08 g	0.08 g
Antifoam	5 drops	5 drops	5 drops	5 drops
SawDust 125-150 µm	**-**	**1 g**	**3 g**	**5 g**
Xanthan Gum	0.5 g	0.5 g	0.5 g	0.5 g

As it is seen from the design tables, difference between this design and whole fluid design is not only Pac & PolyPac, but also two other components – Antifoam and Xanthan Gum. This is an ex-situ situation and decision is made due to the sagging issue of fluids with the absence of polymers. Adding Xanthan Gum helped to get viscosity of the fluid

increased and keep the fluid in suspension. On the other hand, absence of Pac & PolyPac and presence of SD simultaneously ended up generating air bubbles inside the fluid and in the surface. After addition of 0.5 g Xanthan Gum and mixing it well, air bubbles did not disappear, so 5 drops of Antifoam were added as an ex-situ additive, and it was mixed properly as well.

4.1.2.1 Impact of <71 μm SD on the Viscosity of the replacement fluid

It is clearly seen from the Figure 4.12 that the addition of 1 g <71 μm SD and replacement of polymers result in a lower shear stress compared to the reference fluid. This indicates that the presence of sawdust particles has influenced the fluid's viscosity, creating stronger molecular bonds between substances. The reduction in shear stress suggests an increase in the internal friction within the fluid due to the presence of the sawdust particles.

In addition, while examining the shear stress values at 50°C and 80°C, it can be noticed that they represent similar trends in higher RPM. This suggests that the fluid maintains its viscosity consistently within the tested temperature range. The stability implies that it possesses thermal stability, remaining relatively unchanged as it is subjected to higher temperatures. This desirable characteristic ensures consistent performance even under varying thermal conditions.

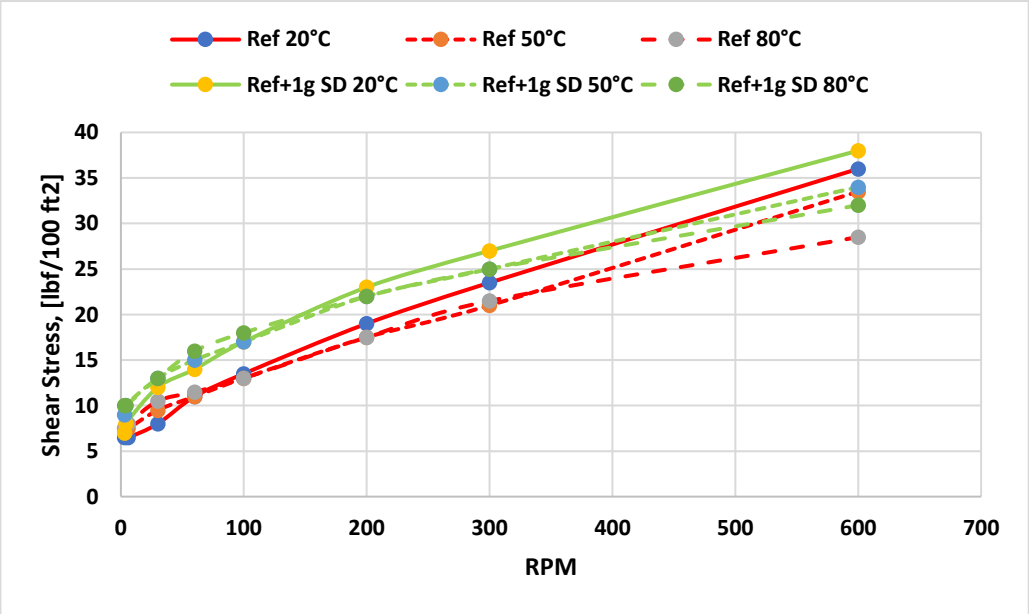

Figure 4.12: Viscometer data at 20°C, 50°C, 80°C for replacement reference and 1 g <71 μm SD fluids

The obtained Bingham yield stress values of replacement bentonite reference fluid and fluid with the abovementioned additive are demonstrated in Figure 4.13. As it is clearly observed from the graph, addition of <71 µm SD in 1 g concentration led to have Bingham yield stress values not much different even after cooked. While addition of 1 g concentration showed increase in yield stress as cooked, 3 g and 5 g concentrations decreased the yields stress at 80°C. Additionally, stress value line for 1 g concentration depicted smoother trendline, making fluids thermally more stable rather than the other two concentrations and replacement base reference fluid without SD.

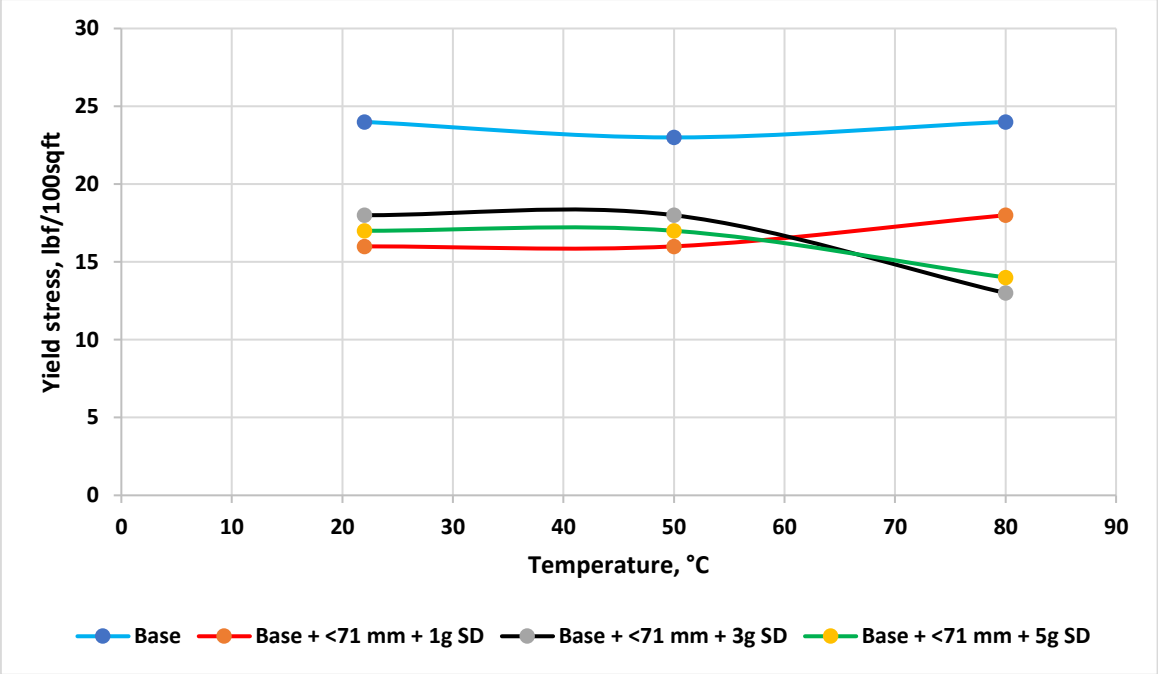

Figure 4.13: Bingham yield stress of replacement bentonite reference and <71 µm SD fluids at different temperatures

4.1.2.2 Impact of <71 µm SD on the pH and Filtrate loss of the base fluid

pH values of the fluids have been measured and the results show some reductions in the values compared to the replacement base fluid. It's worth noting that the pH values of the fluids containing saw dust were slightly lower compared to the base fluid without saw dust (Table 4.7). This decrement of pH value affects mainly 2 points: 1. Clay Swelling Control - Controlling the swelling of clay minerals present in the formation & wellbore stability; 2. Corrosion Control - Controlling corrosiveness towards metal equipment and casing & well integrity.

Table 4.7: pH of replacement bentonite reference and first batch fluids

Drilling Fluid	**Base Fluid**	**Fluid 3.1 SD (<71 µm, 1 g)**	**Fluid 3.2 SD (<71 µm, 3 g)**	**Fluid 3.3 SD (<71 µm, 5 g)**
pH	10.81	10.71	10.38	10.24

Filtrate loss experiment was done with the replacement bentonite fluid containing <71 µm SD with 3 different concentrations is conducted for the first batch of fluids using API filter test rig filter press equipment. After applying 100 psi pressure on the fluids and waiting 7.5 minutes, impact of <71 µm SD has been studied. Results showed that, Fluid 1.1 displayed the best filtrate loss reduction percentage, with 7.1% (Figure 4.14) and only 5.2 ml filtrate loss compared to replacement reference base fluid (Figure 4.14). 1 g concentration of <71 µm SD clearly outplays 0.5 g of Pac & 1.0 g of PolyPac mixture with less filtrate loss values. In real application the only challenge would be keeping SD well sorted and particle size plays an imported role (later sections will show comparison between 71 µm and higher sizes).

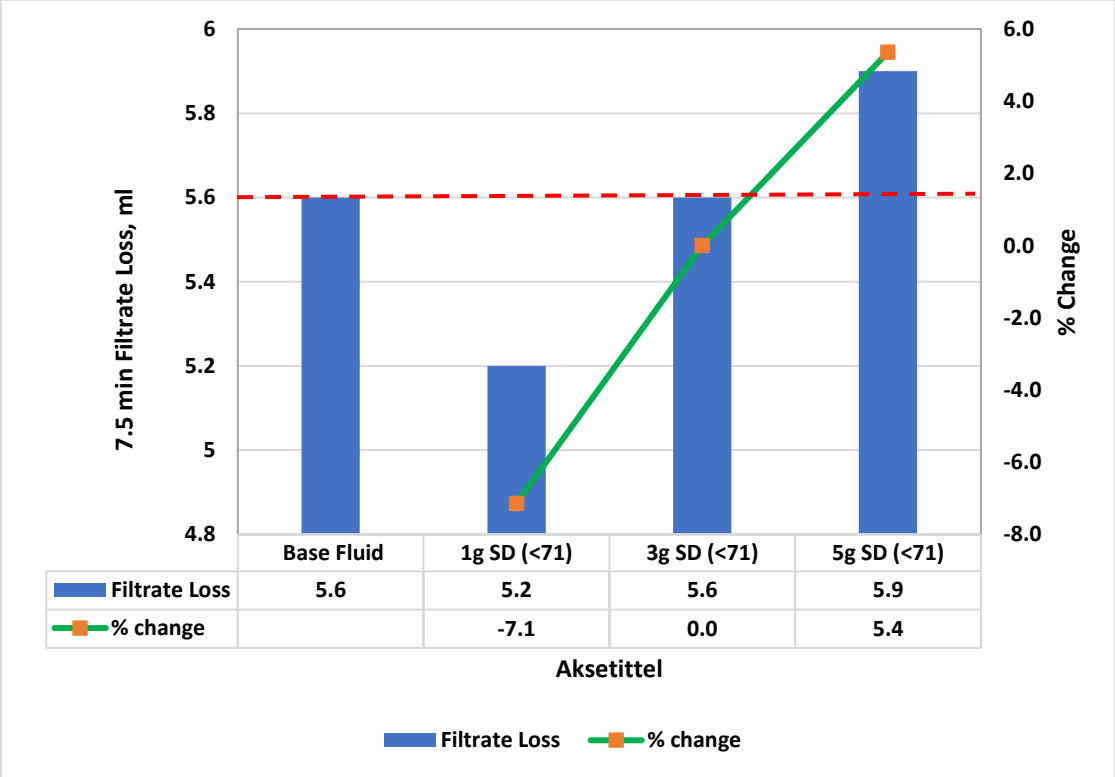

Figure 4.14: Filtrate Loss of replacement bentonite reference and first batch fluids

Also, it is also worth to mention that saw dust is relatively cheaper material than Pac & PolyPac, does not have chemical toxicity and is eco-friendly option. Considering all this advantages, use of particularly successful Fluid 3.1 is an excellent option.

4.1.2.3 Impact of 125-150 μm SD on the Viscosity of the base fluid

The obtained Bingham yield stress values of replacement bentonite reference fluid and fluid with the abovementioned additive are demonstrated in Figure 4.15. As it is clearly observed from the graph, addition of 1 g concentration showed increase in yield stress as cooked, while 3 g and 5 g concentrations relatively kept constant at 50°C and 80°C. Meanwhile, addition of 3 g of SD behaved in an unusual way, decreasing slightly between 22°C - 80°C temperature range.

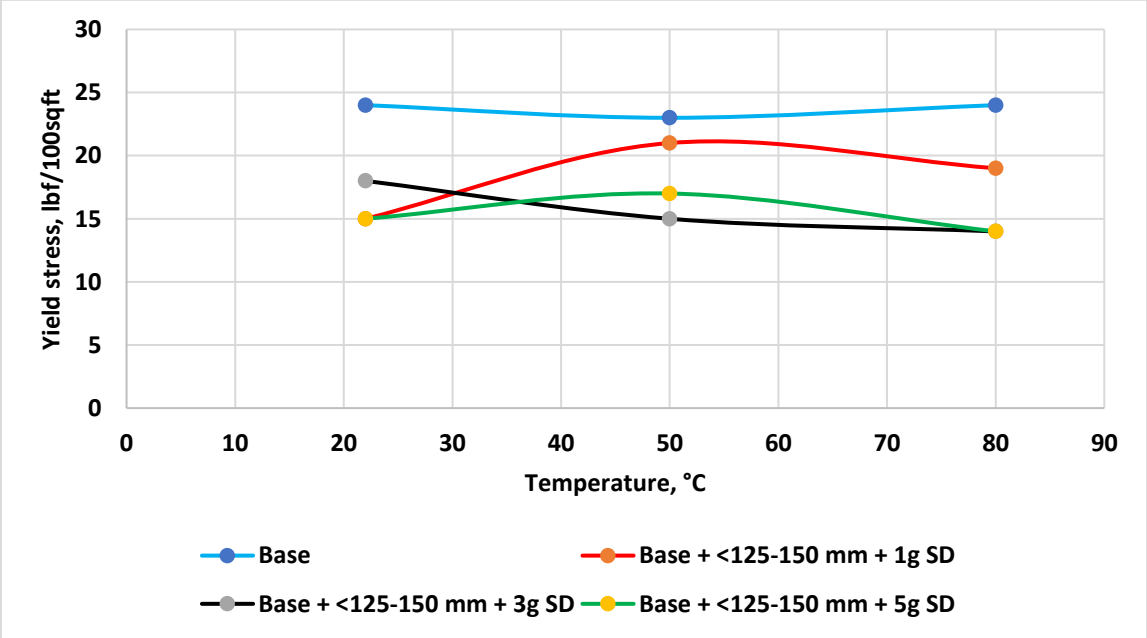

Figure 4.15: Bingham yield stress of replacement bentonite reference and 125-150 μm SD fluids at different temperatures

4.1.2.4 Impact of 125-150 μm SD on the pH and Filtrate loss of the base fluid

pH values of the fluids have been measured and the results show some reductions in the values compared to the replacement base fluid. It's worth noting that the pH values of the

fluids containing saw dust were slightly lower compared to the base fluid without saw dust (Table 4.7). This decrement of pH value affects mainly clay swelling control as controlling the swelling of clay minerals present in the formation & wellbore stability, as well as controlling corrosion, via corrosiveness towards metal equipment and casing & well integrity.

Table 4.8: pH of replacement bentonite reference and second batch fluids

Drilling Fluid	**Base Fluid**	**Fluid 4.1 SD (125-150 µm, 1 g)**	**Fluid 4.2 SD 125-150 µm, 3 g)**	**Fluid 4.3 SD 125-150 µm, 5 g)**
pH	10.81	10.57	10.43	10.31

Filtrate loss experiment was done with the replacement bentonite fluid containing 125-150 µm SD with 3 different concentrations is conducted for the second batch of fluids using API filter test rig filter press equipment. 100 psi pressure was applied on the fluids and 7.5 minutes on the clock was measured, while the impact of 125-150 µm SD has been studied. Results showed that, no fluid displayed filtrate loss reduction percentage. However, fluids with 3 g and 5 g concentrations showed almost same filtrate loss as base fluid (Figure 4.16):

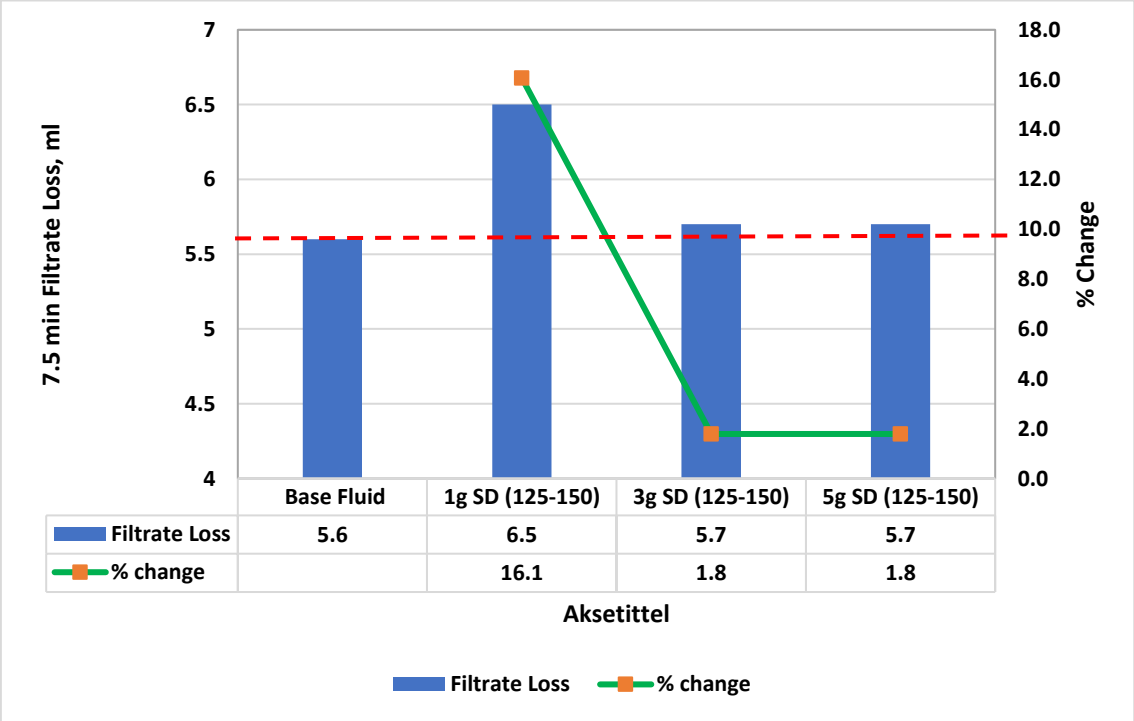

Figure 4.16: Filtrate Loss of replacement bentonite reference and second batch fluids

The obtained results also show that, particle size of saw dust also matters a lot in the absence of Pac & PolyPac. While <71 µm SD showed one particular result with less filtrate loss than base fluid, 125-150 µm SD show no result on that side.

4.2 KCL Drilling Fluid Systems

In this section, filtrate loss, viscosity and pH value results for KCL-based drilling fluids are shown and impact of saw dust in two different particle sizes are discussed (<71 µm & 125-150 µm). All the experiments have been done according to abovementioned design structures and procedures. Ex-situ additions of certain components are shown in the fluid design tables accordingly. In this test, the idea of polymer replacement is employed with the objective of minimizing cost.

4.2.1 Effect of Saw Dust in 1.5 g XG Polymer Replacement KCL Base Fluid

The basis for this fluid is a little different than the bentonite fluid. Since the target of KCL replacement fluid is to reduce the filtrate loss below the reference that contains Pac & PolyPac (i.e 5.6ml), 1.5 g amount of ex-situ Xanthan Gum was introduced. The idea behind that is to reduce the occurrence of high filtrate loss values and depicted spurt loss in the beginning of the experiment after removing Pac & PolyPac. Adding Xanthan Gum also directly affects viscosity of the fluid positively.

Table 4.9: Replacement KCL fluids with three different concentrations of SD (ex-situ 1.5 g XG)

Additives	**Base Fluid**	**Fluid 5.1**	**Fluid 5.2**	**Fluid 5.3**
Water	350 ml	350 ml	350 ml	350 ml
KCL	25 g	25 g	25 g	25 g
Soda ash	0,52 g	0,52 g	0,52 g	0,52 g
Pac	0.5 g	-	-	-
PolyPac	1,0 g	-	-	-
Barite	143 g	143 g	143 g	143 g
Carbopol	0.1 g	0.1 g	0.1 g	0.1 g
SawDust	**-**	**1 g <71** µm SD	**1 g 125-150** µm SD	**3 g 125-150** µm SD
Xanthan Gum (ex-situ)	1.5 g	1.5 g	1.5 g	1.5 g

The main goal of replacing polymers and adding saw dust in not only economic and ecological side, but also to achieve less filtrate loss compared the equivalent fluids in whole system.

Since Fluids 2.1 and 2.2 in whole bentonite system and Fluid 3.1 in replacement bentonite system gave filtrate loss reduction percentages 7.1%, 14.3% and 7.1% respectively, same concentrations of SD have been chosen to test in the KCL system (Table 4.9). 1.5 g Xanthan Gum has been added in both base KCL and replacement KCL fluids as an ex-situ situation, different than in bentonite situation. Addition of XG supposedly prevents sagging fluid issue in the absence of Pac & PolyPac polymers.

4.2.1.1 Impact of <71 μm SD on the Viscosity of the replacement base fluid

The replacement of polymers and addition of 1 g <71 μm SD result in a decreased shear stress when compared to the reference fluid, as is seen from Figure 4.17. This suggests that the viscosity of the fluid has been affected by the presence of sawdust particles, strengthening molecular interactions between components. Because of the presence of the sawdust particles, the drop in shear stress implies an increase in internal friction inside the fluid.

Additionally, it can be shown that similar tendencies are evident above 100 RPM when looking at the shear stress values at 20°C, 50°C, and 80°C. This implies that the fluid consistently maintains its viscosity across the measured temperature range. The stability suggests that it has thermal stability since it maintains its original form even when heated up. This advantageous trait guarantees constant performance even across a range of heat environments.

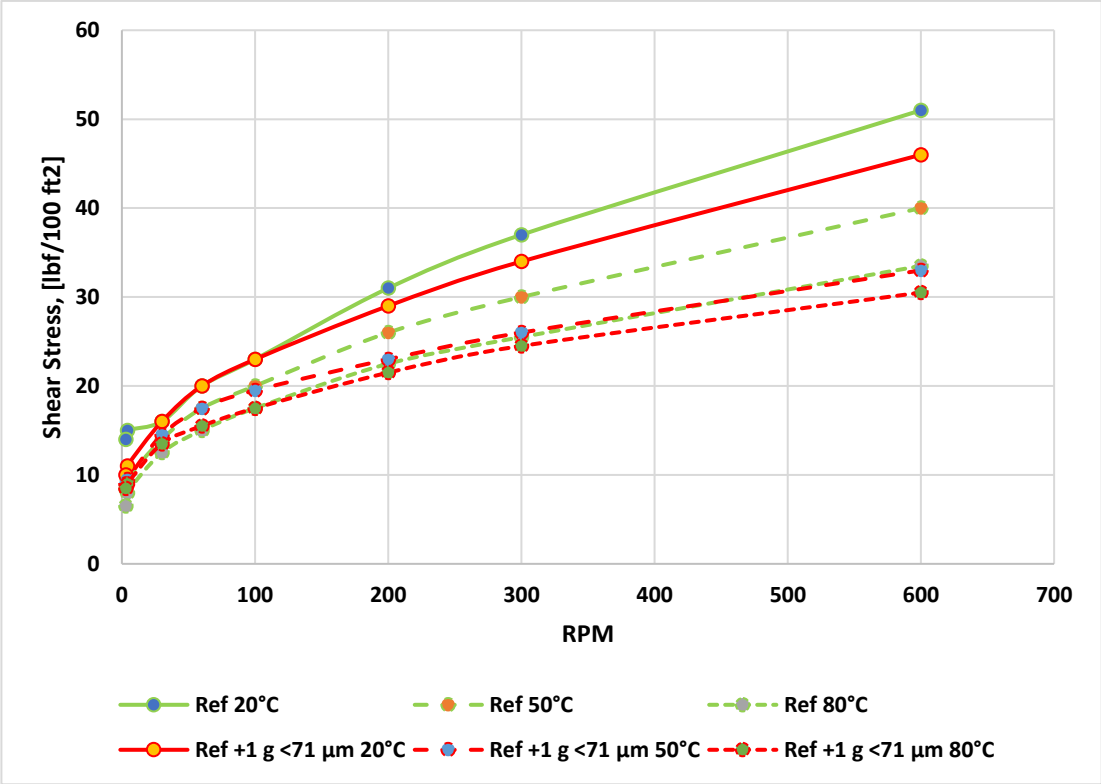

Figure 4.17: Viscometer data at 20°C, 50°C, 80°C for replacement reference and 1 g <71 µm SD fluids

4.2.1.2 Impact of <71 µm SD on the pH and Filtrate loss of the base fluid

Measurements of the fluids' pH values reveal a slight reduction in those levels as compared to the replacement base fluid. In contrast to the base fluid without saw dust, the pH values of the fluids containing saw dust were somewhat lower (Table 4.10). This decrease in pH value primarily impacts wellbore stability and clay swelling control, which regulates the swelling of clay minerals found in the formation.

Table 4.10: pH and FL of replacement Base Fluid and Fluid 5.1 (ex-situ 1.5 g XG)

Drilling Fluid	**Base Fluid**	**Fluid 5.1**
pH	8.90	8.75
Filtrate Loss (ml)	5.6	13.6

Filtrate loss experiment was done with the replacement KCL fluid containing <71 µm SD and the concentration of 1 g. The experiment is conducted for using API filter test rig

filter press equipment. 100 psi pressure was applied on the fluid and 7.5 minutes on the clock was measured, while the impact of <71 µm SD has been studied. While Base Fluid had 5.6 ml filtrate loss, Fluid 5.1 with 1.5 g ex-situ XG showed 13.6 ml filtrate loss in the absence of Pac & PolyPac and replacement of saw dust (Table 4.10).

4.2.1.3 Impact of 125-150 µm SD on the Viscosity of the KCL replacement base fluid

Figure 4.18 immediately represents the decrement of viscosity while adding 125-150 µm SD as original fluid keeps highest shear stress in almost all RPM grades. Meanwhile temperature parameter does its well-known effect onto the viscosity, in the visible example of the case with 80°C (Figure 4.18). On the other hand, 3 g concentration as shown in Figure 4.19, behaves similarly, having negligible difference between 1 g or 3 g dust addition with 125-150 µm sorting level.

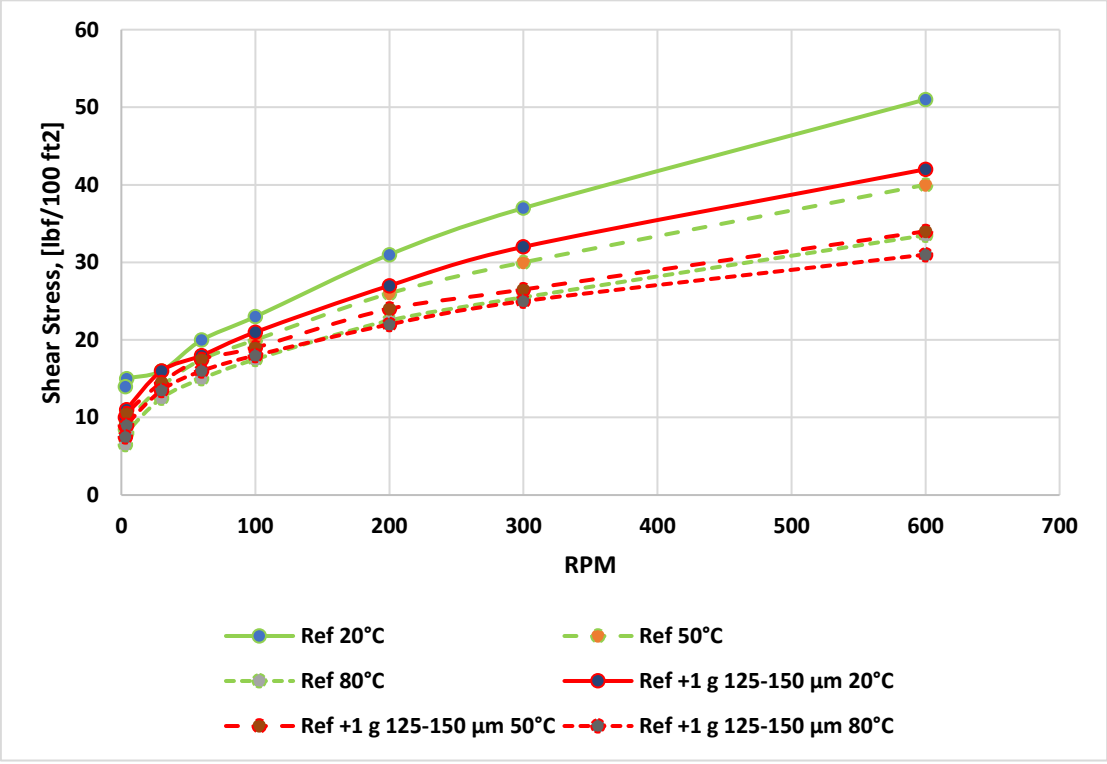

Figure 4.18: Viscometer data at 20°C, 50°C, 80°C for replacement reference and 1 g 125-150 µm SD fluids

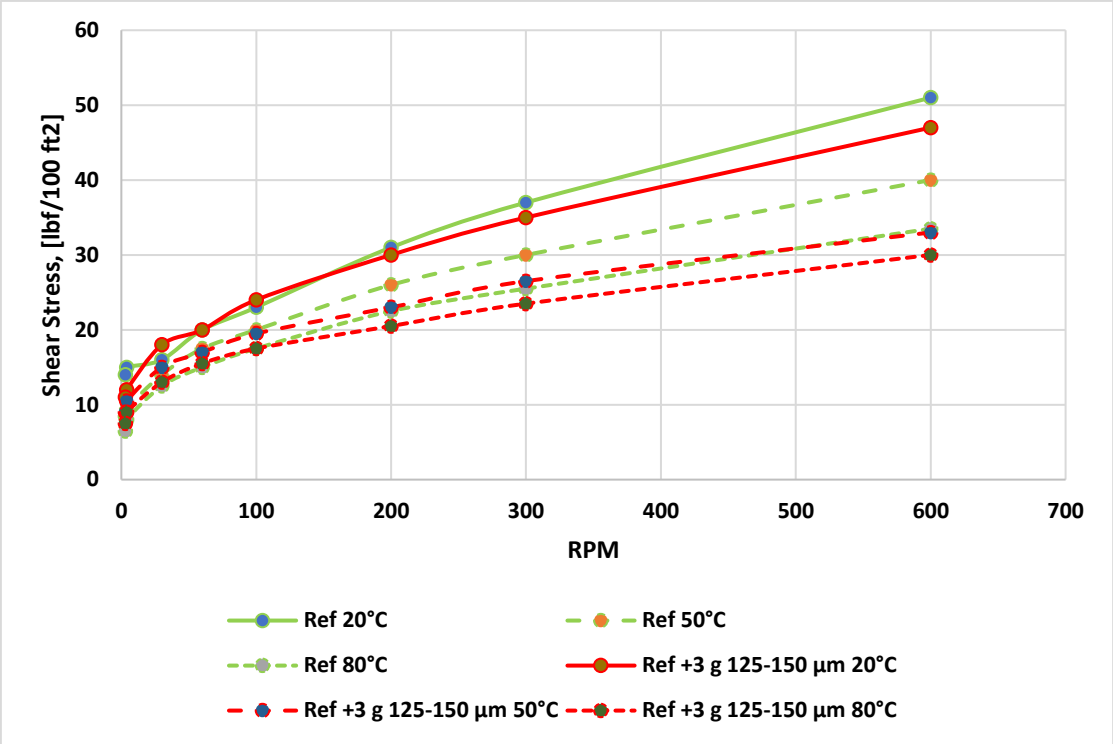

Figure 4.19: Viscometer data at 20°C, 50°C, 80°C for replacement reference and 3 g 125-150 µm SD fluids

Figure 4.20 shows yield stress of sample fluid versus different temperature and concentration cases. Replacement of base fluid with 3 g 125-150 µm SD gave least alteration compared to original fluid. This parameter directly influences to:

- Suspension of Cuttings
- Hole Cleaning Efficiency
- ECD Control
- Pumping and Flowability
- Gel Strength

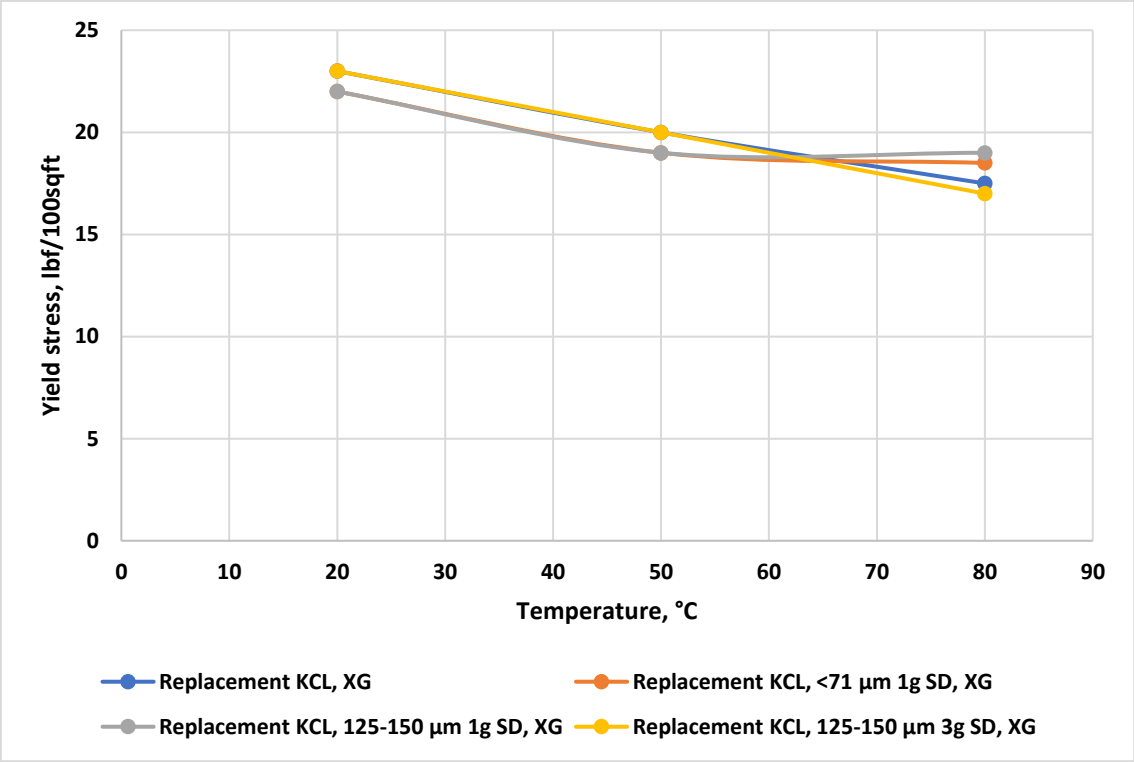

Figure 4.20: Bingham yield stress of replacement KCL fluids at different temperatures

4.2.1.4 Impact of 125-150 µm SD on the pH and Filtrate loss of the KCL replacement base fluid

The fluids' pH levels have been assessed, and the results indicate some decreases in the values as compared to the replacement base fluid. It is important to note that the pH levels of the fluids containing sawdust were marginally lower than those of the base fluid without any sawdust (Table 4.11). The major effects of this pH value decrease on clay swelling control and wellbore stability are the control of the swelling of the clay minerals present in the formation.

Table 4.11: pH and FL of replacement Base Fluid, Fluid 5.2 and Fluid 5.3 (ex-situ 1.5 XG)

Drilling Fluid	**Base Fluid**	**Fluid 5.2** **SD (125-150 µm, 1 g)**	**Fluid 5.3** **SD 125-150 µm, 3 g)**
pH	8.90	8.74	8.55
Filtrate Loss (ml)	5.6	8.8	8.4

After introducing 1.5 g XG, filtrate loss experiment was done with the replacement KCL fluid containing 125-150 μm SD and the concentration of 1 g and 3g. The experiments were conducted for using API filter test rig filter press equipment. 100 psi pressure was applied on the fluid and 7.5 minutes on the clock was measured, while the impact of 125-150 μm SD has been studied. Compared to Base Fluid filtrate loss 5.6 ml, Fluids 5.2 and 5.3 showed slightly higher filtrate loss values of 8.8 ml and 8.4 ml respectively (Table 4.11). On the other hand, pH value made just 5% fluctuation over the options.

Filtrate loss values are slightly higher compared to the base fluid filtrate loss. Considering that 0.5 g Pac and 1.5 g PolyPac have been replaced by small concentration of SD and the filtrate loss percentage increase is only slightly higher, KCL based fluid can be considered as homogenous with SD. In terms of filtrate loss, SD can be used as a replacement material for polymers in order to save cost and conduct the operations in eco-friendly manner.

4.2.2 Effect of 3 g SD in half Pac and PolyPac 1.5 g XG Polymer KCL Base Fluid

The basis for this fluid is a little different than the first KCL fluid. Since the target of KCL replacement fluid was to reduce the filtrate loss below the reference that contains Pac & PolyPac (i.e 5.6ml), 1.5 g amount of ex-situ Xanthan Gum was introduced. The idea behind that is to reduce the occurrence of high filtrate loss values and depicted spurt loss in the beginning of the experiment after removing Pac & PolyPac. Adding Xanthan Gum also directly affects viscosity of the fluid positively.

However, the main objective of this design is to study the replacement of half the amount of polymers rather than replacing whole polymers, as well as to show the performance of SD, according to best KCL system so far, which is fluid 5.3, containing 3 g of 125-150 μm SD. Besides the first fluid design where 0.5 g Pac & 1.0 g PolyPac were in the system, this time their share in the mixture cut by half and reduced to 0.25 g and 0.5 g respectively (Table 4.12):

Table 4.12: Replacement KCL base fluid and fluid 6.1 (half Pac & PPac)

Additives	**Base Fluid**	**Fluid 6.1**
Water	350 ml	350 ml
KCL	25 g	25 g
Soda ash	0,52 g	0,52 g
Pac	0.5 g	0.25
PolyPac	1,0 g	0.5
Barite	143 g	143 g
Carbopol	0.1 g	0.1 g
SawDust	-	**3 g, 125-150**
Xanthan Gum	1.5 g	1.5 g

4.2.2.1 Impact of 125-150 µm SD on the Viscosity of the base fluid

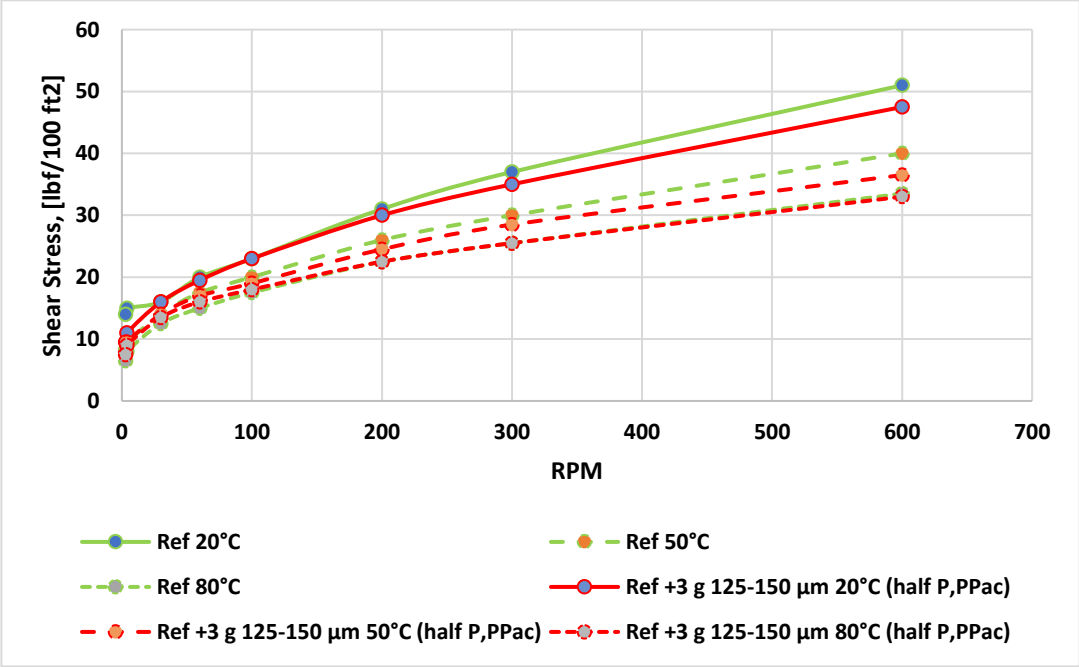

Figure 4.21: Viscometer data at 20°C, 50°C, 80°C for KCL replacement reference and 3 g 125-150 µm SD fluids

Figure 4.21 shows well-known dependency of shear stress from RPM (circulation rate equivalent). In any case, reduction is noticed once SD addition is made. The presence of sawdust particles in the fluid leads to a decrease in shear stress, which indicates an elevation in internal friction within the fluid.

The obtained Bingham yield stress values of replacement KCL reference fluid and fluid with the abovementioned additive with half Pac & PolyPac are demonstrated in Figure 4.22. As it is clearly observed from the graph, fluids show the same tendency in different temperature. The addition of 1 g concentration showed only a slight stability over the reference fluid.

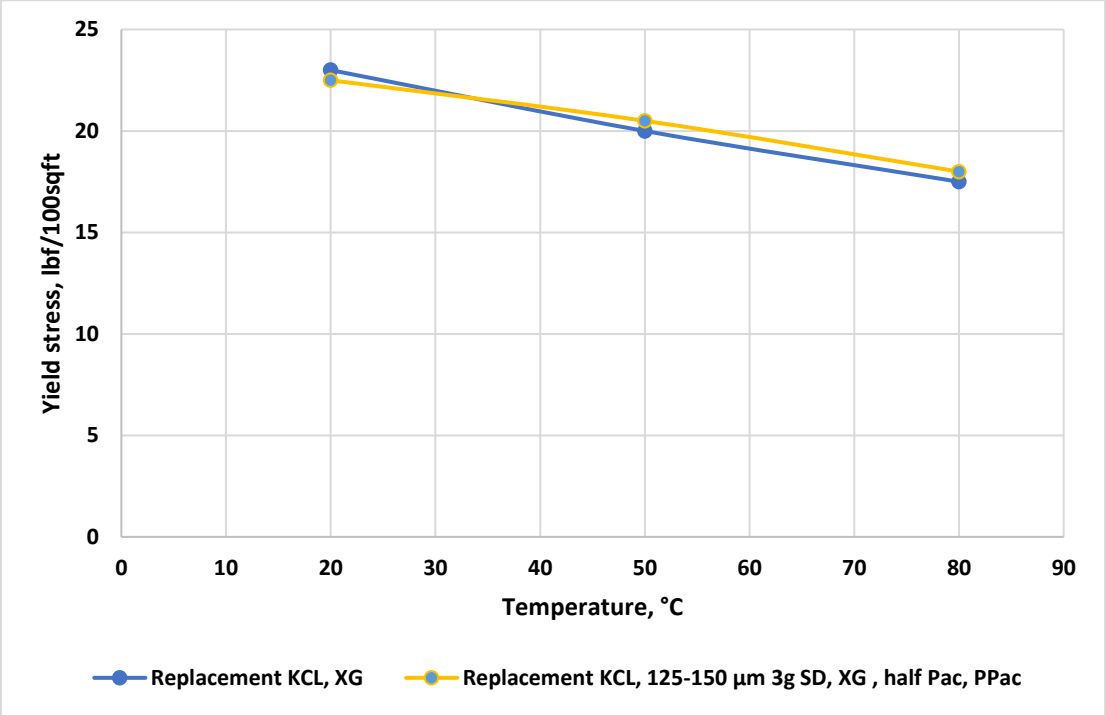

Figure 4.22: Bingham yield stress of replacement reference and half polymer KCL fluids at different temperatures

4.2.2.2 Impact of 125-150 µm SD on the pH and Filtrate loss of the base fluid

pH values of the fluids have been measured and the results show some reductions in the values compared to the replacement base fluid. It's worth noting that the pH values of the fluids containing saw dust were slightly lower compared to the base fluid without saw dust (Table 4.13). This decrement of pH value affects clay swelling and corrosion.

Table 4.13: pH of replacement Base Fluid and Fluid 6.1 (half Pac & PolyPac)

Drilling Fluid	**Base Fluid**	**Fluid 6.1**
pH	8.90	8.61

Filtrate loss experiment was done with the replacement KCL fluid containing 125-150 µm SD and the concentration of 3 g. The experiment is conducted by using API filter test rig filter press equipment. 100 psi pressure was applied on the fluid and 7.5 minutes on the clock was measured, while the impact of 3 g of 125-150 µm SD has been studied. While Base Fluid had 5.6 ml filtrate loss, Fluid 6.1 with half Pac & PolyPac showed 6.6 ml filtrate loss in replacement system (Figure 4.23).

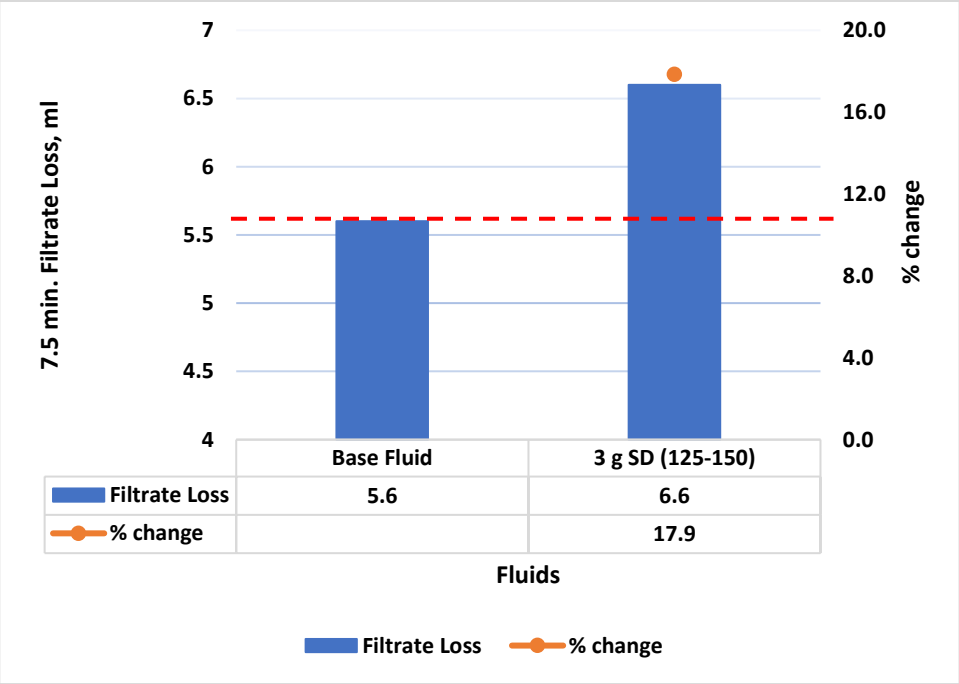

Figure 4.23: FL & FLR of KCL replacement system with half Pac/PolyPac

Figure 4.23 shows that, replacing 0.25 g Pac and 0.5 g PolyPac by 3 g 125-150 µm SD does not provide filtrate loss reduction percentage, but filtrate low increase by just 17.9%. Considering polymer costs, their ecological aspects and performance of saw dust, it can also be considered as a positive result despite the increase in filtrate loss increase.

4.3 Bridging performance of Saw Dust Based Drilling Fluid

Since the drilling formation make up shale dominated formation, it is common practice to drill with KCL based drilling fluids to control shale swelling issues. The KCL based drilling fluid formulated in this thesis is based on the worst-case fluid in sense that the amount of polymers has been reduced and replaced with non-polymeric saw dust. The

idea is to investigate the impact of saw dust. Results showed that the additives of Saw dust compared with the based (more polymeric KCL) drilling fluid exhibited 1.0 ml filtrate loss increment.

The experimental results indicated that the drilling fluid with the inclusion of sawdust exhibited a 1.0 ml increase in filtrate loss compared to the base drilling fluid, which contained more polymers. Additionally, an experimental study was conducted to assess the self-healing performance of the sawdust system when encountering natural fractures, by conducting a lost circulation bridging comparison with the base drilling fluid containing polymeric KCL.

4.3.1 Lost Circulation in the KCL Base Drilling Fluid - with and without SD

The purpose of this experiment is to evaluate the ability of the sawdust system to self-heal by creating natural filter cake when exposed to natural fractures. This is accomplished by comparing the lost circulation bridging between the base drilling fluid containing polymeric KCL and the KCL fluid in which the polymers have been replaced with sawdust. Additionally, studying the average pressure during the bridging experiment can give us the insights of the experiment. The average pressure obtained from the duration of the test provides information about the average pressure during the formation and breakdown of the bridge. Additionally, the mean value is time-averaged over the testing period.

Figure 4.24 shows the bridging test that has been conducted using the Gilson equipment. On the Y-axis is the bridging pressure in megapascals (MPa), and on the X-axis is the time in minutes. The graph depicts 20 minutes of testing the bridging effectiveness of sawdust in a potassium chloride (KCL)-based fluid (Figure 4.24). In the experiment, the slot size is 125 microns, and the particulate size of the sawdust suspended in the water-based drilling fluid is less than 71 microns with 1 g of concentration.

The graph depicts the diagnostic results for both fluids. During the twenty-minute duration of the experiment, both fluids registered a zero MPa bridge pressure. This

indicates that there was no pressure buildup during the test, regardless of whether the fluid contained the conventional polymeric KCL or the sawdust-based alternative.

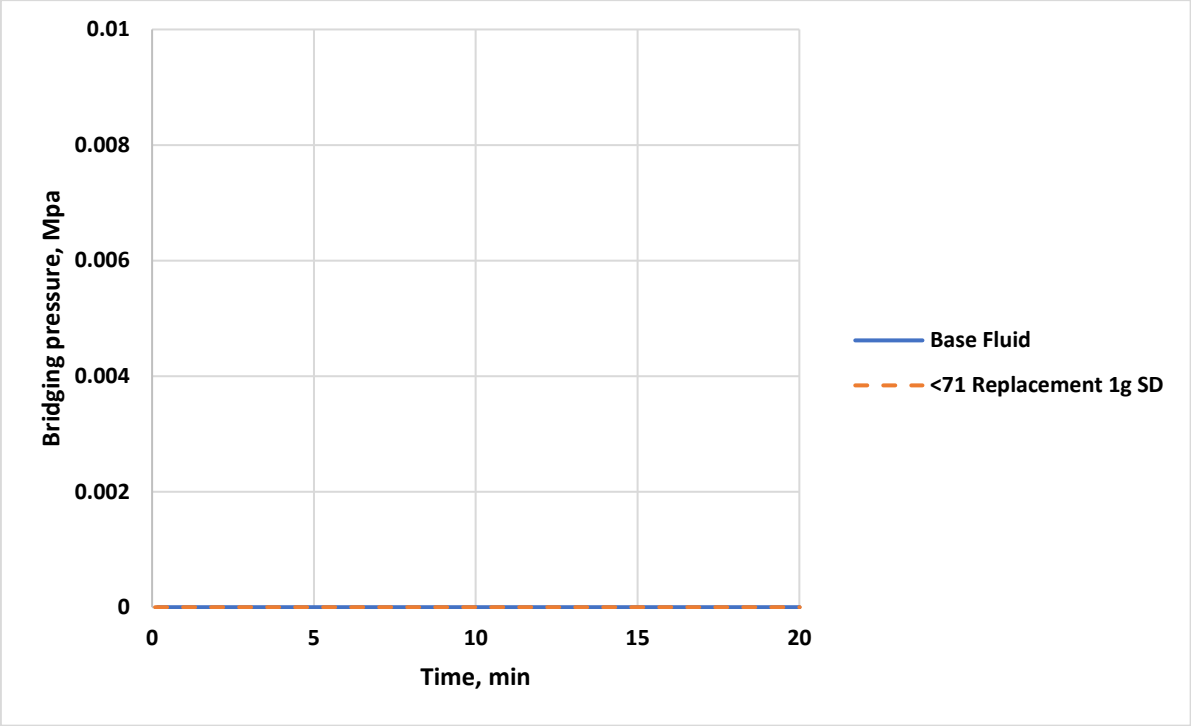

Figure 4.24: Bridging performance of KCL base fluid and 1 g <71 µm replacement fluids in 125-micron slot

The objective of this experiment is to evaluate the self-healing performance of the sawdust system in the presence of natural fractures. This is accomplished by analyzing the lost circulation bridging the KCL fluid in which the polymers have been replaced by sawdust particles between 125 and 150 microns in size. The experiment's slot size is set to 125 microns.

Two distinct sawdust-based fluid concentrations have been evaluated:

1. KCL replacement fluid with a 1 g SD concentration: This concentration of sawdust attained its maximal bridging pressure of 15 MPa in the twenty-first minute, according to the graph. After 20 minutes, it maintained an average bridge pressure of 1.88 MPa.

2. KCL replacement fluid with a 3 g SD concentration: The graph demonstrates that this concentration also experienced pressure buildup, albeit to a lesser extent than the 1-gram concentration.

Figure 4.25 depicts a thirty-minute measurement of the bridging performance of sawdust in a potassium chloride (KCL)-based fluid.

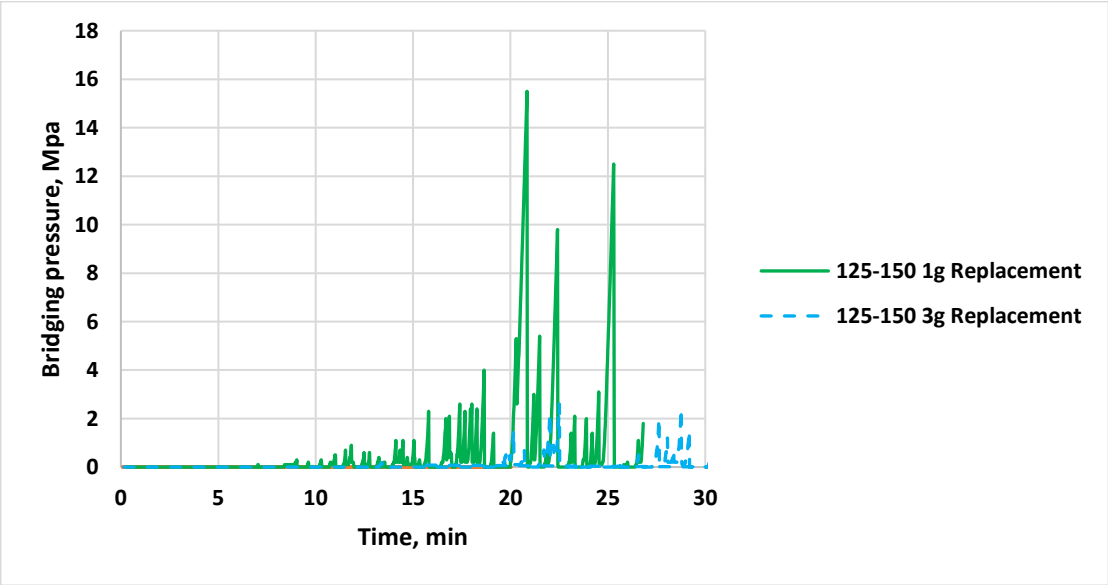

Figure 4.25: Bridging performance of KCL 125-150 µm replacement fluids in 125-micron slot

The pressure build-up observed in the graph is due to the gradual formation of a filter cake (Figure 4.25). As the fluid penetrates through the slot, the sawdust particles in suspension begin to accumulate, forming a filter cake that aids in bridging and sealing the leakage area, thereby mitigating lost circulation issues.

Throughout the testing, the bridging pressure profile displays a zigzag pattern, indicating the intermittent build-up and subsequent collapse of the bridging material over time. This zigzag pattern is frequently observed in bridging experiments and is frequently linked to the dynamic behavior of the bridging particles within the drilling fluid.

Figure 4.26 shows average pressure build-up values for KCL replacement fluids which showed build up values compared to the base fluid. 1 g SD performance as a replacement

additive showed 0.6 MPa build-up value, while 3 g SD performance showed 0.08 MPa on average throughout the test period. One can suggest that SD particles of 125-150 microns are acting as LCM in a 125-micron slot.

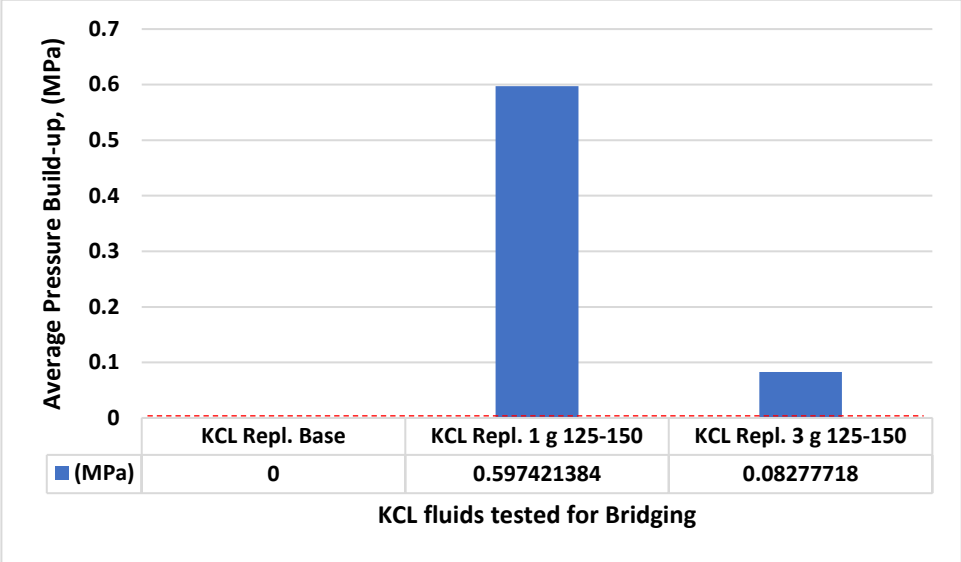

Figure 4.26: Average Pressure Build-up for KCL fluids (with Polymers)

To evaluate the impact of the sawdust in KCL fluid and its performance in bridging system, Fluid 6.1 with half Pac & PolyPac with ex-situ 1.5 g XG was also subjected to be experimented in the presence of natural fractures. This is accomplished by comparing the lost circulation bridging the KCL fluid in which the polymers have been replaced by sawdust particles between 125 and 150 microns in size. The experiment's slot size is set to 125 microns.

The pressure increase observed in the graph is due to the gradual formation of a filter cake (Figure 4.27). As the fluid penetrates through the slot, the sawdust particles in suspension begin to accumulate, forming a filter cake that aids in bridging and sealing the leakage area, thereby mitigating lost circulation issues.

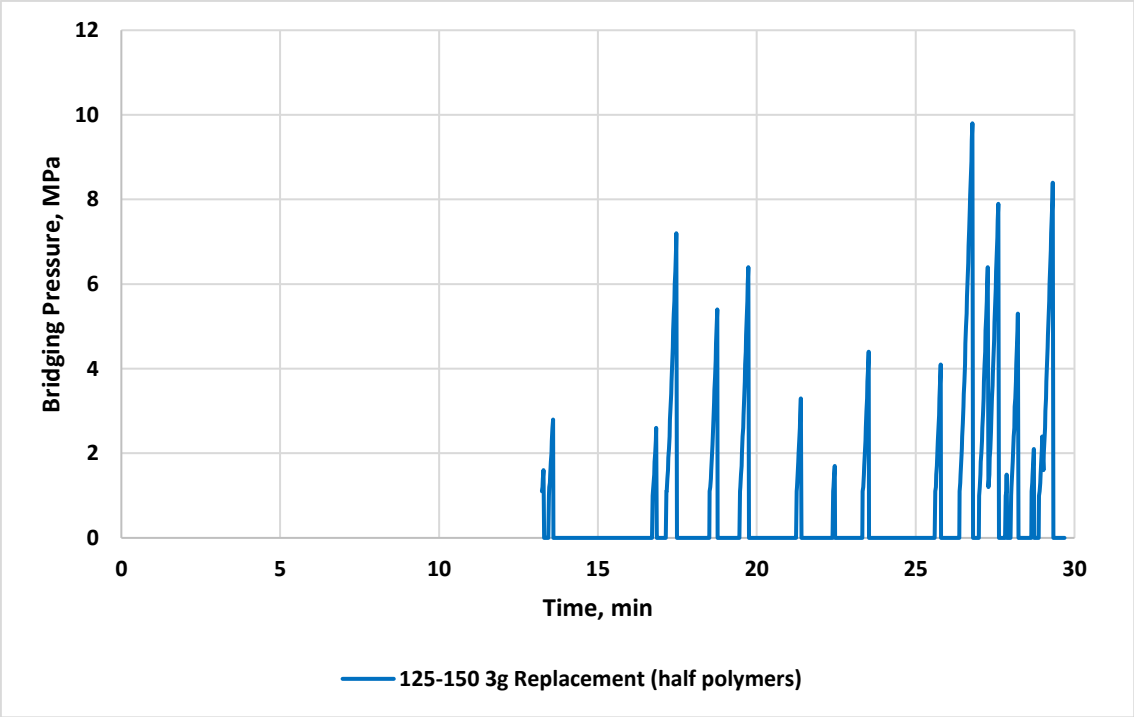

Figure 4.27: Bridging performance of KCL 3g 125-150 µm replacement fluid in 125-micron slot (half polymer)

Throughout the testing, the bridging pressure profile displays a zigzag pattern, indicating the intermittent build-up and subsequent collapse of the bridging material over time. As it is seen from Figure 4.27, it took around 13 minutes for the fluid to form an initial impermeable filter cake. This concentration of sawdust with half Pac & PolyPac attained its maximal bridging pressure of 15.5 MPa in the twenty-first minute, according to the graph. This zigzag pattern is frequently observed in bridging experiments and is frequently linked to the dynamic behavior of the bridging particles within the drilling fluid.

The evaluation of the average pressure build-up values of fluids and the performance of sawdust have been done in the Figure 4.28.

In a 30-minute span it maintained an average bridging pressure of 0.48 MPa. The average build-up for the abovementioned fluid is approximately 6 times higher than the fluid with Pac & PolyPac (Figure 4.28).

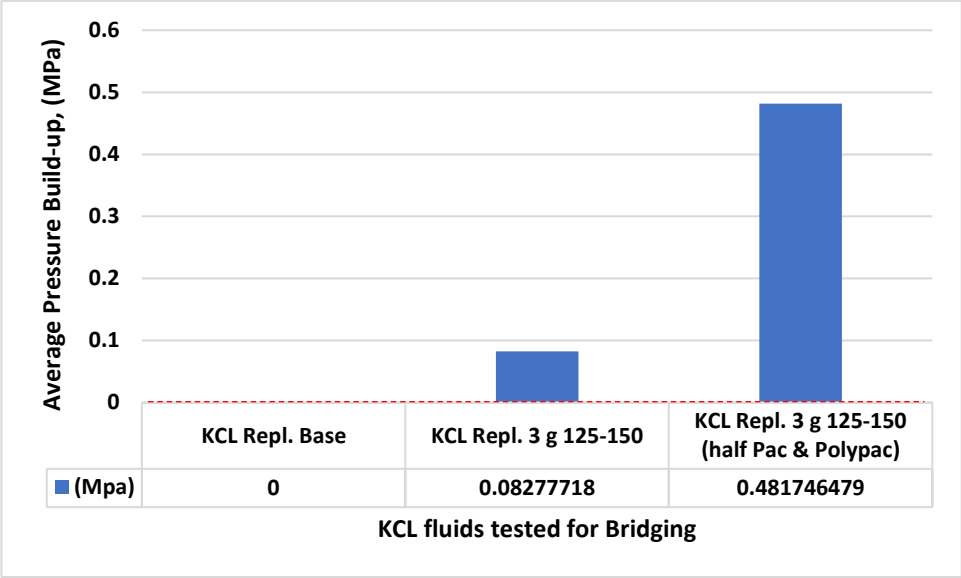

Figure 4.28: Average Pressure Build-up for KCL fluids (with full, no and half Pac and PolyPac)

4.3.2 Lost Circulation in the Bentonite Based Drilling Fluid-with and without SD

The purpose of this experiment is to evaluate the ability of the sawdust system to self-heal by creating natural filter cake when exposed to natural fractures. This is accomplished by comparing the lost circulation bridging between the base drilling fluid containing Bentonite and the Bentonite fluid in which the polymers have been replaced with sawdust. Additionally, studying the average pressure during the bridging experiment can give us the insights of the experiment. The average pressure obtained from the duration of the test provides information about the average pressure during the formation and breakdown of the bridge. Additionally, the mean value is time-averaged over the testing period.

Figure 4.29 shows the bridging test that has been conducted using the Gilson equipment. On the Y-axis is the bridging pressure in megapascals (MPa), and on the X-axis is the time in minutes. The graph depicts 20 minutes of testing the bridging effectiveness of sawdust in a Bentonite-based fluid (Figure 4.29). In the experiment, the slot size is 125 microns, and the particulate size of the sawdust suspended in the water-based drilling fluid is less than 71 microns with 1 g of concentration.

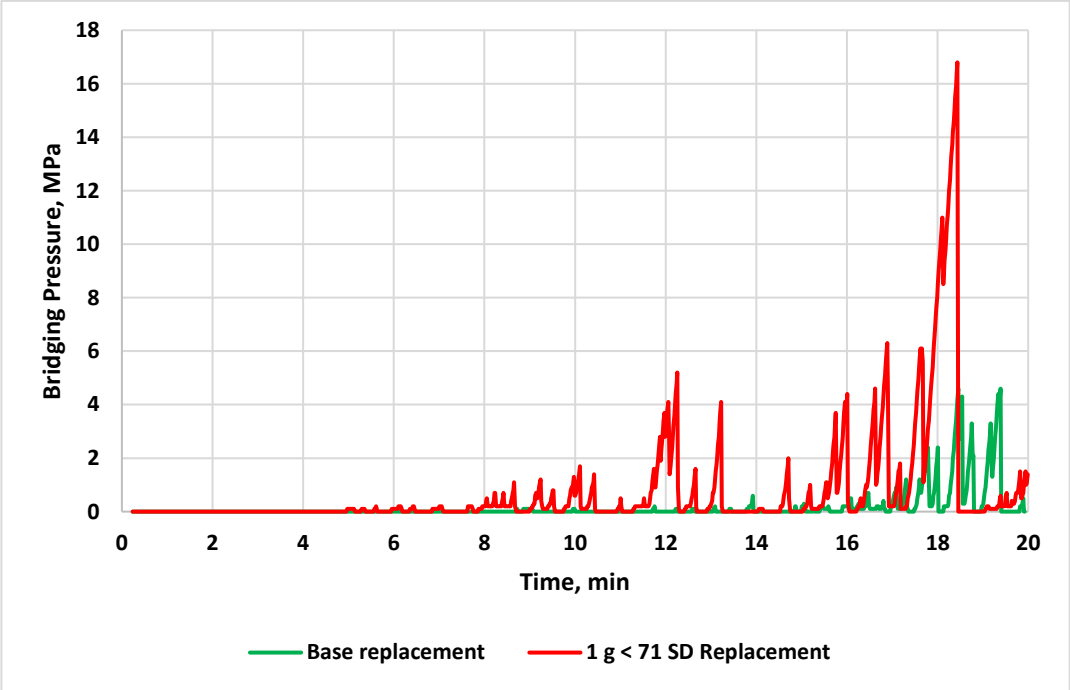

Figure 4.29: Bridging performance of Bentonite base fluid and 1 g <71 µm SD replacement fluids in 125-micron slot

The graph depicts the diagnostic results for both fluids. Base fluid showed only a little pressure build-up during the twenty-minute duration of the experiment, reaching maximum of 4.5 MPa. On the other hand, replacing Pac and PolyPac with 1 g <71 µm SD showed an improvement in the bridging pressure, as overall trend was higher than the bas fluid. The maximum build up was 17 MPa for replacement fluid, while an average value after the build-up started was 1.24 MPa (after 7 minutes), (Figure 4.29). It is around 1 MPa higher than the same span for the base fluid (0.24 MPa after 7 minutes).

The evaluation of the average pressure build-up values of fluids and the performance of sawdust have been done in the Figure 4.30.

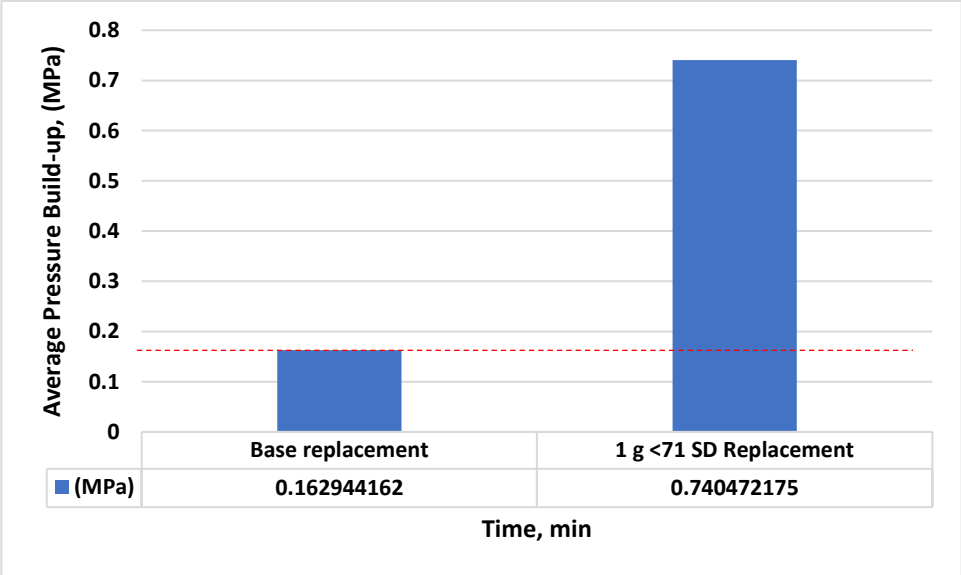

Figure 4.30: Average Pressure Build-up for Bentonite replacement fluids

In a whole span, replacement fluid with 1 g concentration showed 0.74 MPa average build-up value while base fluid had 0.16 MPa (Figure 4.30). The results prove that saw dust performance for bridging and preventing loss of circulation by creating filter cake is inevitable, despite the fluctuating trends.

These findings suggest that the inclusion of sawdust as a replacement for Pac and PolyPac in the drilling fluid formulation contributes to enhanced bridging pressure and demonstrates the potential of sawdust as an effective bridging agent for preventing circulation loss in drilling operations.

Figure 4.31 shows bridging performance of whole base bentonite fluid and performance after adding two different concentrations of 125-150 μm SD. After around 7 minutes into the experiment, pressure build up starts for both fluids with saw dust on it while base fluid was still losing the circulation until minute 9. Overall, what stands out from the chart is that addition of 1 g and 3 g concentrations showed slightly more build-up sections in 20 minutes span compared to the base fluid (Figure 4.31).

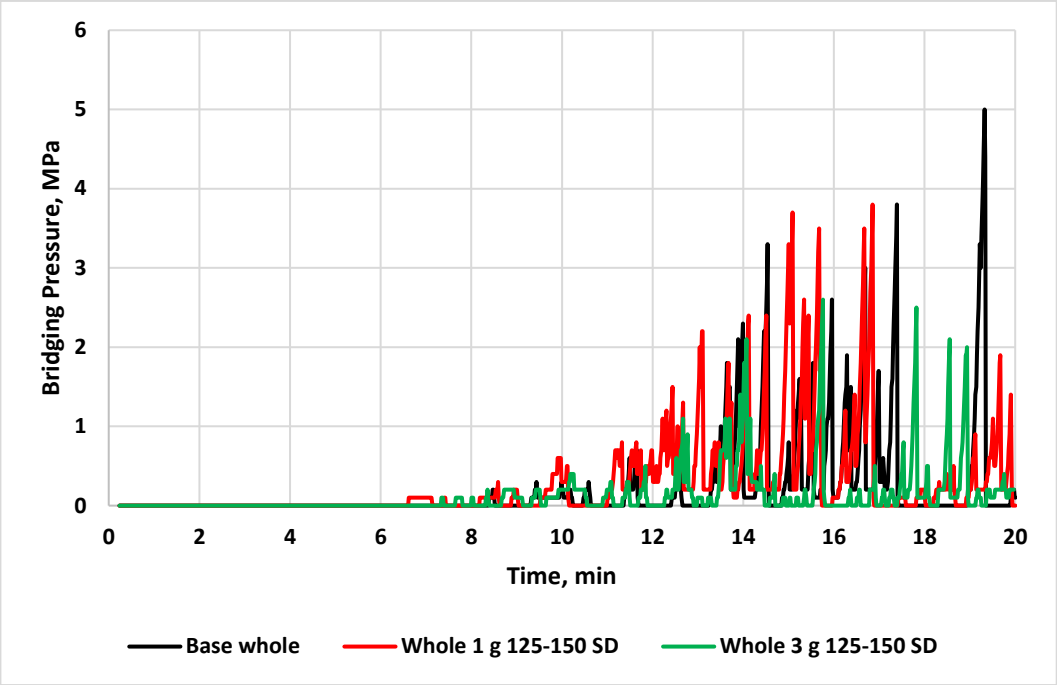

Figure 4.31: Bridging performance of Whole Bentonite base and 125-150 µm SD fluids in 125-micron slot

Figure 4.32 shows average pressure build-up values for the abovementioned whole fluids. 1 g addition of 125-150 µm SD as a whole additive builds up more pressure than whole base fluid. It also suggests that, 125-150 µm particle sized SD creates bonds and easily generates filter cake in 125-micron slot.

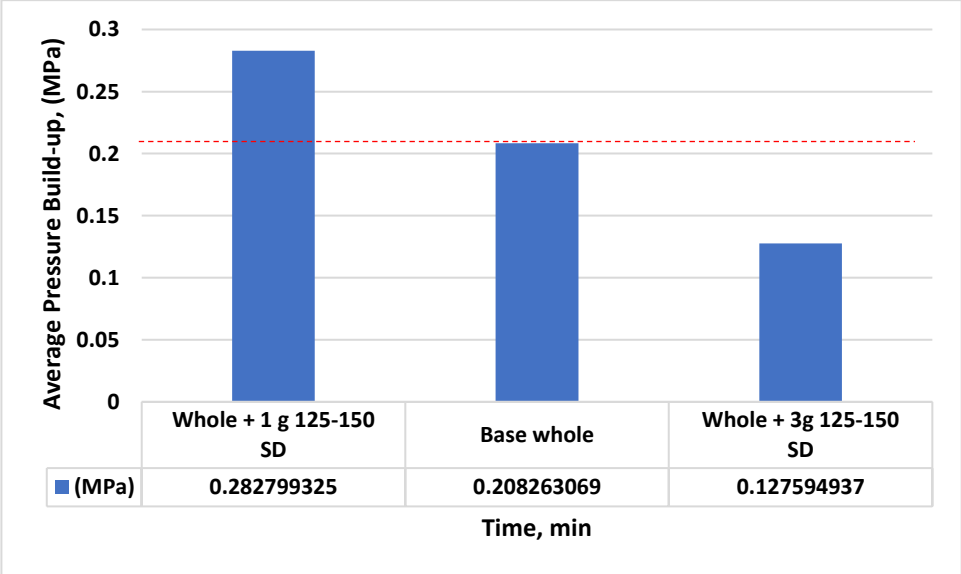

Figure 4.32: Average Pressure Build-up for Bentonite whole fluids

The same fluid in whole bentonite system has been studied closely and decision was made to add industrial quartz to the system and check the bridging again, but this time in a bigger slot size of 250 microns as quartz is added. The main objective behind the idea was to improve the performance of 3 g 125-150 µ SD whole fluid and making it have more average pressure build-up values than the base fluid. 190 ml of each fluid were mixed with 2% equivalent of quartz (3.8 g) and Gilson equipment has been employed for another test.

Figure 4.33 depicts the saw dust + quartz performance as a Lost Circulation Material (LCM) together in 250-micron test slot. Results show that since the start of the experiment all the fluids started to show pressure build-up.

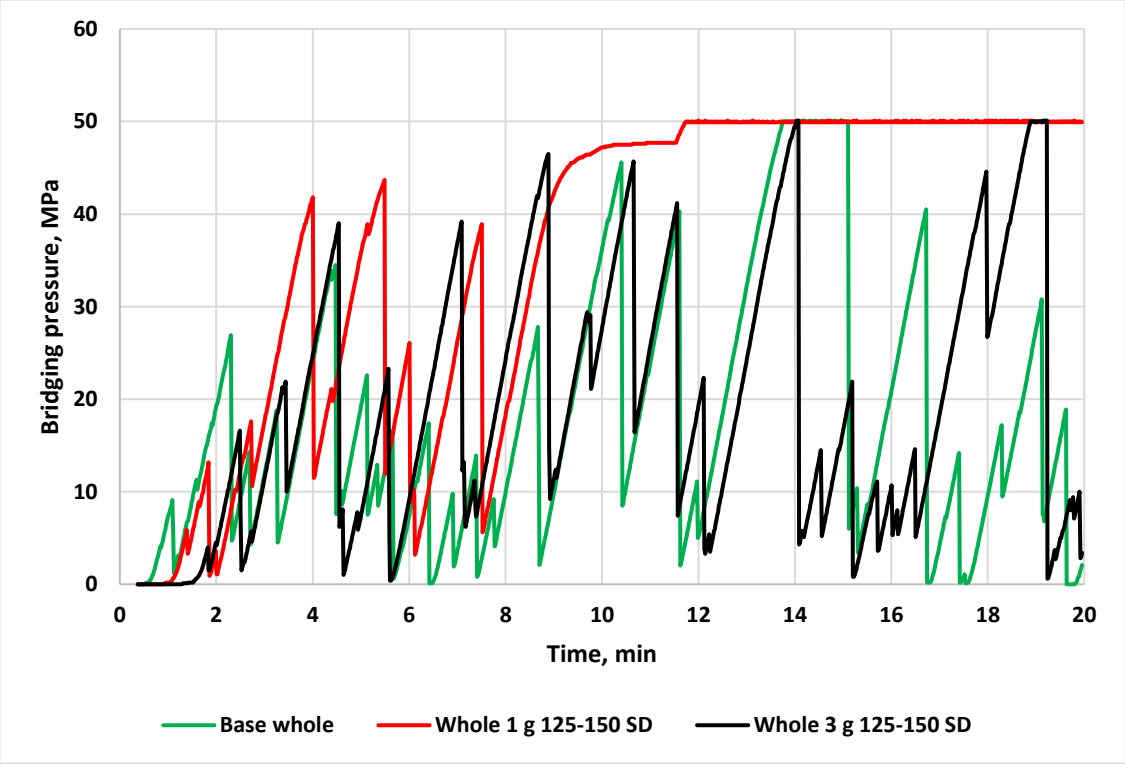

Figure 4.33: Bridging performance of Whole Bentonite base and 125-150 µm SD fluids with quartz added in 250-micron slot

Figure 4.33 shows that, after achieving stable build up pressure at around 50 MPa, but it might be because of the limits set in the Gilson equipment. The equipment itself has 50

MPa reading capacity, but it is suggested that the numbers could have been higher if the reading were able to be read in greater values.

While base fluid showed an average of 18 MPa build-up pressure, 3 g concentration of SD improved an average and have recorded 19 MPa (Figure 4.34). The greater achievement has been recorded in 1 g concentration of SD in 125–150-micron size, having 36 MPa average and creating proper filter cake without collapsing after 11 minutes (Figure 4.34).

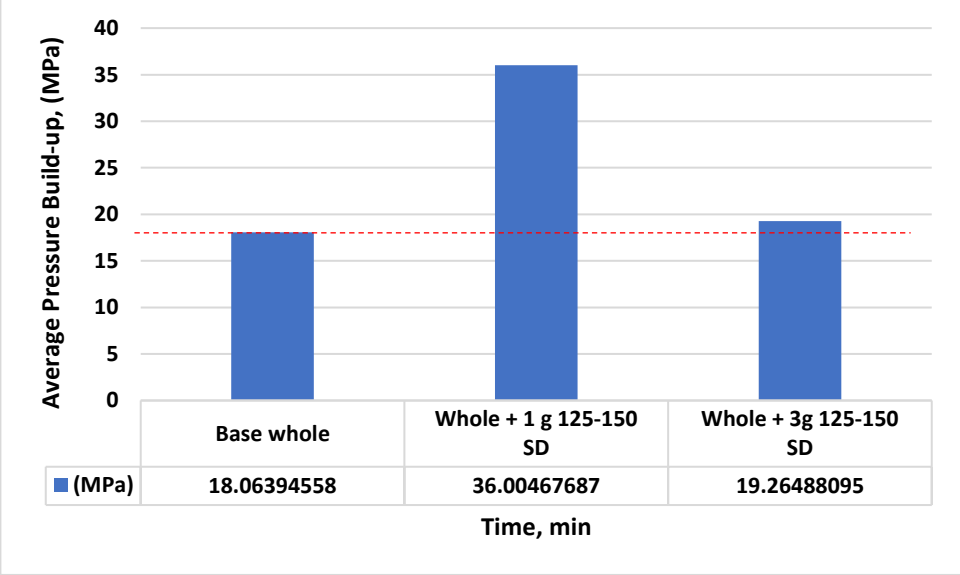

Figure 4.34: Average Pressure Build-up for Bentonite whole fluids with quartz added

Quartz, however, together with SD in both concentrations worked as a proper LCM and showed zig-zag build-ups over the 20 minutes span of experiment. The experiment was conducted in 250-micron size slot compared to the previous experiment without quartz, where the slot was 125 microns in size. It is suggested that the compatibility of quartz and SD provides positive synergy as LCM materials, creating proper filter cake.

4.4 Viscoelasticity of drilling fluids

The amplitude sweeps tests were conducted on the drilling fluids blended with and without the saw dust. The viscoelastic properties of the drilling fluids describe the internal

structure of the drilling fluids up on oscillatory dynamic loading. The gel structure has direct relation with the drilling fluid's solid suspension behavior.

4.4.1 Effect of SD in whole and polymer replacement bentonite drilling fluids

Figure 4.35 shows the oscillatory amplitude test results of the bentonite drilling fluids. As shown in the figure, the saw dust free based fluid possesses the higher storage and loss moduli. However, for better evaluation, the viscoelastic parameters are quantified below. The main parameters used for the assessment are the linear viscoelastic zone, the yield point and the flow point, the strains at the yield point and at the flow point. The precise values of these parameters are extracted using interpolation technique.

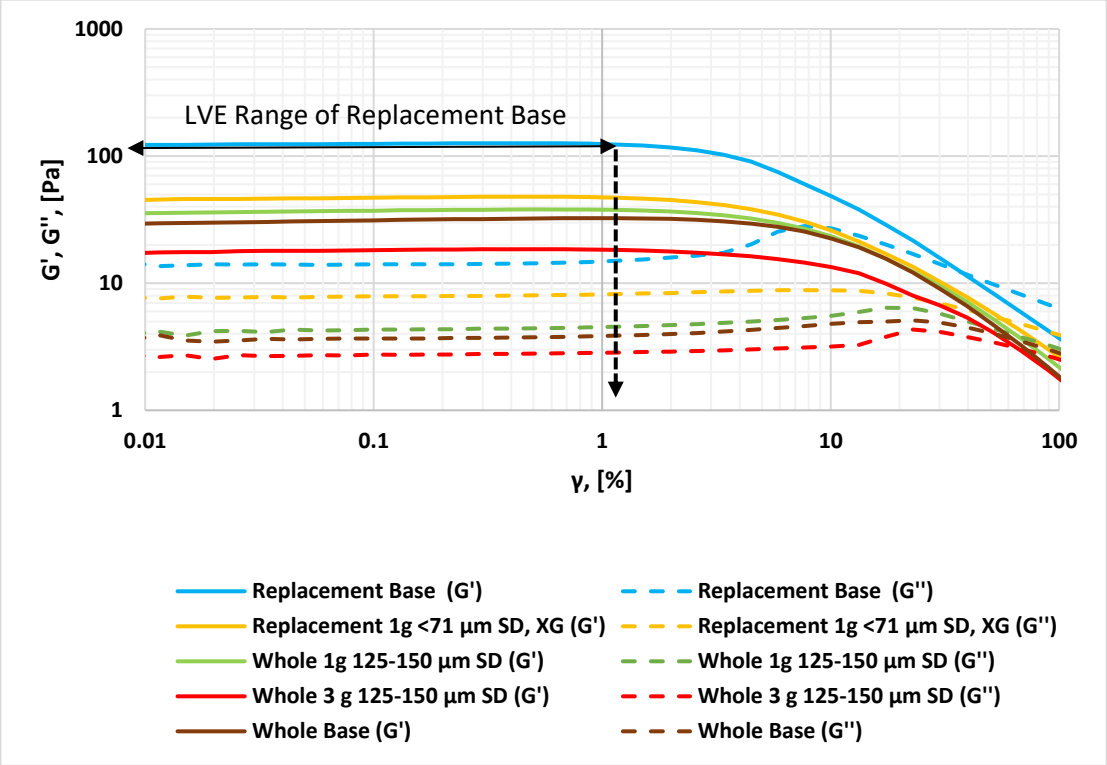

Figure 4.35: Amplitude sweep results for Bentonite fluids

Table 4.14 and Table 4.15 provide the summary of the viscoelastic fluids obtained from whole and polymer replacement fluids blended with saw dust, respectively. Results show that the addition of 1 g and 3 g SD on the whole bentonite drilling fluid increased and decreased the shear yield stress and the shear flow, respectively. On the other hand, on the polymer replacement system, the additive of 1 g SD reduced both shear stress.

Table 4.14: Summary of parameters obtained from the whole Bentonite fluids

Drillig fluid	Shear yield	Shear flow	Stain yield	Strain flow
Whole Base	0.6395	3.227376762	1.98	62.683
Bent whole. 125-150 1g SD, XG	0.93674	3.575683746	2.6	65.695
Bent whole. 125-150 3g SD, XG	0.28	2.861493151	1.51	65.374

Table 4.15: Summary of parameters obtained from the Bentonite Replacement fluids

Drillig fluid	Shear yield	Shear flow	Stain yield	Strain flow
Bentonite Repl. Base	1.8432	6.440123529	1.51	37.741
Bent Repl. 71 1g SD	0.55079	4.1029	1.15	56.857

4.4.2 Effect of SD in polymer replacement KCL drilling fluids

The amplitude sweep responses of the KCL based drilling fluid are depicted in Figure 4.36. These responses provide valuable insights into the rheological behavior of the fluid system. A comparison between the Bentonite fluid system and the KCL based drilling fluid system reveals interesting findings. The storage moduli of the systems blended with sawdust (SD) exhibited higher values than the reference drilling fluid that did not contain sawdust. The observed increase in storage moduli suggests that the incorporation of sawdust in the drilling fluid positively impacts its structural stability and resistance to deformation. The higher storage moduli of the SD blended systems indicate enhanced elasticity and rigidity, which can be beneficial in preventing wellbore instability and maintaining wellbore integrity during drilling operations. These findings highlight the potential of utilizing sawdust as a promising additive in KCL based drilling fluids to improve their mechanical properties and overall performance. Further investigations are warranted to explore the specific mechanisms by which the presence of sawdust contributes to the increased storage moduli of the drilling fluid, allowing for a more comprehensive understanding of its effectiveness and potential applications.

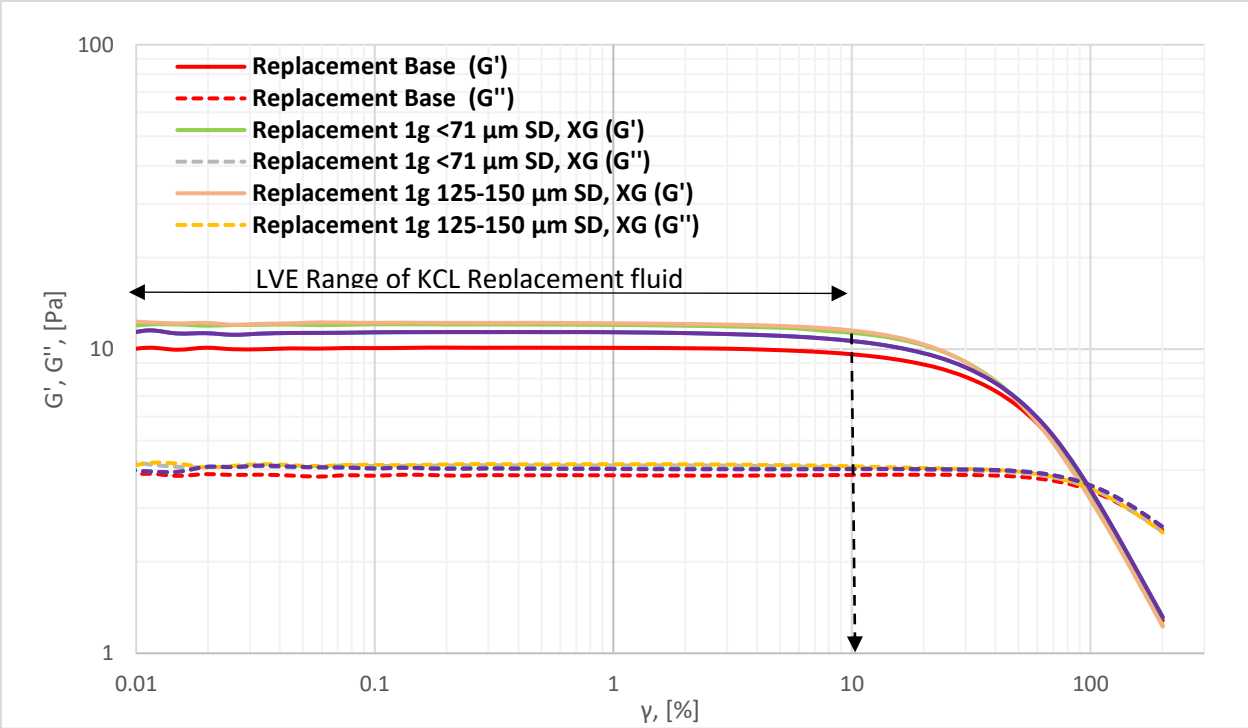

Figure 4.36: Amplitude sweep results for KCL fluids

Unlike the Bentonite drilling fluid, the addition of saw dust in the KCL drilling fluid, the additives increase the shear yield stress. But the impact on the shear flow stress is not significant. On the other hand, the additives increase the yield shear rate by over 2.4%-4.3%.

Table 4.16: Summary of parameters obtained from the amplitude sweeps of KCL fluids

Drilling Fluids	Shear yield stress	Flow shear stress	Shear rate yield	Shear rate flow
KCl Base	0.366	4.736	3.410	97.711
KCl Repl. 71 1g SD, XG	0.728	4.685	5.880	93.679
KCl Repl. 125-150 1g SD, XG	0.738	4.629	5.880	91.992
KCl Repl. 125-150 3g SD, XG	0.760	4.751	5.880	92.558
KCl Repl. Half Pac, PPac, 125-150 3g SD, XG	0.899	4.916	7.710	97.319

It is visible that last version of mixture (KCl Repl. Half Pac, PPac, 125-150 3g SD, XG) behaved remarkably different compared to others having a slight reduction in Shear rate flow from 97.711 to 97.319.

5 Modelling and Simulation Study

This chapter present the modelling and performance simulation studies of the best drilling fluids formulated in Chapter 4. The hydraulics simulation evaluates the equivalent circulating density (ECD). The rheological models are also used to calculate the rheological parameters are also modelled with rheological models to determine the rheological parameters.

5.1 Rheological modeling

The non-Newtonian rheological models presented in section 2.4 are used for the rheological parameters' determinations. The models are [19]:

1. Bingham Plastic model.
2. Power law model
3. Unified model
4. Herschel Buckley model.
5. Robertson stiff model.

The selection of the drilling fluids for the rheological modelling is based on the best SD performance. As shown in section 4.1, the following fluids are selected.
Table 5.1 shows the drilling fluid formulation based on polymer replacement method. Results shows that the addition of 1 g SD replacing 0.5 g Pac and 1.0 g PolyPac, reduced the filtrate loss from 5.6 to 5.2, which is 7.14 % reduction.

Table 5.1: Replacement bentonite fluid with 1 g <71 µm SD

Additives	**Base Fluid**	**Fluid 3.1**
Water	350 ml	350 ml
Soda ash	3.2 g	3.2 g
Pac	0.5 g	-
PolyPac	1.0 g	-
Bentonite	10 g	10 g
Barite	150 g	150 g
Carbopol	0.08 g	0.08 g
Antifoam	5 drops	5 drops
SawDust <71 µm	**-**	**1 g**
Xanthan Gum	0.5 g	0.5 g
Filtrate loss	**5.6ml**	**5.2 ml**

Unlike polymer replacement method, Table 5.2 shows the drilling fluid formulation based the addition of saw dust on the based drilling fluid that contains both 0.5 g Pac and 1.0 g PolyPac. Results showed that the 3 g SD (125-150 μm) reduced the filtrate loss by from 3.5 to 3.0, which is 14.3 % reduction.

Table 5.2: Whole bentonite fluid with 3 g 125-150 μm SD

Additives	**Base Fluid**	**Fluid 2.2**
Water	350 ml	350 ml
Soda ash	3.2 g	3.2 g
Pac	0.5 g	0.5 g
PolyPac	1.0 g	1.0 g
Bentonite	10 g	10 g
Barite	150 g	150 g
Carbopol	0.08 g	0.08 g
SawDust 125-150 μm	**-**	**3 g**
Filtrate loss	**3.5**	**3.0**

In both cases Bentonite plays a crucial role for essential values: fluid loss control, lubrication, borehole stability, and contamination control.

In addition to filtrate loss, the drilling fluids are modelled by the rheology models presented in section 2.4 and the calculated rheological parameters along with the % change due to the additives are presented in Table 5.3 and Table 5.4.

5.1.1 Saw dust (1 g, <71 μm) in polymer replacement bentonite fluid

The viscometer data of the sawdust-based bentonite drilling fluid modeled with the non-Newtonian fluids. The comparison of the model predicted with the measurements are shown in Figure 5.1 and Figure 5.2. As shown the Herschel-Bulkley, Unified and the Robertson and Stiff models fits most of the dataset better than the Bingham Plastic and the Power law models. Table 5.3 shows the summary of the models generated.

Table 5.3: Summary of Rheological models for 1 g <71 SD based bentonite fluid

Model	Equation
Herschel-Bulkley	8.391 + 0.547*γ^0.566
Unified	8.536+0.477*γ^0.587
Power Law	6.296*γ^0.232
Bingham	0.024*γ+12.569
Robertson and Stiff	3.094*(23.629+γ)^0.345

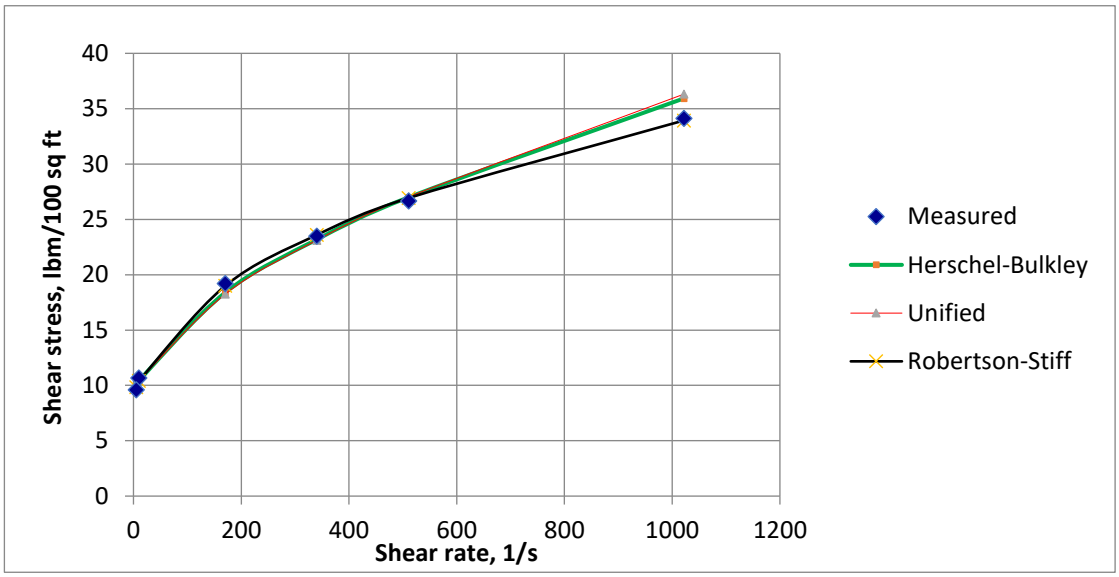

Figure 5.1: Comparison of Herschel-Bulkley, Unified and Robertson and Stiff models with 1 g <71 µm SD blended drilling fluids measurement

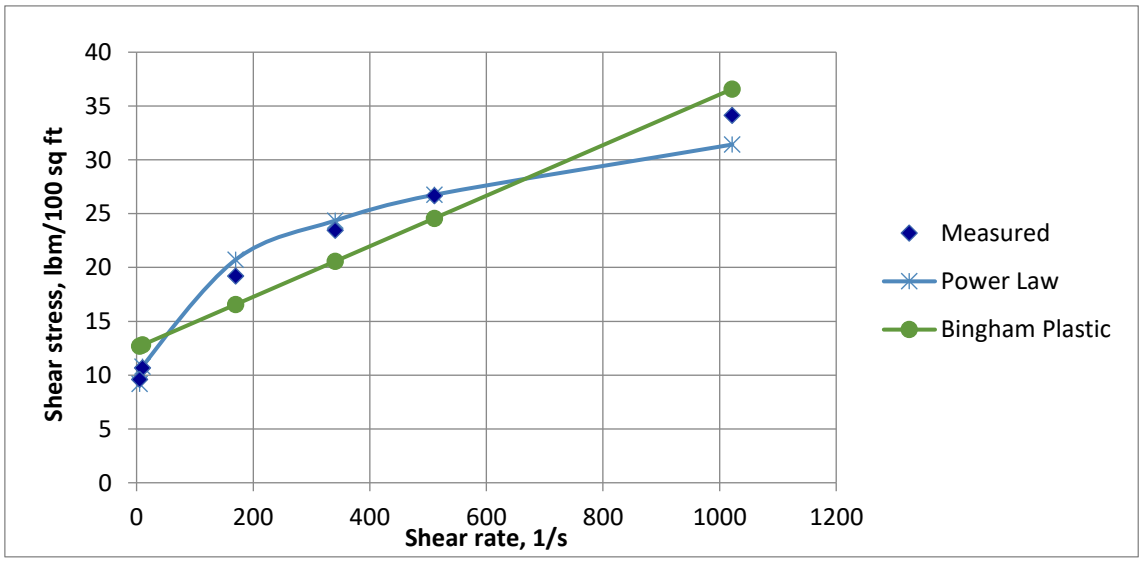

Figure 5.2: Comparison of Bingham Plastic and Power law with 1 g <71 µm SD blended drilling fluids measurement

To analyze the percentile error deviation between the models, the measurements are calculated as the absolute mean of sum of the dataset. The comparison results shows that the Herschel-Bulkley, Unified, Power law and the Robertson-Stiff models cumulative mean error deviation records in the following order:

- Roberson and Stiff (1.4) > Herschel Bulkley (2.7) > Unified (3.1) > Power law (4.2) > Bingham Plastic (15.5)

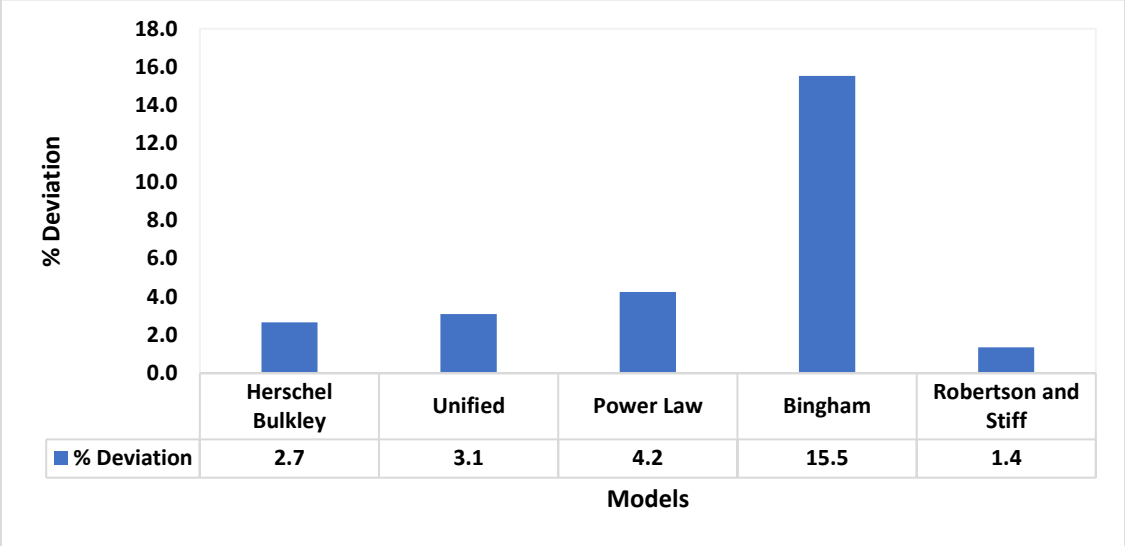

Figure 5.3: Error deviation of models with 1 g <71 µm SD blended drilling fluids measurement

5.1.2 Saw dust (3 g, 125-150 mm) in whole Bentonite fluid

Similarly, the 3g 125-150 µm SD blended drilling fluid modeled, and the results are provided in Table 5.4 below. The model prediction data are also compared with the measurement and the results are displayed in Figure 5.4 and Figure 5.5. As shown, the Hershel-Bulkley, Unified and the Robertson-Stiff models describe the drilling fluids viscosity property.

Table 5.4: Summary of Rheological models for 3 g 125-150 SD based bentonite fluid

Model	Equation
Herschel-Bulkley	7.630 + 0.1159*γ^0.8092
Unified	7.469+0.1687*γ^0.7493
Power Law	4.577*γ^0.2751
Bingham	0.0298*γ+9.149
Robertson and Stiff	0.46*(89.9973+γ)^0.6291

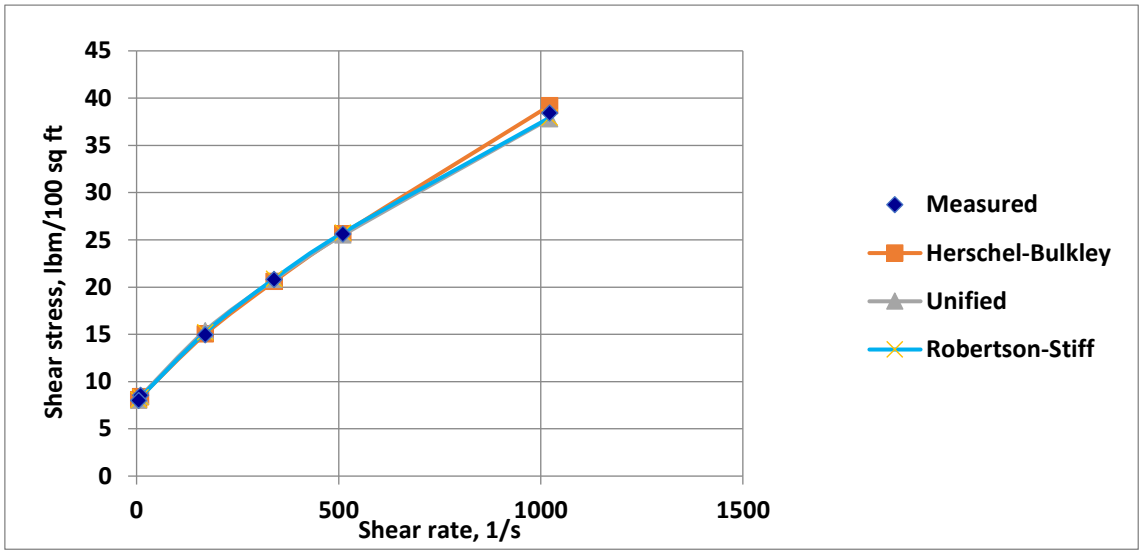

Figure 5.4: Comparison of Herschel-Bulkley, Unified and Robertson-Stiff models with 3 g 125-150 µm SD blended drilling fluids measurement

On the other hand, both the Power Law and the Bingham Plastic models exhibited higher deviation from the measurement. It is interesting to note that the Power Law for the <71µm SD based drilling fluid prediction showed less deviation and was better than the Bingham plastic. But for the 125-150 µm SD, the Power Law model prediction was the worst. This shows that the rheological models' prediction is not consistent.

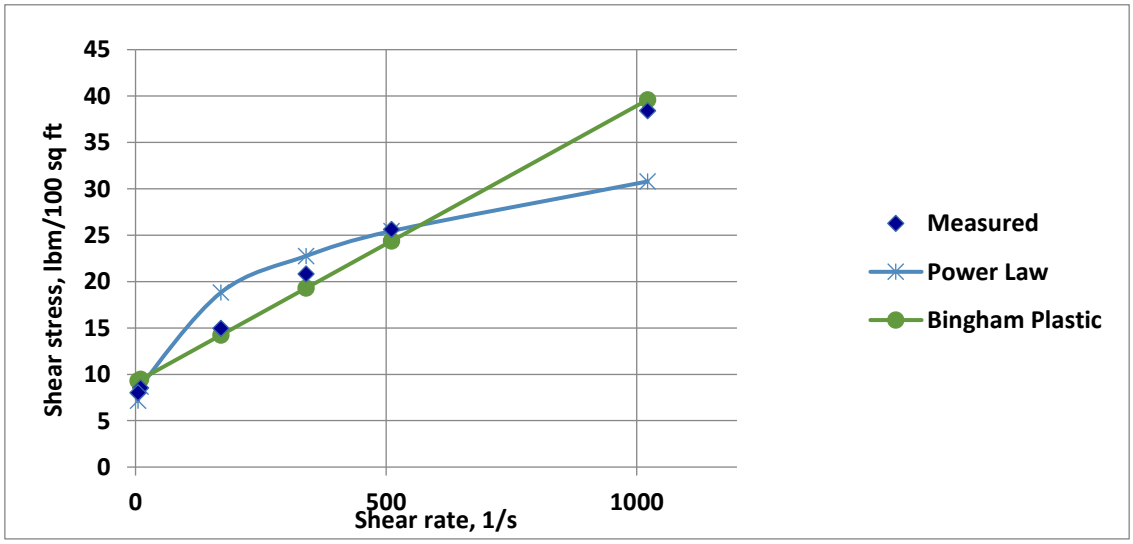

Figure 5.5: Comparison of Bingham Plastic and Power law with 125-150 µm blended drilling fluids measurement

Figure 5.6 shows the calculated error deviations obtained from the models. Results shows in the order of best prediction as:

- Herschel Bulkley (1.05) > Unified (1.13) > Robertson and Stiff (1.20) > Bingham Plastic (7.82) > Power law (11.30)

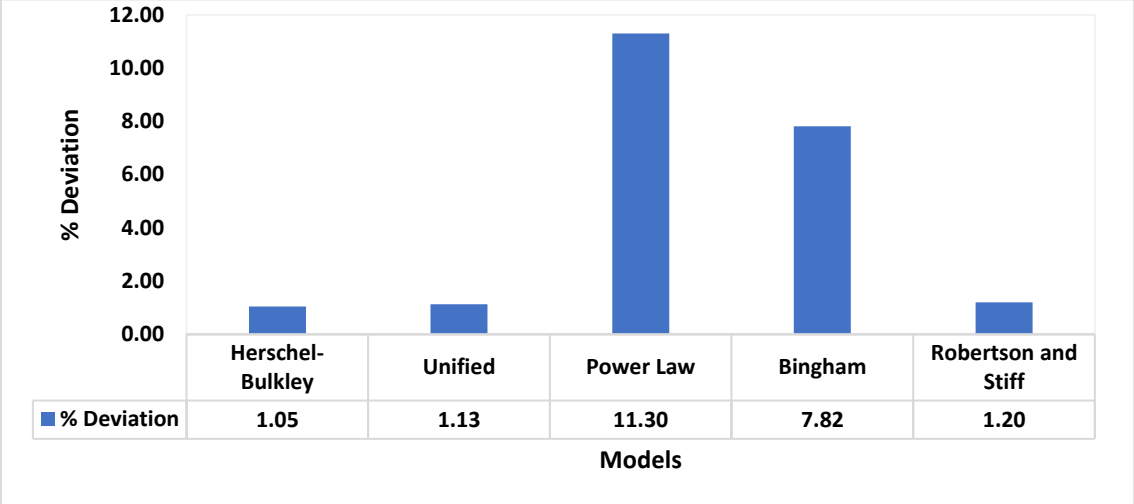

Figure 5.6: Error deviation of models with 1 g <71 µm SD blended drilling fluids measurement

5.2 Hydraulics simulation

In this subsection the hydraulics performance of the drilling fluids that modelled in section 5.1 are simulated with the Unified hydraulics model summarized in Table 5.3 and Table 5.4.

5.2.1 Simulation setup

Figure 5.7 shows a hydraulic experimental simulation well used to calculate the impact of the saw dust drilling fluids on the ECD. The simplified 10000 ft length simulation well was constructed with 8.5” casing. An inner diameter (ID) of 4.8” and an outer diameter (OD) of 5” of the drill string was used for the set up. Since the pump is placed at the top of the drill string, the pressure loss along the surface flow line is neglected. Moreover,

the drill string is designed without BHA element that contains only drill pipe and drill bit having three nozzles at the size of (3*28/32”). During the simulation, the injection rates are between 50 and 600 gpm and the drilling fluids’ densities are 1.3 sg respectively.

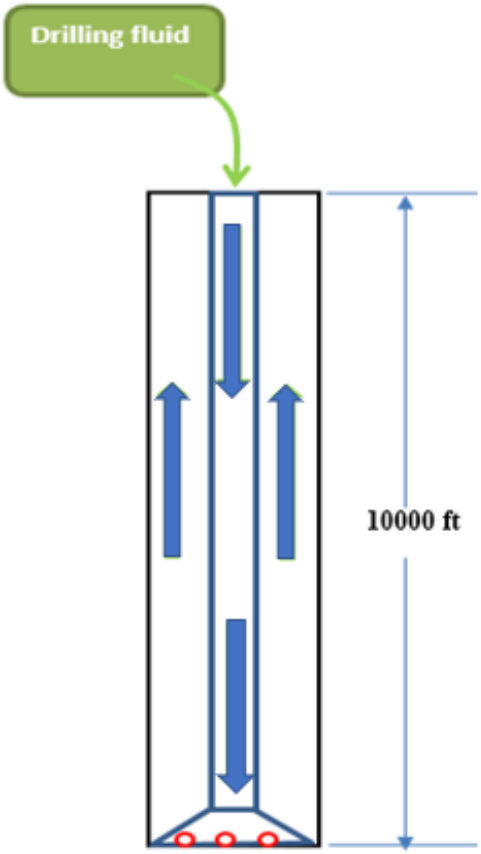

Figure 5.7: Illustration of hydraulics simulation setup

5.2.2 Simulation results

Two drilling fluids we injected in the simulation well. The selected of the fluids was here again based on the best filtrate loss performance. The viscosity of the drilling fluids used were the one measured at 80°C. The reason for high temperature selection is to have more realistic case to the real drilling data, considering the well to be under reservoir conditions.

5.2.2.1 ECD vs Flowrate <71µm SD, 80°C

Figure 5.8 shows the simulated ECD as the fluid flows increases from 50-600 gpm. As shown, the base fluid’s (Reference) ECD is higher than the saw dust blended drilling fluids. From the simulation results, one can observe that the ECD variation is non-linearly

with the saw dust concentration. Moreover, the flow pattern of the base fluid is of laminar, whereas the saw dust fluids showed transitional flow behavior at a higher flow rate. For instance, the flow pattern transition of the 1 g SD, 3 g SD and the 5 g SD are at around 400, 500 and 550 pgm respectively. After 550 rpm level all 3 versions have similar slope of ECD vs RPM dependency.

Overall, the additives do not increase the ECD of the drilling fluids. Since the saw dust is light, the high concentration of saw dust could reduce the density of the drilling fluids and hence one could expect more ECD reduction.

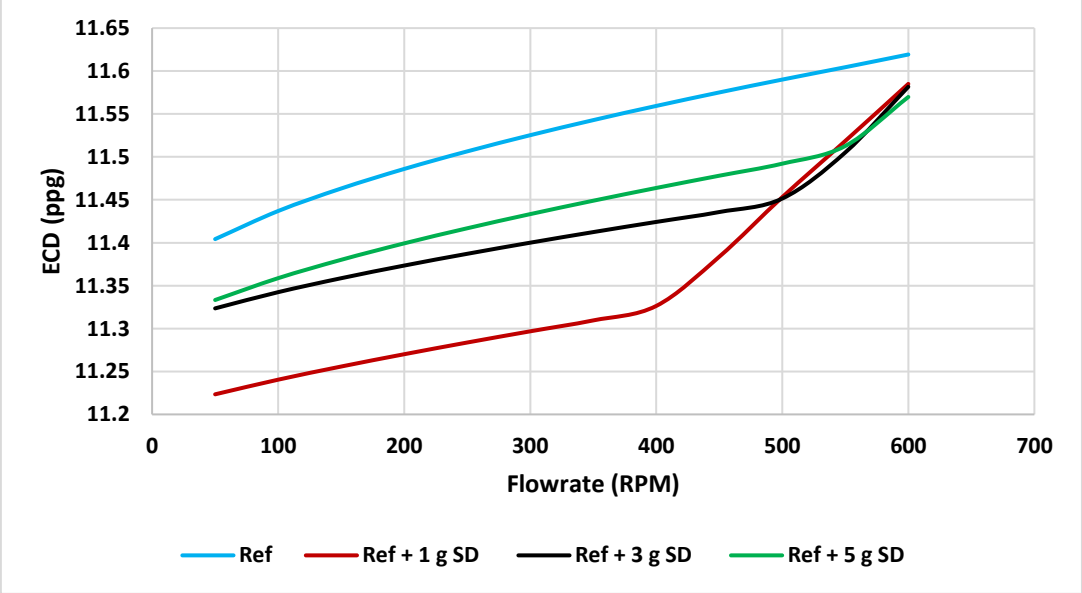

Figure 5.8: Illustration of <71 μm SD fluid ECD variation in different flow rates, at 80°C

For better evaluation, the percentile deviation of the Saw dust blended drilling fluids ECD from the Reference fluid are calculated and the results are displayed in Figure 5.9.

As shown in the Figure 5.9, the percentile deviation varies as the flow rate changes. The maximum percentile deviation of the 1 g, 3 g and 5 g SD based drilling fluids showed -2.02, % -1.2% and 0.79%, respectively. Most abrupt alteration is noticed for the case of 1 g SD addition starting at roughly 390 RPM later behaving similarly as other options.

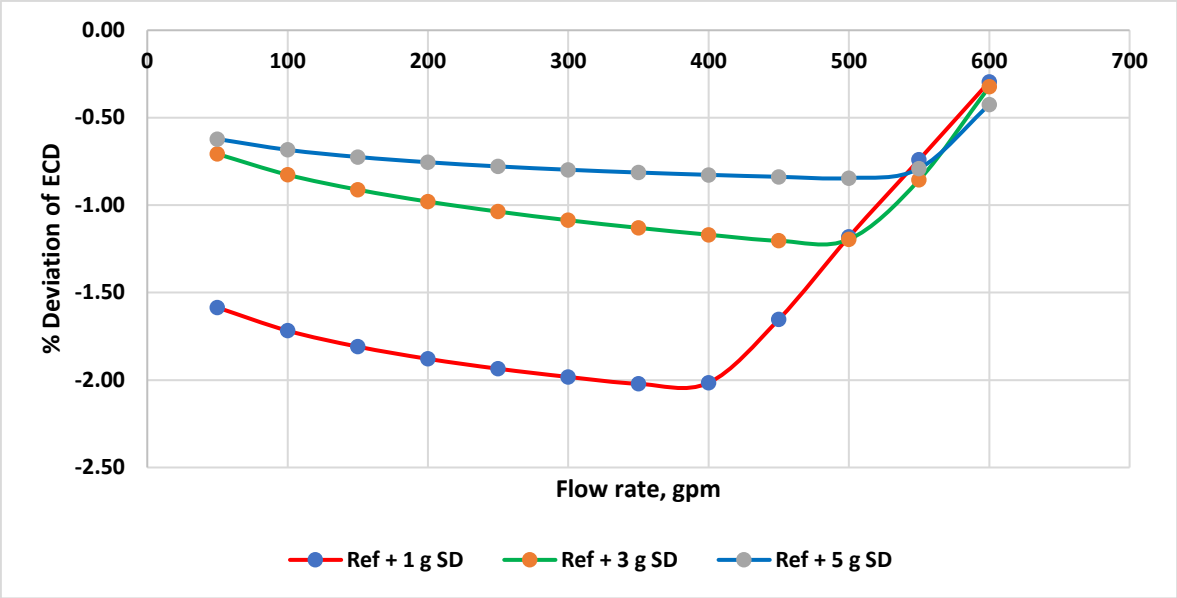

Figure 5.9: Illustration of percentile deviation of <71 µm SD fluid ECD in different flow rates, at 80°C

5.2.2.2 Annular Pressure Loss vs Flowrate <71µm SD 80°C

Figure 5.10 indicates annular pressure loss in psi versus flowrate in RPM for the <71 µm SD fluid. This pressure loss occurs due to the friction factor between the designed fluid and wellbore wall. The graph clearly indicates the positive performance of replacement sawdust which also reduces annular pressure loss, complying in all concentrations.

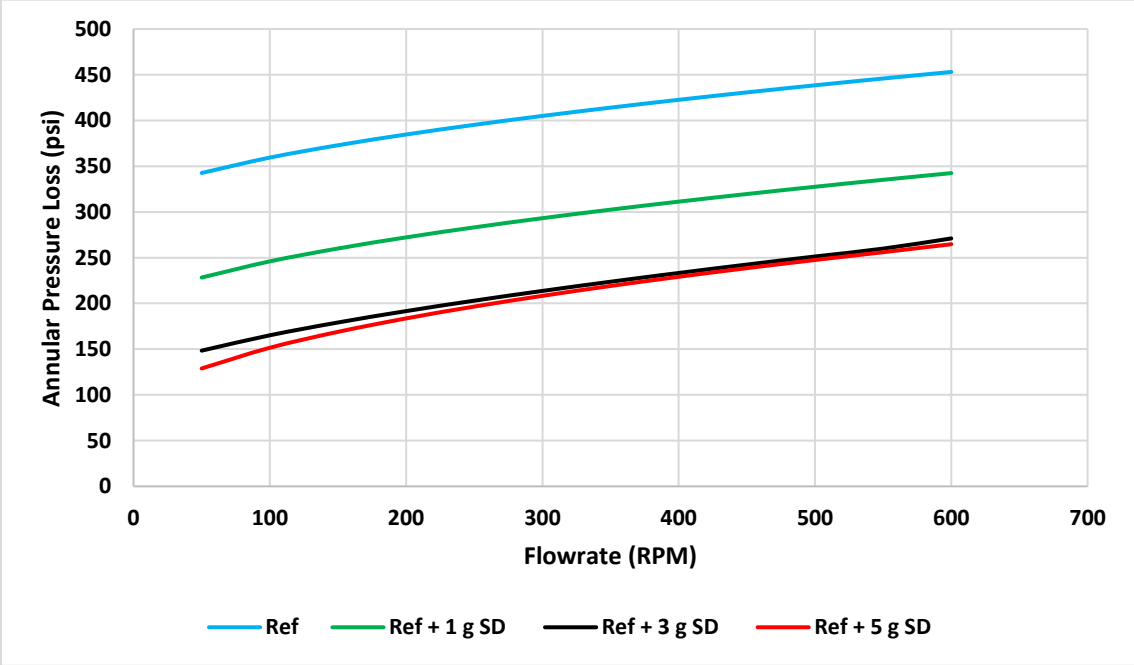

Figure 5.10: Annular Pressure Loss vs Flowrate <71µm 80°C

5.2.2.3 ECD vs Flowrate 125-150 µm 80°C

Similarly, the simulation results obtained from the 125-150 µm SD blended drilling fluids is plotted in Figure 5.11 comparing with the base fluid. Unlike the <71 µm SD blended system, the deviation of the 125-150 µm SD based drilling fluid from the base fluid is relatively less. This is due to the viscosity resemblance at the 80°C where the viscosity reduction of new mixture is compensated via thermal increment of viscosity.

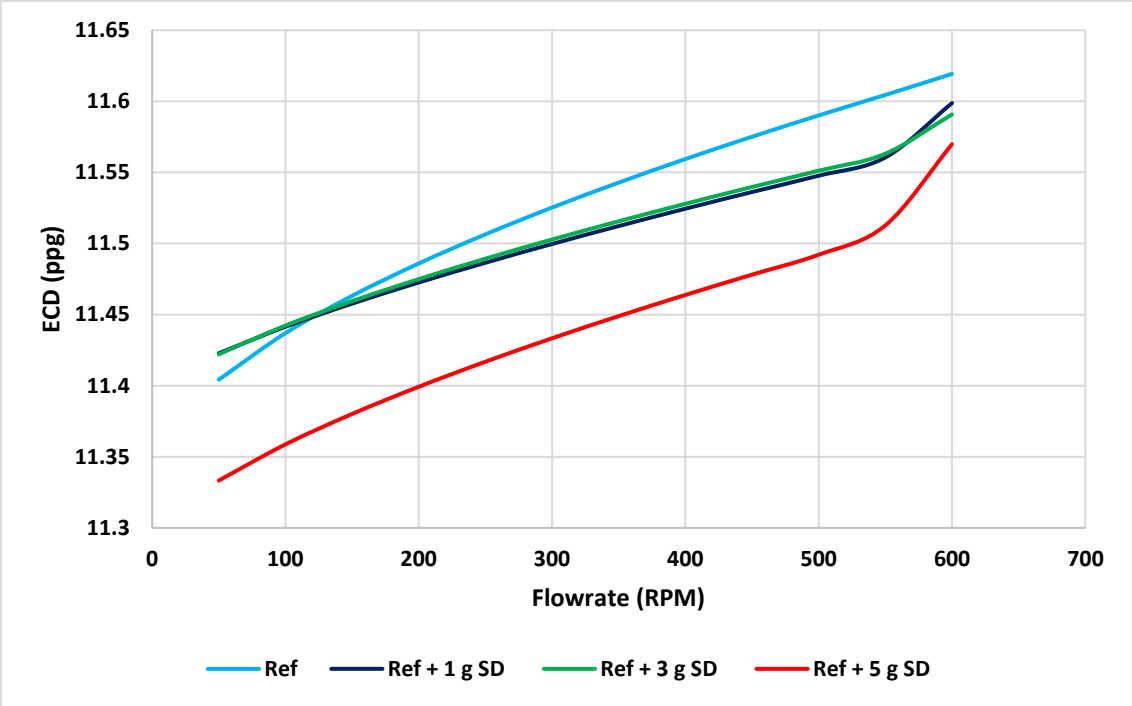

Figure 5.11: Illustration of 125-150 µm SD fluid ECD variation in different flow rates, at 80°C

The maximum error comparisons results show that of the 1 g, 3 g and 5 g SD based drilling fluids showed -0.36 % -0.36% and -0.80%, respectively.

It should be noted that the main objective this part of the simulation to investigate how the additives impact on the rheological parameters and hence on the hydraulics performance. Overall, the saw dust impact on the drilling fluids is negligible.

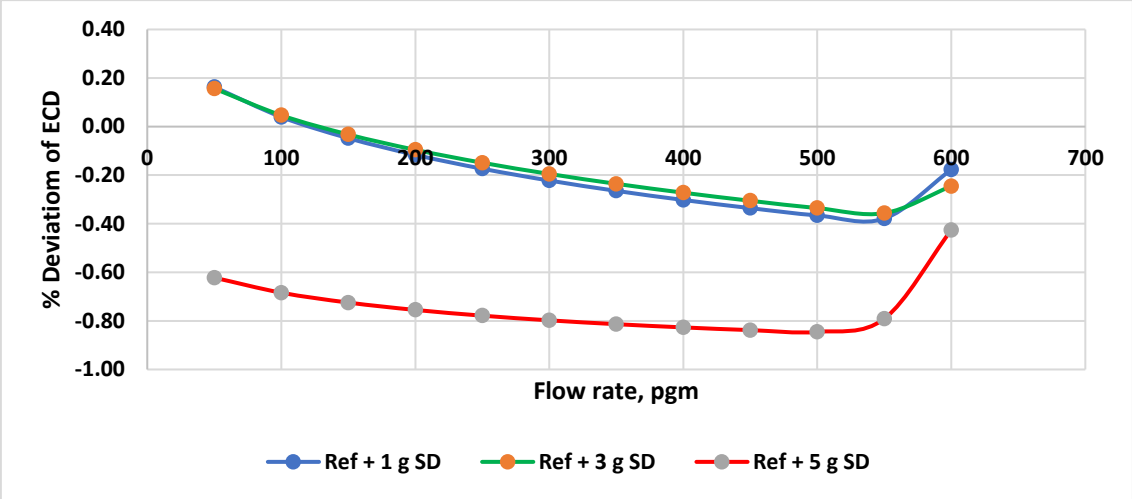

Figure 5.12: Illustration of percentile deviation of 125-150 µm SD fluid ECD in different flow rates, at 80°C

5.2.2.4 Annular Pressure Loss vs Flowrate 125-150 µm SD 80°C

Figure 5.13 indicates annular pressure loss in psi versus flowrate in RPM for the 125-150 µm SD fluid. This pressure loss occurs due to the friction factor between the designed fluid and wellbore wall. The graph clearly indicates the increased pressure loss in higher flowrates for the fluids with SD additions. Still, this margin is less than reference fluid, which is logical considering the presence of SD particles.

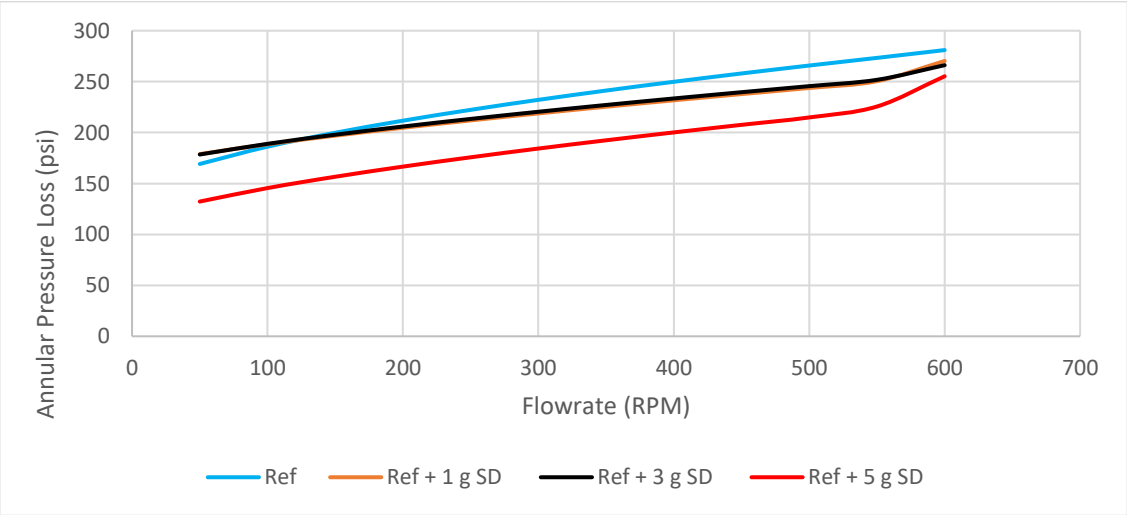

Figure 5.13: Annular Pressure Loss vs Flowrate 125-150 µm 80°C

6 Summary and Conclusion

The main objectives of this thesis work were to designing Bentonite and KCL based water-based fluids and studying impact of addition and replacement of saw dust over polymers on rheological properties of the fluids, with two different particle sizes and three different concentrations. Rheological (viscosity, pH values), filtrate loss, viscoelastic, lost circulation bridging experiments have been conducted, as well as rheological modelling have been developed for the best fluid performances in a virtual well. Resulting data have been applied on and hydraulic simulation for further hydraulic investigations.

Conclusions are made based on the obtained results from experimental and simulation studies:

- For filtrate loss performance, the best fluid and saw dust concentration were fluid 2.2 in whole bentonite system with 3 g 125-150 μm SD. The fluid showed 14.3 % reduction after adding sawdust to the system, reducing filtrate loss value from 3.5 ml to 3 ml.
- Bingham yield stress values showed that, whole bentonite fluids with both particle sizes of saw dust provide thermally stable fluid in terms of viscosity.
- Bridging experiment results suggest that addition of saw dust as a replacement particle shows pressure build-up over the 20-30 minutes. Also, addition of 2 wt% quartz and positive synergy produced from quartz and sawdust creates filter cake pressure build-up.
- From amplitude sweep measurements one can conclude that all fluids behaved as elastic fluids with a structure possession of gel, proving they all have viscoelastic properties.
- Based on Rheological model deviations for best bentonite fluids, the model selection was made for 1 g <71 μm SD and 3 g 125-150 μm SD fluids respectively according to percentile deviation with the following order:
    1. Roberson and Stiff (1.4) > Herschel Bulkley (2.7) > Unified (3.1) > Power law (4.2) > Bingham Plastic (15.5)
    2. Herschel Bulkley (1.05) > Unified (1.13) > Robertson and Stiff (1.20) > Bingham Plastic (7.82) > Power law (11.30)

- Sawdust prevents sagging issue of water-based fluid alongside with the polymers. It can be also noticed from obtained filtrate loss values.
- Hydraulics Simulation proved the thermal stability of the fluids as both ECD and pump pressure values kept stability with three different temperature values.
- The viscoelastic measurements have suggested a conclusion that addition of saw dust increased the LVE range value, alongside with flow point and yield stress with most of the designed fluids.

It should be remarked that, all the observations and conclusions provided above are based on the results of this thesis and the scope of this project. Varying concentrations of saw dust additive might behave differently in Bentonite and KCL based fluids, as well as when experimentally tested in different temperature, pressure and other rheological and physical conditions.

References

[1] H. Mahmoud *et al.*, "Pilot-scale study on the suspension of drill cuttings: Effect of fiber and fluid characteristics," *Journal of Natural Gas Science and Engineering*, vol. 101, p. 104531, May 2022, doi: 10.1016/j.jngse.2022.104531.

[2] E. E. Okoro *et al.*, "Radiological and toxicity risk exposures of oil based mud: health implication on drilling crew in Niger Delta," *Environ Sci Pollut Res*, vol. 27, no. 5, pp. 5387–5397, Feb. 2020, doi: 10.1007/s11356-019-07222-3.

[3] Z. Vryzas, V. Zaspalis, L. Nalbantian, O. Mahmoud, H. A. Nasr-El-Din, and V. C. Kelessidis, "A Comprehensive Approach for the Development of New Magnetite Nanoparticles Giving Smart Drilling Fluids with Superior Properties for HP/HT Applications," in *Day 3 Wed, November 16, 2016*, Bangkok, Thailand: IPTC, Nov. 2016, p. D031S053R001. doi: 10.2523/IPTC-18731-MS.

[4] M. Sadeghalvaad and S. Sabbaghi, "The effect of the TiO2/polyacrylamide nanocomposite on water-based drilling fluid properties," *Powder Technology*, vol. 272, pp. 113–119, Mar. 2015, doi: 10.1016/j.powtec.2014.11.032.

[5] N. Mohamadian, H. Ghorbani, D. A. Wood, and M. A. Khoshmardan, "A hybrid nanocomposite of poly(styrene-methyl methacrylate- acrylic acid) /clay as a novel rheology-improvement additive for drilling fluids," *J Polym Res*, vol. 26, no. 2, p. 33, Feb. 2019, doi: 10.1007/s10965-019-1696-6.

[6] O. Mahmoud, A. Mady, A. S. Dahab, and A. Aftab, "Al_2O_3 and CuO nanoparticles as promising additives to improve the properties of KCl -polymer mud: An experimental investigation," *Can J Chem Eng*, vol. 100, no. 6, pp. 1384–1397, Jun. 2022, doi: 10.1002/cjce.24285.

[7] N. M. Taha and S. Lee, "Nano Graphene Application Improving Drilling Fluids Performance," in *Day 2 Mon, December 07, 2015*, Doha, Qatar: IPTC, Dec. 2015, p. D021S013R005. doi: 10.2523/IPTC-18539-MS.

[8] M. Belayneh, B. Aadnøy, and S. M. Strømø, "MoS2 Nanoparticle Effects on 80 °C Thermally Stable Water-Based Drilling Fluid," *Materials*, vol. 14, no. 23, p. 7195, Nov. 2021, doi: 10.3390/ma14237195.

[9] C. O. Nwaoji, G. Hareland, M. Husein, R. Nygaard, and M. F. Zakaria, "Wellbore Strengthening-Nano-Particle Drilling Fluid Experimental Design Using Hydraulic

Fracture Apparatus," in *All Days*, Amsterdam, The Netherlands: SPE, Mar. 2013, p. SPE-163434-MS. doi: 10.2118/163434-MS.

[10] M. Laudon, B. F. Romanowicz, and D. L. Laird, *Clean Technology 2010: bioenergy, renewables, storage, grid, waste and sustainability : technical proceedings of the 2010 CTSI Clean Technology and Sustainable Industries Conference and Expo*. Boston, Danville, CA, Boca Raton, FL: Clean Technology and Sustainable Industries Organization ; Nano Science and Technology Institute ; CRC Press, 2010.

[11] S. Davoodi, A. Ramazani S.A., S. Jamshidi, and A. Fellah Jahromi, "A novel field applicable mud formula with enhanced fluid loss properties in High Pressure-High Temperature well condition containing pistachio shell powder," *Journal of Petroleum Science and Engineering*, vol. 162, pp. 378–385, Mar. 2018, doi: 10.1016/j.petrol.2017.12.059.

[12] R. Caenn, H. C. H. Darley†, and G. R. Gray†, "Introduction to Drilling Fluids," in *Composition and Properties of Drilling and Completion Fluids*, Elsevier, 2017, pp. 1–34. doi: 10.1016/B978-0-12-804751-4.00001-8.

[13] J. Nwaiche, "Selection and Application of Drilling Fluids," 2015, doi: 10.13140/RG.2.1.3243.4722.

[14] L. W. Lake, J. R. Fanchi, and Society of Petroleum Engineers (U.S.), Eds., *Petroleum engineering handbook*. Richardson, TX: Society of Petroleum Engineers, 2006.

[15] M. F. Zakaria, M. Husein, and G. Hareland, "Novel Nanoparticle-Based Drilling Fluid with Improved Characteristics," in *All Days*, Noordwijk, The Netherlands: SPE, Jun. 2012, p. SPE-156992-MS. doi: 10.2118/156992-MS.

[16] "Yield Point (YP) of Drilling Fluids," Jan. 21, 2016. https://www.drillingformulas.com/yield-point-yp-of-drilling-fluids/

[17] R. Caenn, H. C. H. Darley†, and G. R. Gray†, "Evaluating Drilling Fluid Performance," in *Composition and Properties of Drilling and Completion Fluids*, Elsevier, 2017, pp. 55–91. doi: 10.1016/B978-0-12-804751-4.00003-1.

[18] F. Pedraza, B. Rannou, G. Boissonnet, B. Bouchaud, and Z. Maache-Rezzoug, "Rheological Behaviour, Synthesis and Performance of Smart Thermal Barrier

Coating Systems Based on Hollow Alumina," *MSCE*, vol. 03, no. 12, pp. 17–22, 2015, doi: 10.4236/msce.2015.312004.

[19] M. VILORIA OCHOA, "Analysis Of Drilling Fluid Rheology And Tool Joint Effect To Reduce Errors In Hydraulics Calculations," PhD Dissertation, Texas A&M University, Texas, USA, 2006.

[20] A. T. Bourgoyne, Ed., *Applied drilling engineering*. in SPE textbook series, no. vol. 2. Richardson, TX: Society of Petroleum Engineers, 1986.

[21] R. F. Mitchell, S. Miska, B. S. Aadnøy, and Society of Petroleum Engineers (U.S.), Eds., *Fundamentals of Drilling Engineering*. in SPE textbook series, no. v. 12. Richardson, TX: Society of Petroleum Engineers, 2011.

[22] S. E. Haaland, "Simple and Explicit Formulas for the Friction Factor in Turbulent Pipe Flow," *Journal of Fluids Engineering*, vol. 105, no. 1, pp. 89–90, Mar. 1983, doi: 10.1115/1.3240948.

[23] T. Zeynalov, "Effect of Boron nitride (BN) and surface modified BN on the properties of laboratory water-based drilling fluid formulated in Duovis/XG polymers: Experimental and Simulation studies," Master's Thesis, University of Stavanger, Stavanger, Norway, 2018. [Online]. Available: https://uis.brage.unit.no/uis-xmlui/bitstream/handle/11250/2570233/Zeynalov_Tofig.pdf?sequence=1&isAllowed=y

[24] J. Sadigov, "Comparisons of Rheology and Hydraulics Prediction of Mud Systems in Concentric and Eccentric Well Geometry," Master's Thesis, University of Stavanger, 2013.

[25] D. I. G. Jones, *Handbook of viscoelastic vibration damping*. Chichester ; New York: J. Wiley, 2001.

[26] T. G. Mezger, *Rheology handbook: for users of rotational and oscillatory rheometers*. Place of publication not identified: Vincentz Network, 2006.

[27] D. M. Carberry, M. A. B. Baker, G. M. Wang, E. M. Sevick, and D. J. Evans, "An optical trap experiment to demonstrate fluctuation theorems in viscoelastic media," *J. Opt. A: Pure Appl. Opt.*, vol. 9, no. 8, pp. S204–S214, Aug. 2007, doi: 10.1088/1464-4258/9/8/S13.

[28] T. Sharman, "Characterization and Performance Study of OBM at Various Oil-Water Ratios," Master's Thesis, University of Stavanger, Stavanger, Norway, 2015. [Online]. Available: http://hdl.handle.net/11250/300921

[29] O. Skjeggestad, *Boreslamteknologi: teori og praksis*. Bergen: Alma Mater, 1989.

[30] A. Grbeš, G. Bedeković, and I. Sobota, "Bentonite processing," vol. 24, pp. 61–65, Jan. 2013.

[31] R. Caenn, H. C. H. Darley, and G. R. Gray, "Clay Mineralogy and the Colloid Chemistry of Drilling Fluids," in *Composition and Properties of Drilling and Completion Fluids*, Elsevier, 2011, pp. 137–177. doi: 10.1016/B978-0-12-383858-2.00004-4.

[32] "Potassium Chloride," 2023. https://www.chemicalbook.com/ChemicalProductProperty_EN_CB9137176.htm

[33] "Sodium Carbonate." https://www.sigmaaldrich.com/catalog/product/sial/330361?lang=en&region=NO

[34] "Viscosifier. Polyanionic Cellulose." https://www.irooildrilling.com/Viscosifier/PAC.htm

[35] "PolyPac." https://www.slb.com/products-and-services/innovating-in-oil-and-gas/drilling/drilling-fluids-and-well-cementing/drilling-fluids/drilling-fluid-additives/filtration-reducers/PolyPac-ul-ultralow-viscosity-cellulose

[36] A. K. Mohamed, S. A. Elkatatny, M. A. Mahmoud, R. A. Shawabkeh, and A. A. Al-Majed, "The Evaluation of Micronized Barite As a Weighting Material for Completing HPHT Wells," in *Day 3 Wed, March 08, 2017*, Manama, Kingdom of Bahrain: SPE, Mar. 2017, p. D031S027R005. doi: 10.2118/183768-MS.

[37] V. C. Kelessidis, E. Poulakakis, and V. Chatzistamou, "Use of Carbopol 980 and carboxymethyl cellulose polymers as rheology modifiers of sodium-bentonite water dispersions," *Applied Clay Science*, vol. 54, no. 1, pp. 63–69, Nov. 2011, doi: 10.1016/j.clay.2011.07.013.

[38] E. Ayodele and Bekwuchi Ogbonda, "Laboratory and Performance Analysis of Sawdust as a Lost Circulation Material in Water Based Mud," 2019, doi: 10.13140/RG.2.2.33575.88485.

[39] J. Götze, "Chemistry, textures and physical properties of quartz — geological interpretation and technical application," *Mineral. mag.*, vol. 73, no. 4, pp. 645–671, Aug. 2009, doi: 10.1180/minmag.2009.073.4.645.

Appendix A: Filtrate loss and pH data

A.1 Impact of <71 µm SD on the Filtrate loss of the base KCL fluid

Filtrate loss experiment was done with the replacement KCL fluid containing <71 µm SD and the concentration of 1 g. The experiment is conducted for using API filter test rig filter press equipment. 100 psi pressure was applied on the fluid and 7.5 minutes on the clock was measured, while the impact of <71 µm SD has been studied. While Base Fluid had 16.4 ml filtrate loss, absence of Pac & PolyPac couldn't be quite replaced by saw dust after getting 35.6 ml filtrate loss and filtrate loss increase percentage of 117.1% (Table A.1 and Figure A.1). This still shows the importance of polymer-based additives especially in pay-zones with sandstone (prone to mud loss).

Table A.1: pH, FL and FLR of replacement Base Fluid and Fluid 3.1 (ex-situ 0.5 XG)

Drilling Fluid	**Base Fluid**	**Fluid 3.1**
pH	9.46	9.36
Filtrate Loss (ml)	16.4	35.6
Filtrate Loss Reduction (%)	-	117.1

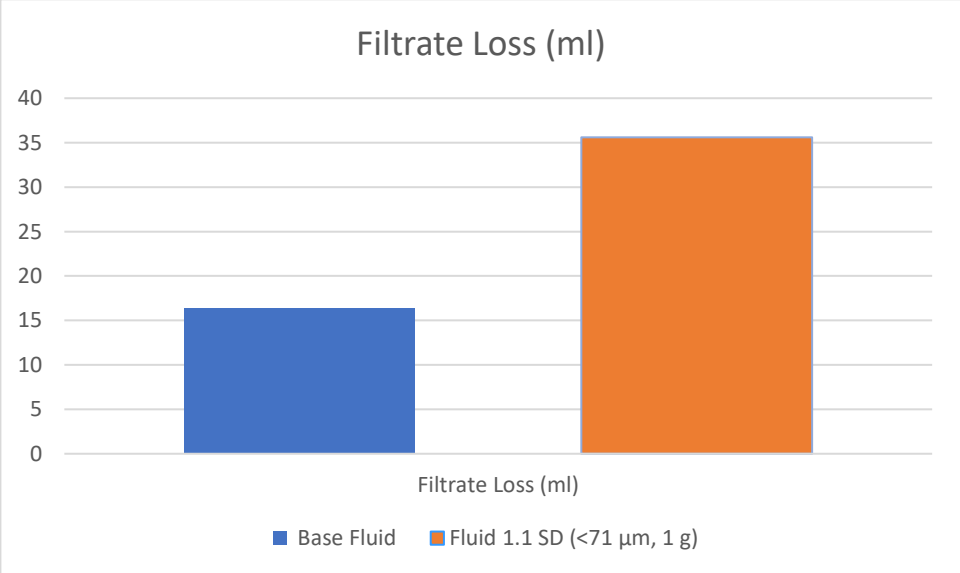

Figure A.1: Filtrate Loss of replacement KCL base fluid and 1 g <71 µm SD fluid (ex-situ 0.5 XG)

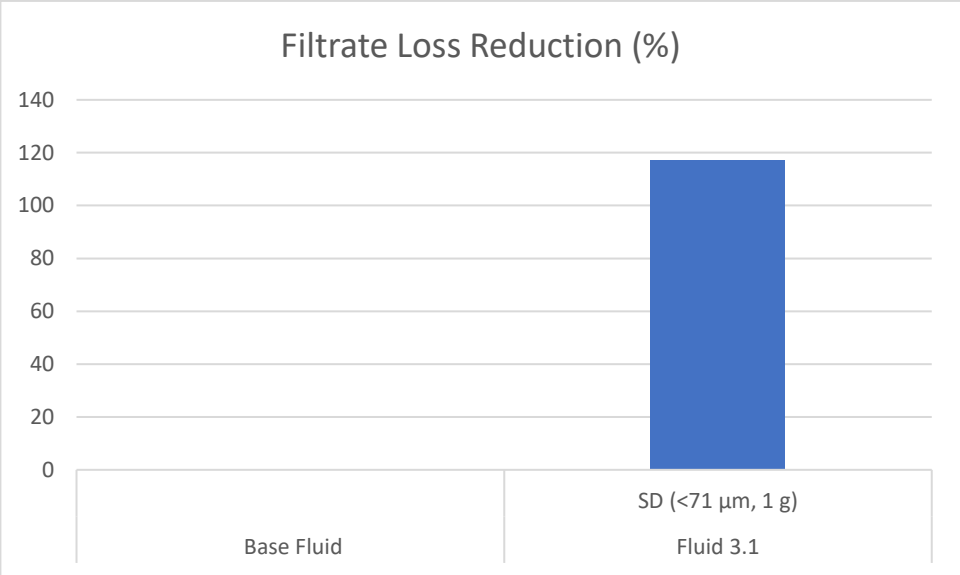

Figure A.2: FLR of replacement KCL <71 µm SD fluid compared to base fluid (ex-situ 0.5 XG)

A.2 Impact of 125-150 µm SD on the Filtrate loss of the base KCL fluid

Filtrate loss experiment was done with the replacement KCL fluid containing 125-150 µm SD and the concentration of 1 g and 3g. The experiments were conducted for using API filter test rig filter press equipment. 100 psi pressure was applied on the fluid and 7.5 minutes on the clock was measured, while the impact of 125-150 µm SD has been studied. Compared to Base Fluid filtrate loss 16.4 ml, Fluids 3.2 and 3.3 showed way higher filtrate loss values of 51.1 ml and 58.6 ml, and Filtrate loss increase percentages of 211.5% and 257.3% respectively (Table A.2 and Figure A.3).

Table A.2: pH, FL and FLR of replacement Base Fluid, Fluid 3.2 and Fluid 3.3 (ex-situ 0.5 XG)

Drilling Fluid	**Base Fluid**	**Fluid 3.2 SD (125-150 µm, 1 g)**	**Fluid 3.3 SD 125-150 µm, 3 g)**
pH	9.46	9.30	9.14
Filtrate Loss (ml)	16.4	51.1	58.6
Filtrate Loss Reduction (%)	-	211.6	257.3

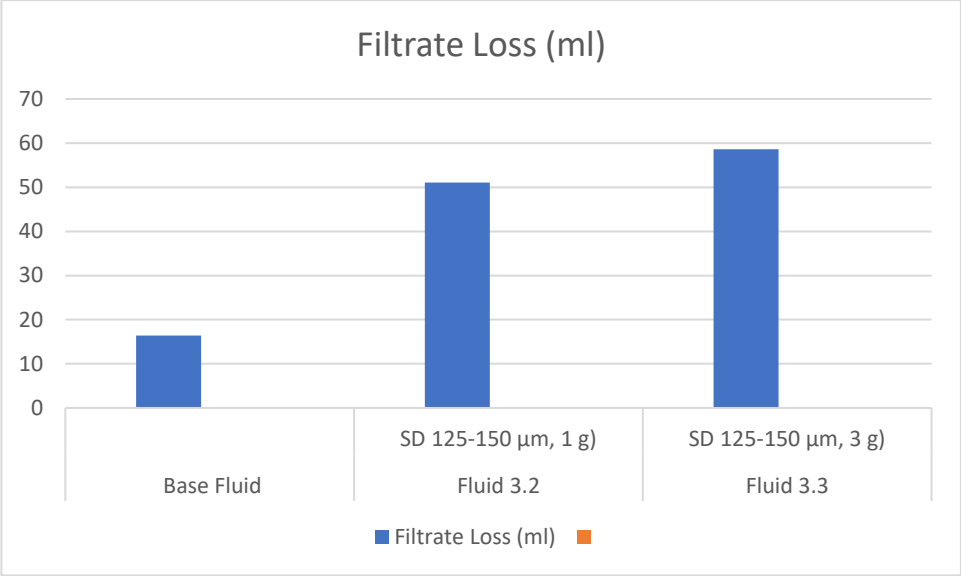

Figure A.3: Filtrate Loss of replacement KCL base fluid and 125-150 µm SD fluids (ex-situ 0.5 XG)

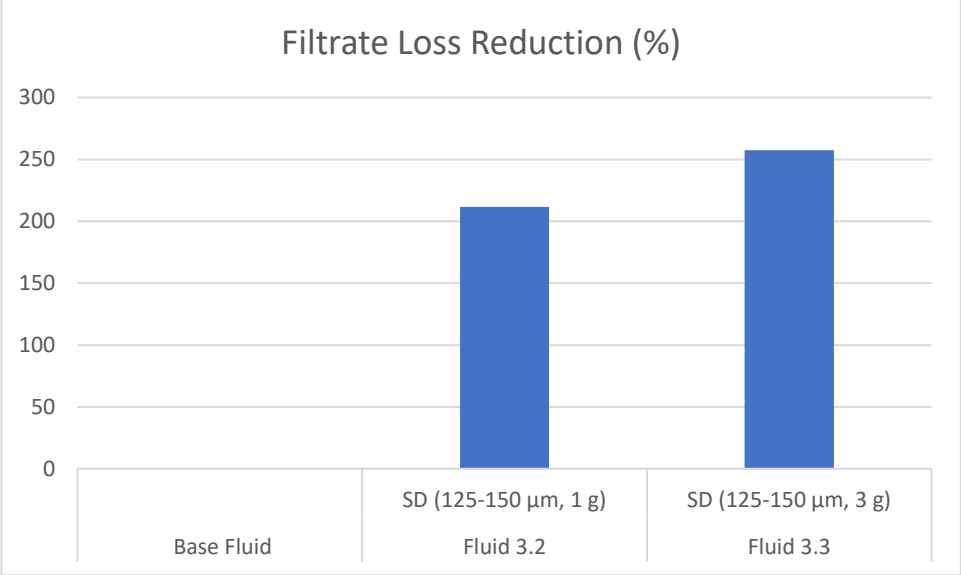

Figure A.4: FLR of replacement KCL 125-150 µm SD fluids compared to base fluid (ex-situ 0.5 XG)

A.3 Effect of Saw Dust in 0.5 XG Polymer Replacement KCL Base Fluid

The basis for this fluid is a little different than bentonite-based fluid due to several reasons. As replacing Pac & PolyPac polymers reduced the filtrate loss in three different fluids, the primary focus was given to replacement of the polymers again, but this time using KCL over Bentonite to see how fluid will work in the totally different fluid system. The main goal of replacing polymers and adding saw dust in not only economic and ecological side, but also to achieve less filtrate loss compared the equivalent fluids in whole system.

Table A.3: KCL fluids and with three different concentrations of SD (ex-situ 0.5 XG)

Additives	**Base Fluid**	**Fluid 5.1**	**Fluid 5.2**	**Fluid 5.3**
Water	350 ml	350 ml	350 ml	350 ml
KCL	25 g	25 g	25 g	25 g
Soda ash	0,52 g	0,52 g	0,52 g	0,52 g
Pac	0.5 g	-	-	-
PolyPac	1,0 g	-	-	-
Barite	143 g	143 g	143 g	143 g
Carbopol	0.1 g	0.1 g	0.1 g	0.1 g
SawDust	-	**1 g <71 µm SD**	**1 g 125-150 µm SD**	**3 g 125-150 µm SD**
Xanthan Gum (ex-situ)	0.5 g	0.5 g	0.5 g	0.5 g

Since Fluids 2.1 and 2.2 in whole bentonite system and Fluid 3.1 in replacement bentonite system gave filtrate loss reduction percentages 7.1%, 14.3% and 7.1% respectively, same concentrations of SD have been chosen to test in the KCL system (Table A.3). 0.5 g Xanthan Gum has been added in both base KCL and replacement KCL fluids as an ex-situ situation same as in bentonite, because of sagging fluid issue in the absence of Pac & PolyPac polymers.

Appendix B: Viscometer data

B.1 Viscometer data for KCL fluids

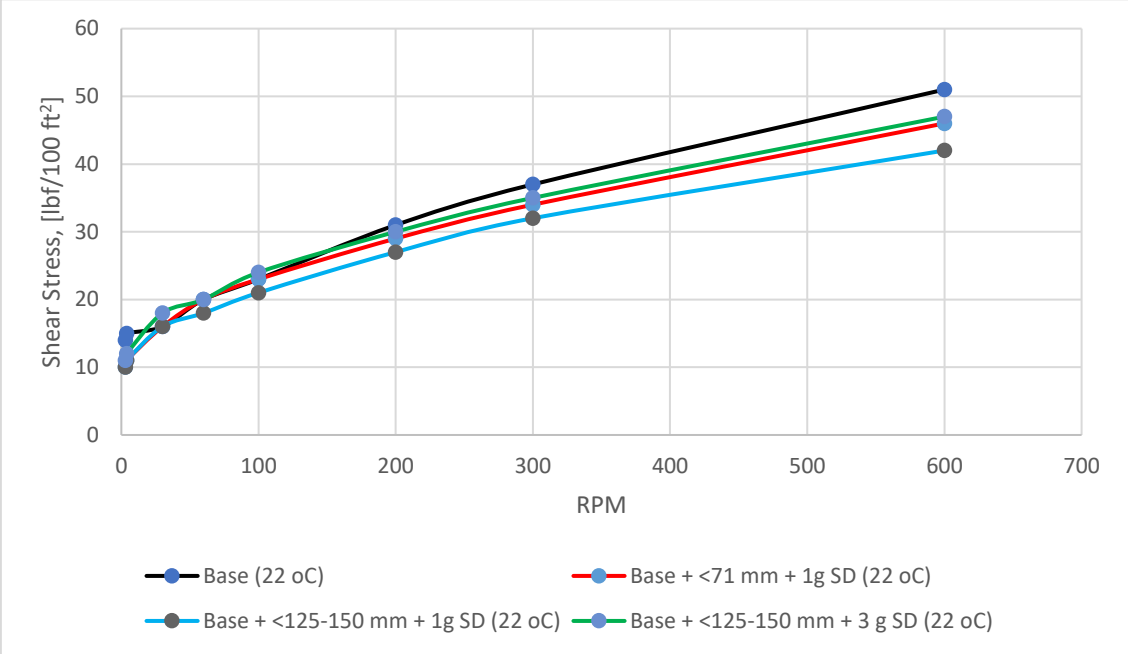

Figure B.1: Viscometer data at 20°C for KCL replacement fluids

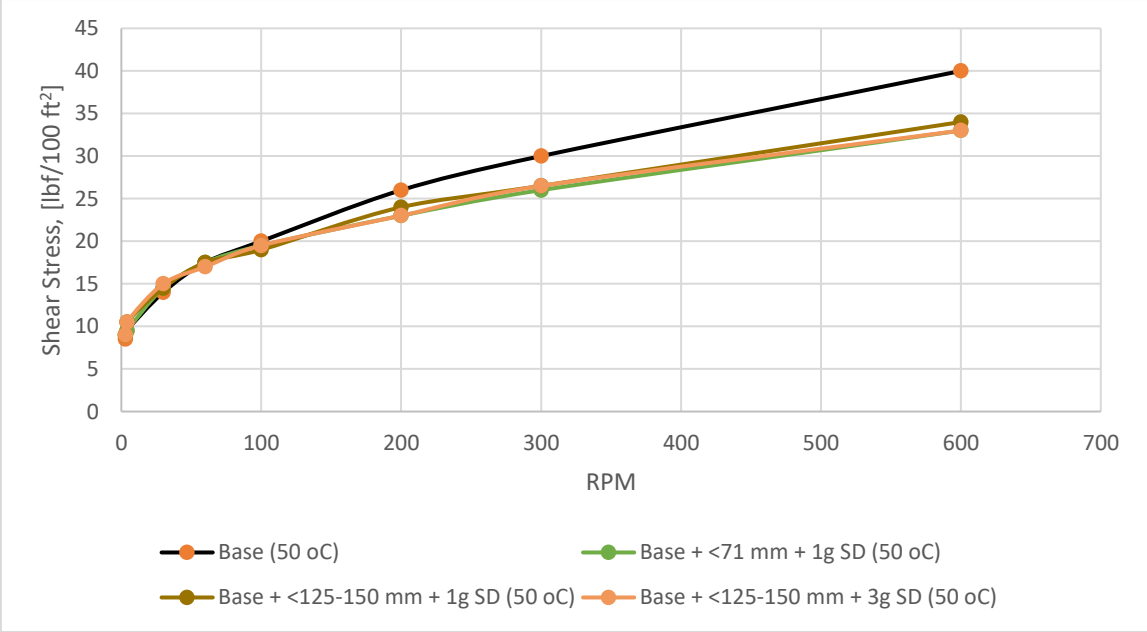

Figure B.2: Viscometer data at 50°C for KCL replacement fluids

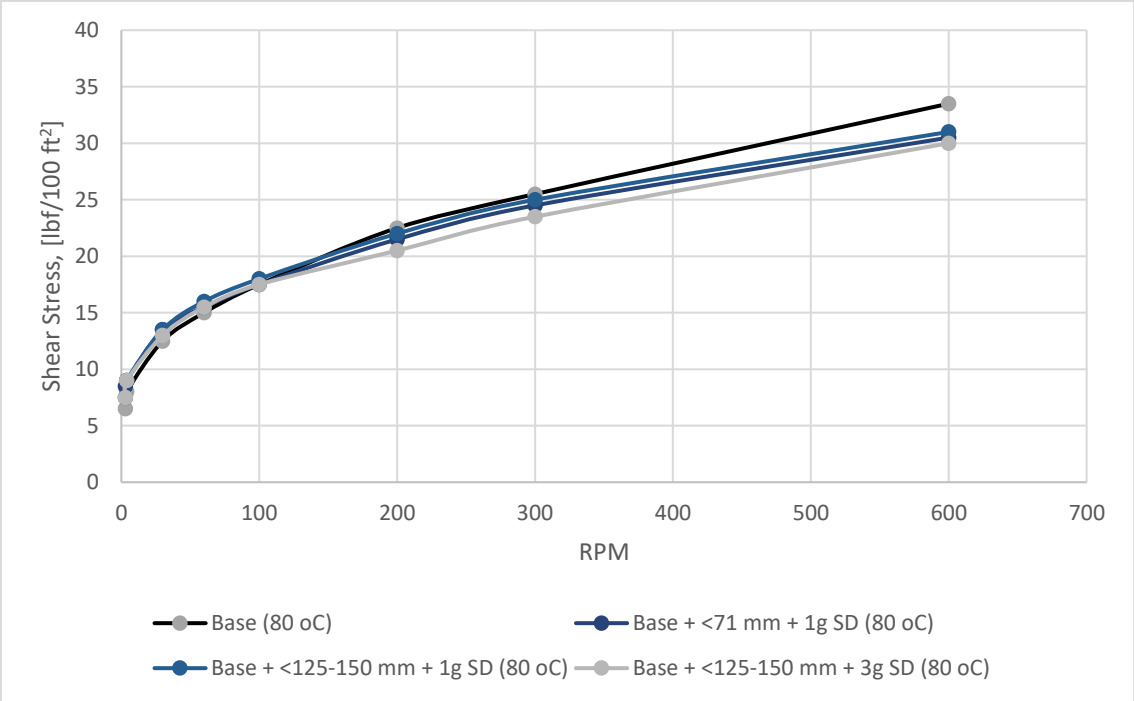

Figure B.3: Viscometer data at 80°C for KCL replacement fluids

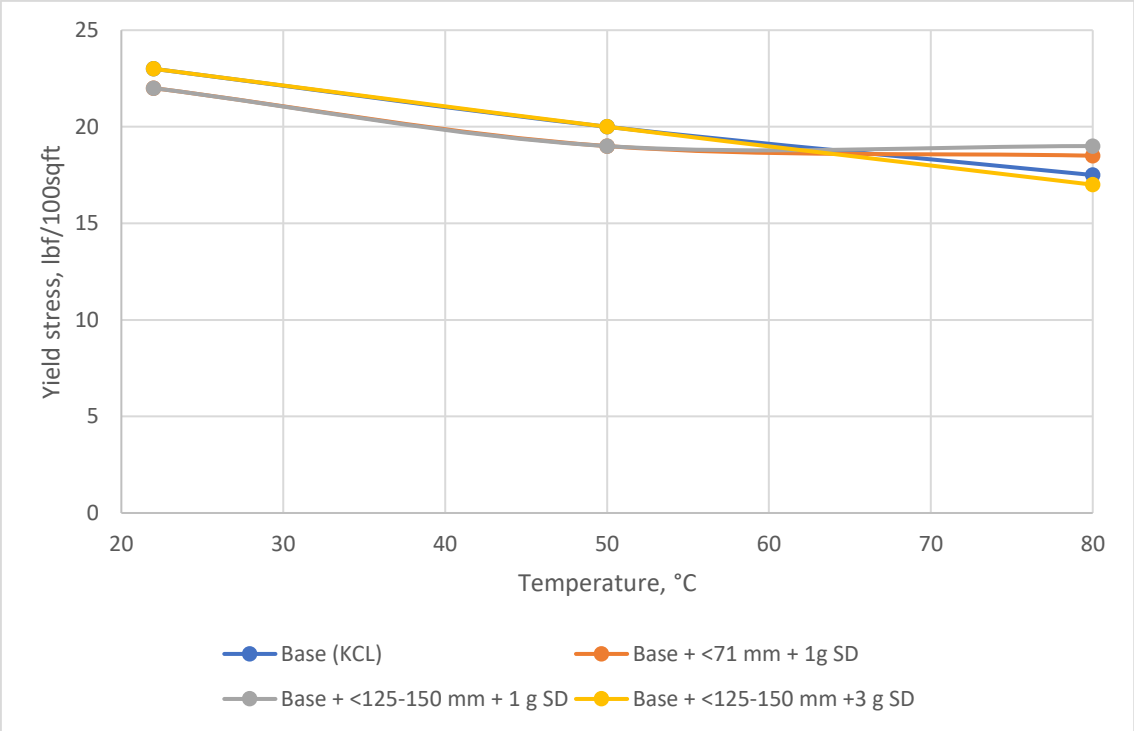

Figure B.4: Bingham yield stress data for KCL replacement fluids at 20°C, 50°C, 80°C

B.2 Viscometer data for Bentonite fluids

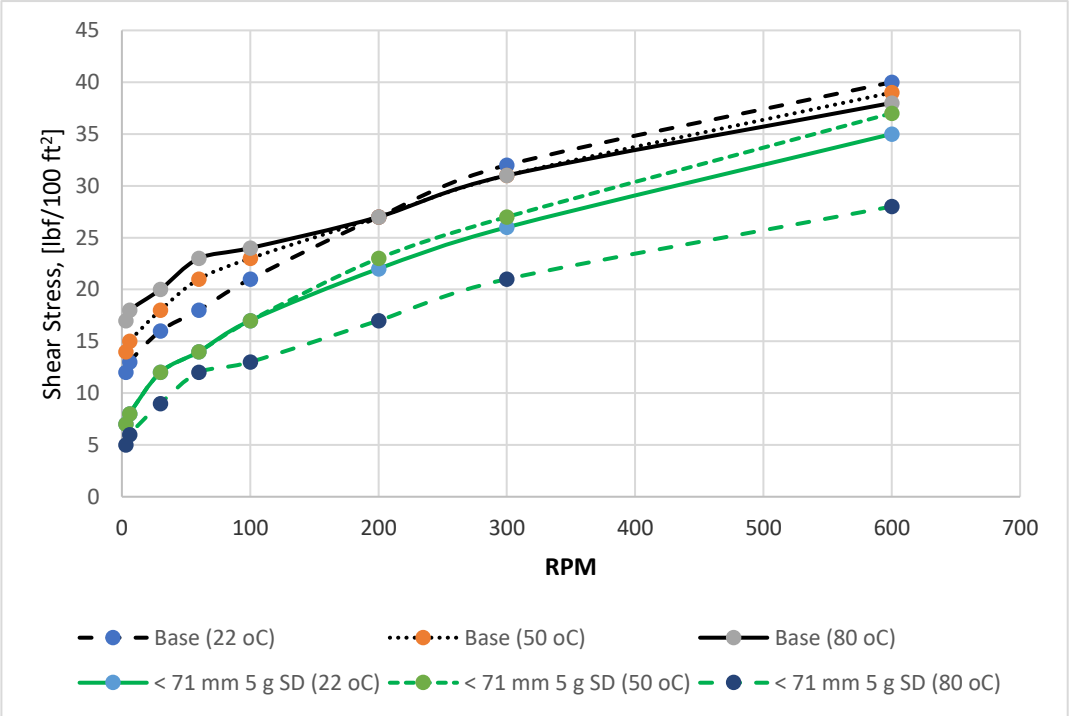

Figure B.5: Viscometer data at 20°C, 50°C, 80°C for bentonite replacement reference and 5 g <71 µm SD fluids

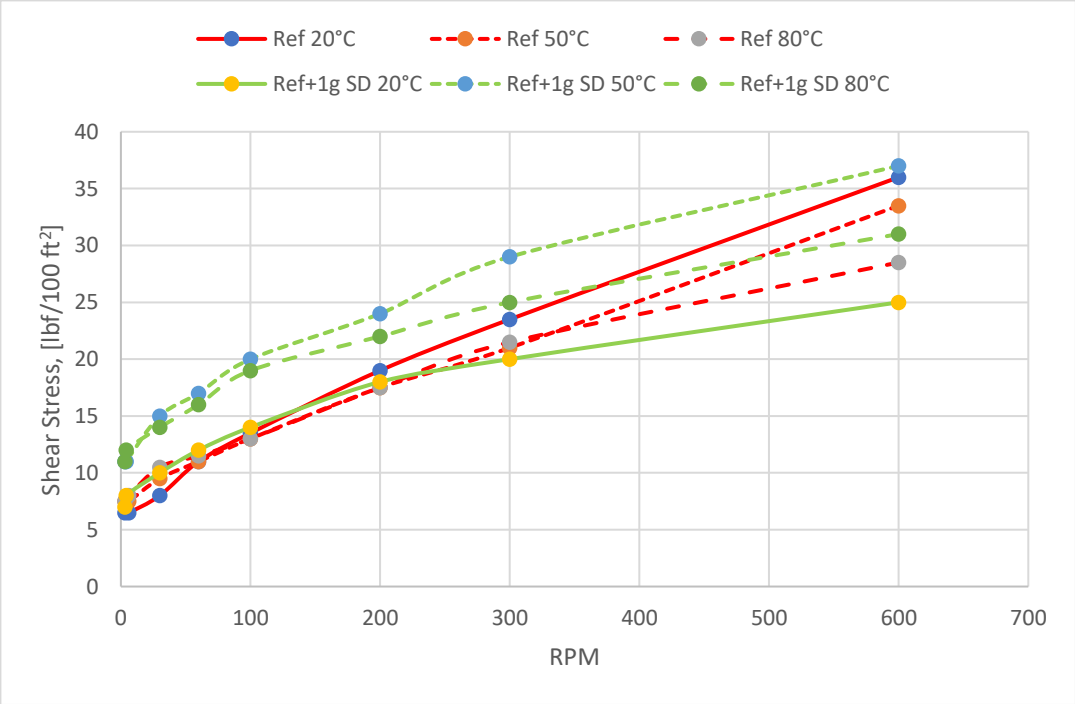

Figure B.6: Viscometer data at 20°C, 50°C, 80°C for bentonite replacement reference and 1 g 125-150 µm SD fluids

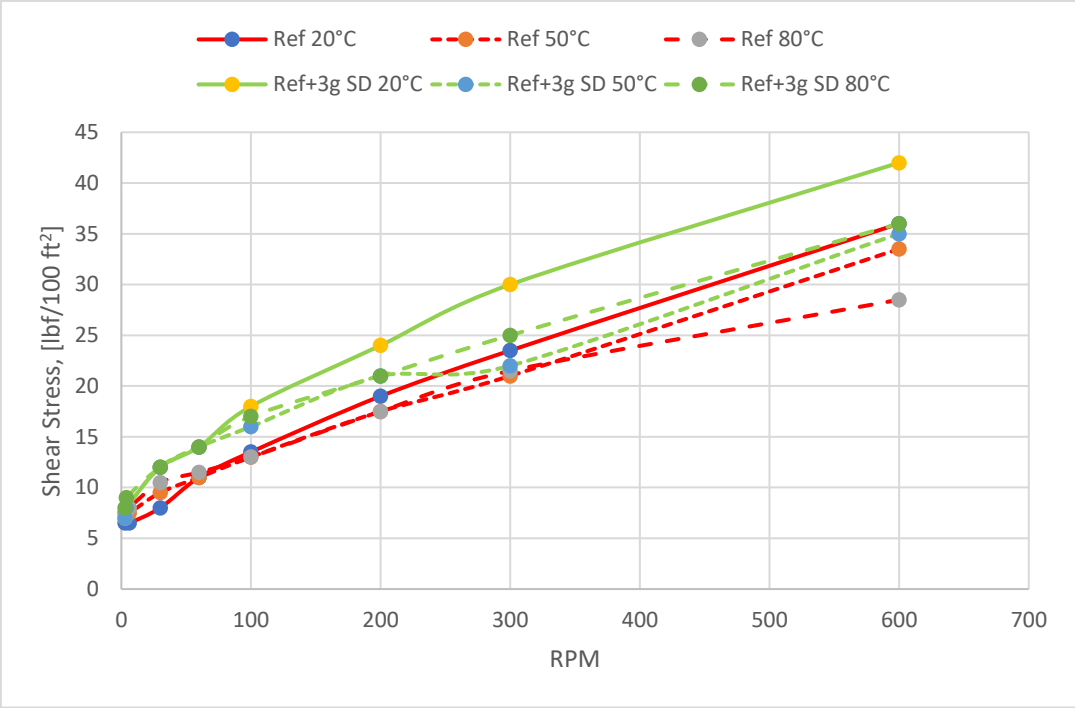

Figure B.7: Viscometer data at 20°C, 50°C, 80°C for bentonite replacement reference and 3 g 125-150 µm SD fluids

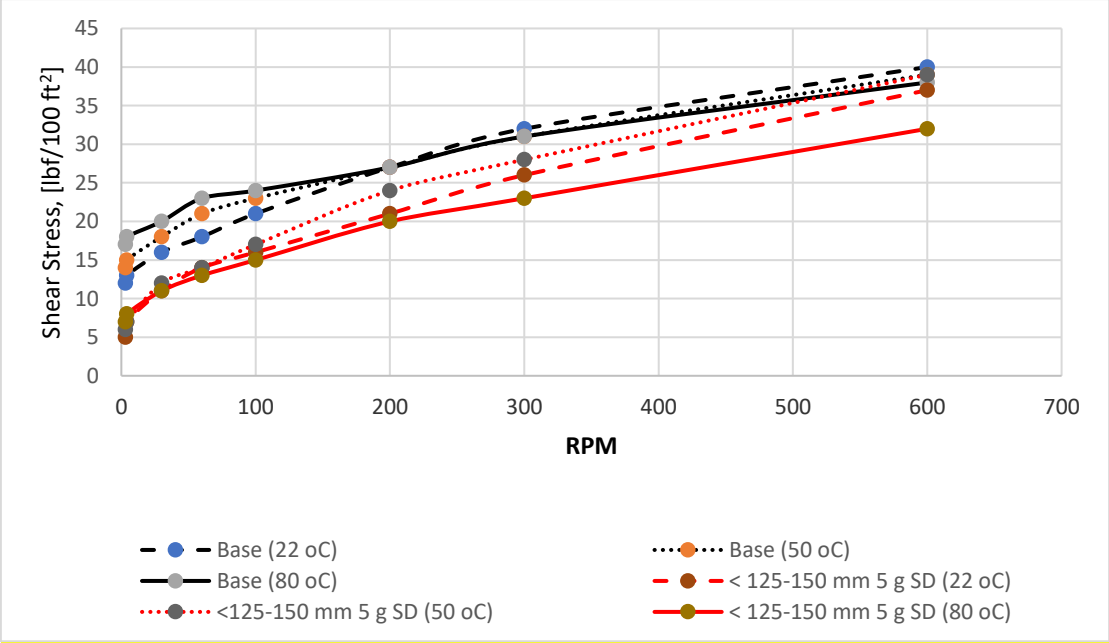

Figure B.8: Viscometer data at 20°C, 50°C, 80°C for bentonite replacement reference and 5 g 125-150 µm SD fluids

Appendix C: Rheology modelling and Parameters determination

C.1 Saw dust (1g <71 µm) in polymer replacement bentonite drilling fluid modeling

Below representations visualizes that Power law and Bingham models suffers from lack of preciseness.

Table C.1: Viscosity data for Bentonite Replacement base fluid and Fluid 3.1

	Reference (Polymer replacement Base fluid (Table formulation)			**<71 Mm Bent.F. + 1g SD (Polymer replacement Base fluid (Table formulation) Fluid 3.1**		
RPM	**22°C**	**50°C**	**80°C**	**22°C**	**50°C**	**80°C**
600	40	39	38	38	34	32
300	32	31	31	27	25	25
200	27	27	27	23	22	22
100	21	23	24	17	17	18
4	13	15	18	8	10	10

		Reference (0.5 gPac+1.0 gPolypac)				Reference (0.0 gPac+0.0 gPolypac)+1g<71 mm SD		
Model		**22°C**	**50°C**	**80°C**		**22°C**	**50°C**	**80°C**
Herschel-Bulkley	τ_0	11.898	13.87	17.317	τ0	6.493	8.766	8.391
	% deviation		16.60 %	45.50 %	% deviation		35.00 %	29.20 %
	k	0.367	0.463	0.377	k	0.388	0.359	0.547
	% deviation		26.20 %	2.80 %	% deviation		-7.50 %	41.10 %
	n	0.652	0.598	0.596	n	0.654	0.632	0.566
	% deviation		-8.30 %	-8.50 %	% deviation		-3.30 %	-13.50 %
Unified	τ_y	11.737	13.871	17.072	τψ	6.402	8.536	8.536
	% deviation		18.20 %	45.50 %	% deviation		33.30 %	33.30 %
	k	0.436	0.463	0.496	k	0.426	0.463	0.477
	% deviation		6.10 %	13.60 %	% deviation		8.60 %	11.90 %
	n	0.625	0.598	0.554	n	0.639	0.592	0.587
	% deviation		-4.30 %	-11.30 %	% deviation		-7.30 %	-8.20 %
Power Law	k	8.412	10.548	13.869	k	4.231	6.165	6.296
	% deviation		25.40 %	64.90 %	% deviation		45.70 %	48.80 %
	n	0.219	0.183	0.138	n	0.308	0.237	0.232
	% deviation		-16.70 %	-37.00 %	% deviation		-23.30 %	-24.80 %
Bingham Plastic	τ_y	15.728	17.686	20.164	τ y	10.366	11.993	12.569
	% deviation		12.40 %	28.20 %	% deviation		15.70 %	21.30 %
	µp	0.029	0.026	0.022	µπ	0.032	0.026	0.024
	% deviation		-12.30 %	-26.30 %	% deviation		-19.70 %	-26.60 %
Robertson-Stiff	A	2.744	4.627	5.717	A	1.453	2.022	3.094
	% deviation		68.70 %	108.40 %	% deviation		39.10 %	112.90 %
	C	46.631	39.209	62.357	C	27.782	41.803	23.629
	% deviation		-15.90 %	33.70 %	% deviation		50.50 %	-15.00 %
	B	0.395	0.312	0.276	B	0.477	0.412	0.345
	% deviation		-20.90 %	-30.00 %	% deviation		-13.80 %	-27.80 %
Newtonian	μ_y	0.052	0.051	0.05	µ y	0.047	0.043	0.041
	% deviation		-1.60 %	-2.70 %	% deviation		-8.60 %	-11.60 %

Figure C.1: Rheology modeling data for Bentonite Replacement base fluid and Fluid 3.1

Table C.2: Base replacement Bentonite fluid at 20°C

Model	Equation	τo,τy, A	k, C	n, B	μp, μ	% Deviation	cP
Herschel-Bulkley	11.898 + 0.3671*γ^0.6516	11.898	0.3671	0.65160		2.43	
Unified	11.737+0.4363*γ^0.6247	11.737	0.4363	0.6247		2.15	
Power Law	8.4115*γ^0.2192		8.4115	0.2192		6.82	
Bingham	0.0293*γ+15.727	15.728			0.0293	12.49	14.02884
Robertson and Stiff	2.744*(46.631+γ)^0.3948	2.7436	46.6310	0.3948		1.69	

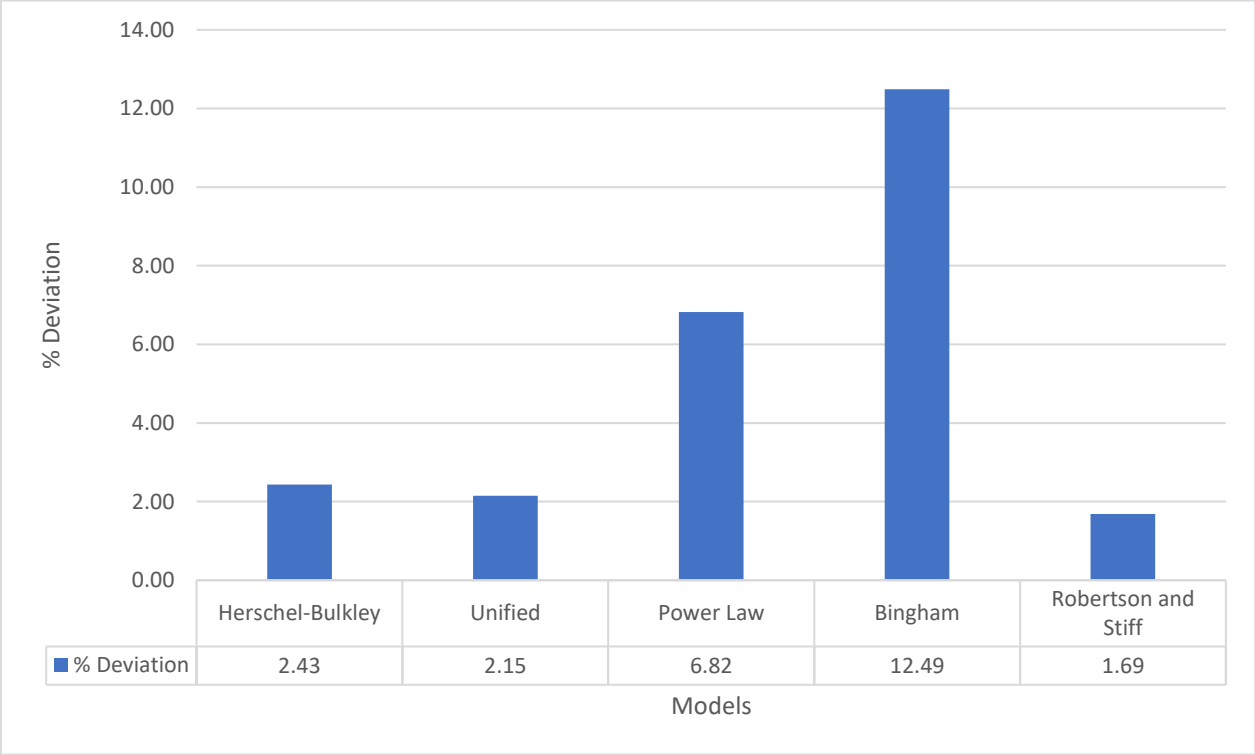

Figure C.2: Deviation of Models for base replacement Bentonite fluid at 20°C

Table C.3: Base replacement Bentonite fluid at 50°C

Model	Equation	τo,τy, A	k, C	n, B	μp, μ	% Deviation	cP
Herschel-Bulkley	13.870 + 0.463*γ^0.598	13.870	0.463	0.598		1.6	
Unified	13.871+0.463*γ^0.598	13.871	0.463	0.598		1.6	
Power Law	10.548*γ^0.183		10.548	0.183		5.4	
Bingham	0.026*γ+17.686	17.686			0.026	10.4	12.305
Robertson and Stiff	4.627*(39.209+γ)^0.3123	4.627	39.209	0.3123		1.4	

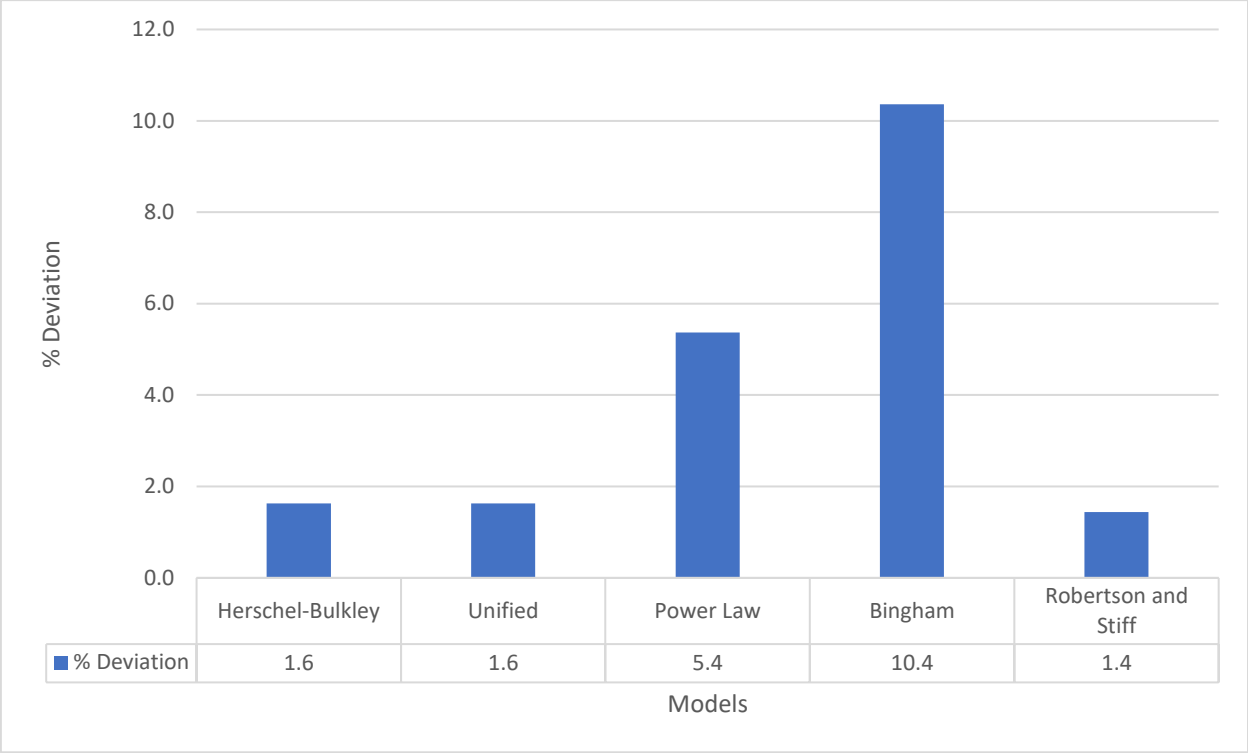

Figure C.3: Deviation of Models for base replacement Bentonite fluid at 50°C

Table C.4: Base replacement Bentonite fluid at 80°C

Model	Equation	τo,τy, A	k, C	n, B	μp, μ	% Deviation	cP
Herschel Bulkley	17.317 + 0.377*γ^0.596	17.317	0.377	0.596		1.3	
Unified	17.072+0.496*γ^0.554	17.072	0.496	0.554		1.2	
Power Law	13.869*γ^0.138		13.869	0.138		5.7	
Bingham	0.022*γ+20.164	20.164			0.022	6.5	10.342
Robertson and Stiff	5.717*(62.357+γ)^0.276	5.717	62.357	0.276		1.9	

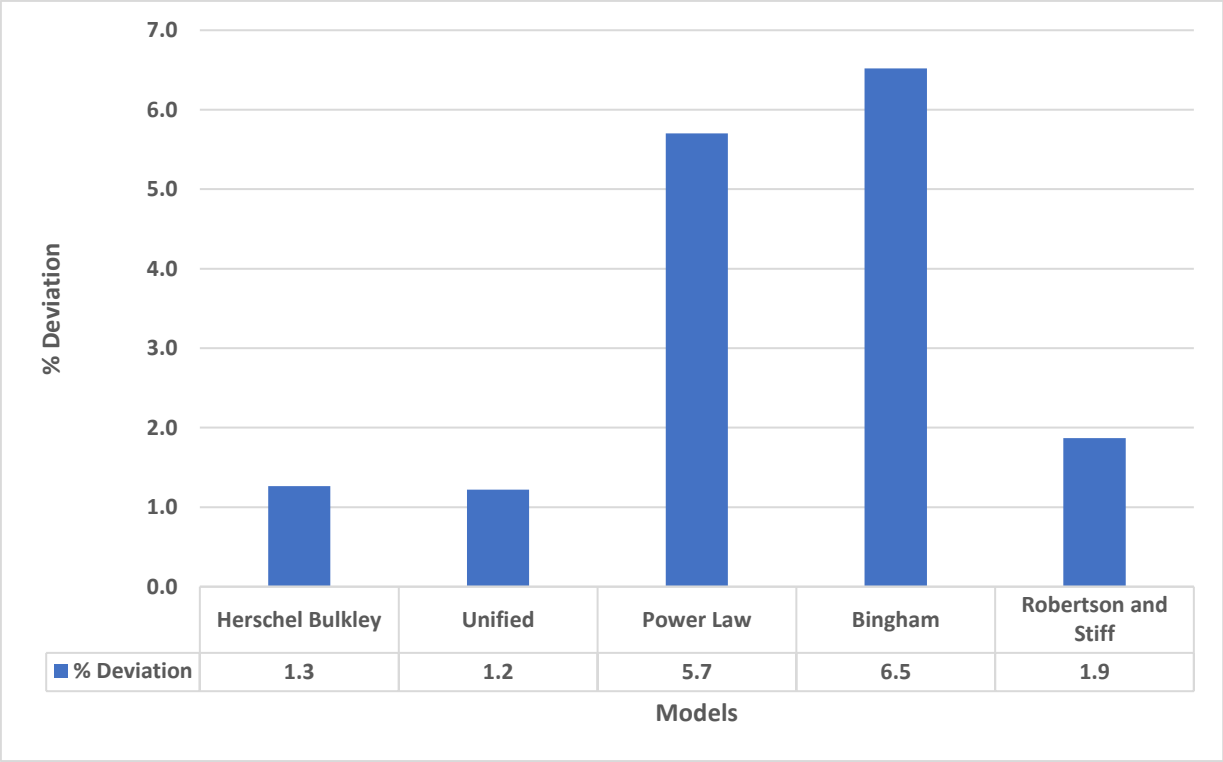

Figure C.4: Deviation of Models for base replacement Bentonite fluid at 80°C

Table C.5: Replacement Bentonite Fluid 3.1 at 20°C

Model	Equation	τo,τy, A	k, C	n, B	μp, μ	% Deviation	cP
Herschel-Bulkley	6.493+ 0.3876*γ^0.6535	6.493	0.3876	0.65350		2.75	
Unified	6.402+0.4263*γ^0.6387	6.402	0.4263	0.6387		2.38	
Power Law	4.2309*γ^0.3084		4.2309	0.3084		6.29	
Bingham	0.032*γ+10.366	10.366			0.032	17.65	15.3216
Robertson and Stiff	1.453*(27.7819+γ)^0.4774	1.4534	27.7819	0.4774		1.57	
Newtonian					0.0467	52.90	22.35996

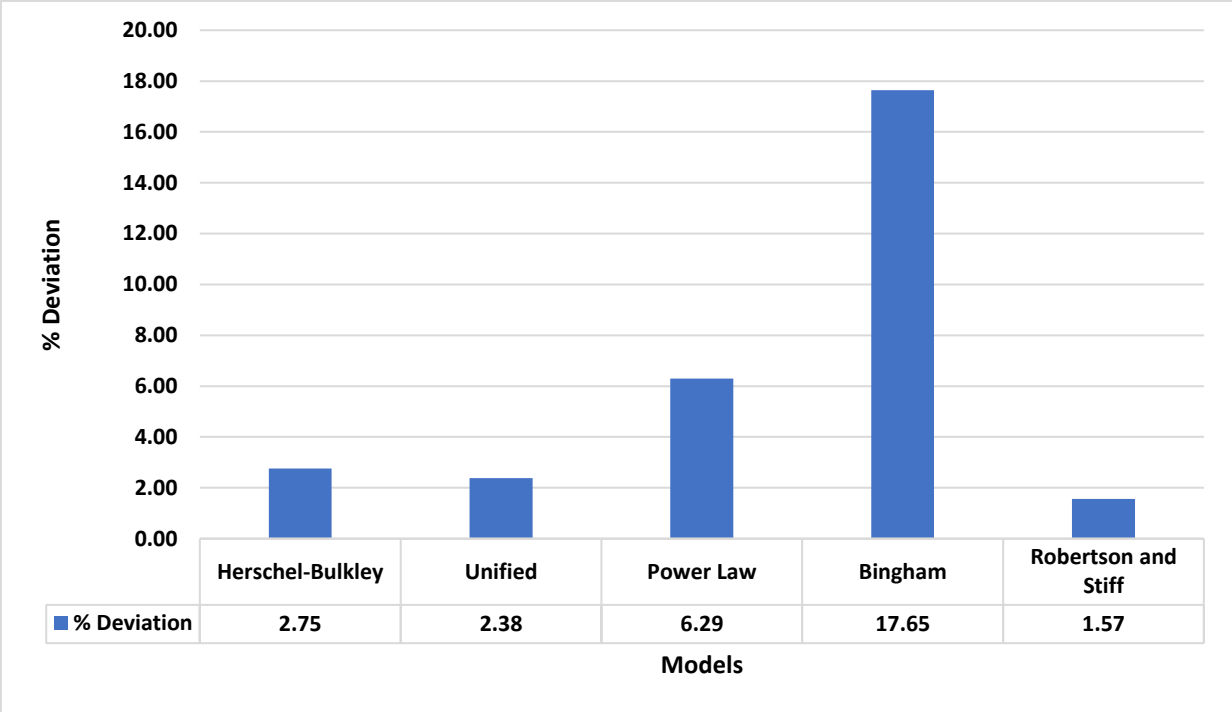

Figure C.5: Deviation of Models for Replacement Bentonite Fluid 3.1 at 20°C

Table C.6: Replacement Bentonite Fluid 3.1 at 50°C

Model	Equation	τo,τy, A	k, C	n, B	μp, μ	% Deviation	cP
Herschel-Bulkley	8.766 + 0.359*γ^0.632	8.766	0.359	0.632		2.1	
Unified	8.536+0.463*γ^0.592	8.536	0.463	0.592		1.5	
Power Law	6.165*γ^0.237		6.165	0.237		6.4	
Bingham	0.026*γ+11.993	11.993			0.026	12.3	12.305
Robertson and Stiff	2.022*(41.803+γ)^0.4117	2.022	41.803	0.4117		1.9	

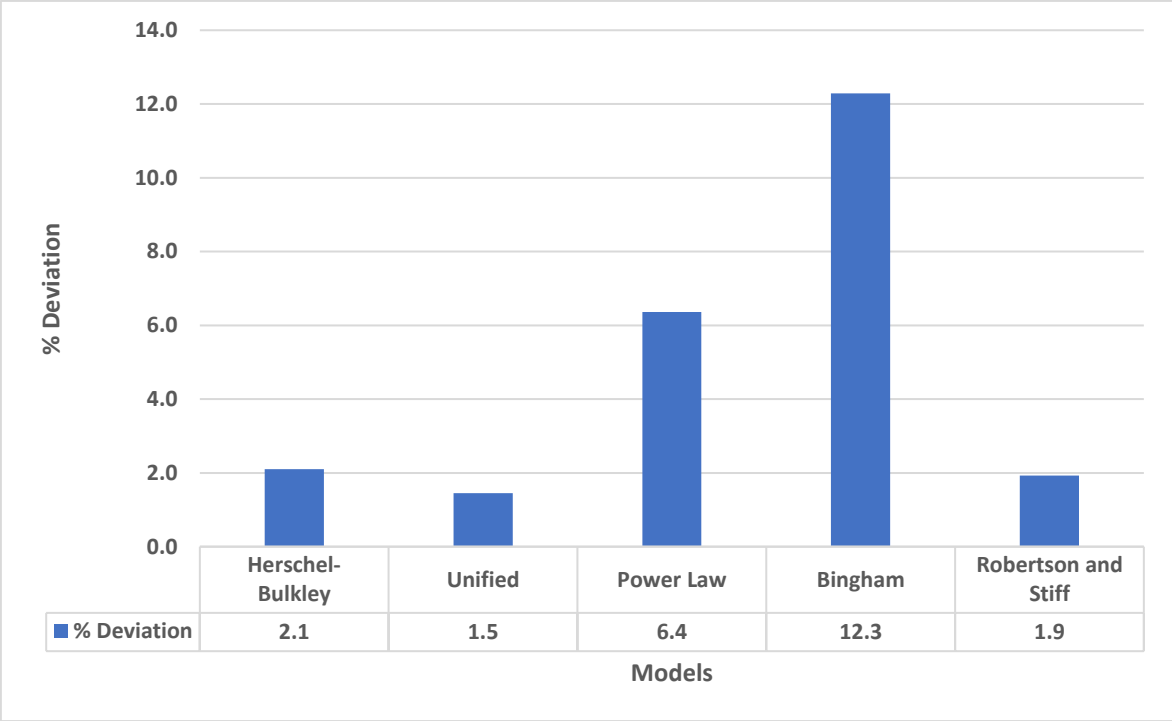

Figure C.6: Deviation of Models for Replacement Bentonite Fluid 3.1 at 50°C

Table C.7: Replacement Bentonite Fluid 3.1 at 80°C

Model	Equation	τo,τy, A	k, C	n, B	μp, μ	% Deviation	cP
Herschel Bulkley	8.391 + 0.547*γ^0.566	8.391	0.547	0.566		2.7	
Unified	8.536+0.477*γ^0.587	8.536	0.477	0.587		3.1	
Power Law	6.296*γ^0.232		6.296	0.232		4.2	
Bingham	0.024*γ+12.569	12.569			0.024	15.5	11.252
Robertson and Stiff	3.094*(23.629+γ)^0.345	3.094	23.629	0.345		1.4	

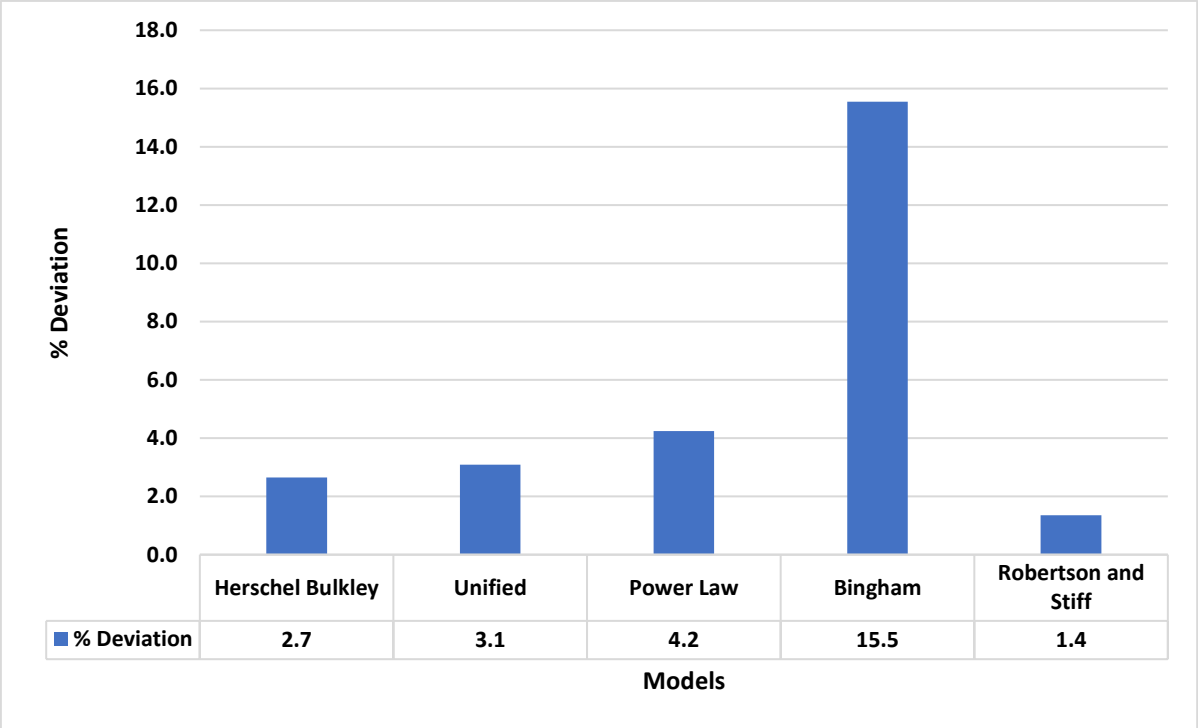

Figure C.7: Deviation of Models for Replacement Bentonite Fluid 3.1 at 80°C

C.2 Saw dust (3g 125-150 µm) in whole Bentonite drilling fluid modeling

Table C.8: Viscosity data for Bentonite whole base fluid and Fluid 2.2

	Reference (Polymer whole Base fluid (Table 1 formulation) Fluid 1.1			125-150 Mm Bent.F. + 3g SD (Polymer whole Base fluid (Table 2 formulation) Fluid 2.2		
RPM	**22°C**	**50°C**	**80°C**	**22°C**	**50°C**	**80°C**
600	36	33.5	28.5	36	30.5	25.5
300	23.5	21	21.5	24	21.5	19
200	19	17.5	17.5	19.5	18	16
100	13.5	13	13	14	14	13
6	6.5	7.5	8	8	8	9
3	6.5	7.5	7.5	7.5	7.5	8.5

		Reference			Reference + 3g SD (125-150 μm)			
Model		**22°C**	**50°C**	**80°C**		**22°C**	**50°C**	**80°C**
Herschel-Bulkley	τ_0	6.208	7.388	7.609	τ0	7.63	7.512	8.722
	% deviation		19.00 %	22.60 %	% deviation		-1.50 %	14.30 %
	k	0.107	0.079	0.136	k	0.116	0.168	0.132
	% deviation		-25.40 %	27.40 %	% deviation		45.30 %	13.90 %
	n	0.832	0.849	0.75	n	0.809	0.727	0.715
	% deviation		2.00 %	-9.90 %	% deviation		-10.20 %	-11.60 %
Unified	τ_y	6.295	7.362	7.469	τ y	7.469	7.469	8.536
	% deviation		16.90 %	18.60 %	% deviation		0.00 %	14.30 %
	k	0.082	0.087	0.187	k	0.169	0.184	0.206
	% deviation		6.20 %	128.50 %	% deviation		9.10 %	22.00 %
	n	0.875	0.834	0.699	n	0.749	0.713	0.645
	% deviation		-4.60 %	-20.00 %	% deviation		-4.90 %	-13.90 %
Power Law	k	3.478	4.429	4.958	k	4.577	4.886	6.195
	% deviation		27.30 %	42.60 %	% deviation		6.80 %	35.40 %
	n	0.317	0.265	0.239	n	0.275	0.249	0.189
	% deviation		-16.50 %	-24.40 %	% deviation		-9.70 %	-31.40 %
Bingham Plastic	τ_y	7.92	8.359	9.462	τ y	9.149	9.502	10.11
	% deviation		5.50 %	19.50 %	% deviation		3.90 %	10.50 %
	μp	0.031	0.027	0.022	μ y	0.03	0.024	0.018
	% deviation		-12.50 %	-28.80 %	% deviation		-19.80 %	-40.60 %
Robertson-Stiff	A	0.513	0.395	0.857	A	0.46	1.138	1.19
	% deviation		-23.00 %	66.90 %	% deviation		147.40 %	158.70 %
	C	58.153	100.731	75.769	C	89.997	55.724	94.835
	% deviation		73.20 %	30.30 %	% deviation		-38.10 %	5.40 %
	B	0.615	0.636	0.511	B	0.629	0.476	0.443
	% deviation		3.30 %	-16.90 %	% deviation		-24.30 %	-29.60 %
Newtonian	μ_y	0.042	0.039	0.036	μ y	0.043	0.037	0.032
	% deviation		-7.50 %	-16.00 %	% deviation		-12.60 %	-25.00 %

Figure C.8: Rheology modeling data for Bentonite whole base fluid and Fluid 2.2

Table C.9: Base whole Bentonite fluid at 20°C

Model	Equation
Herschel-Bulkley	6.208 + 0.1065*γ^0.8323
Unified	6.295+0.0818*γ^0.8746
Power Law	3.4778*γ^0.3167
Bingham	0.0312*γ+7.920
Robertson and Stiff	0.513*(58.1534+γ)^0.6152

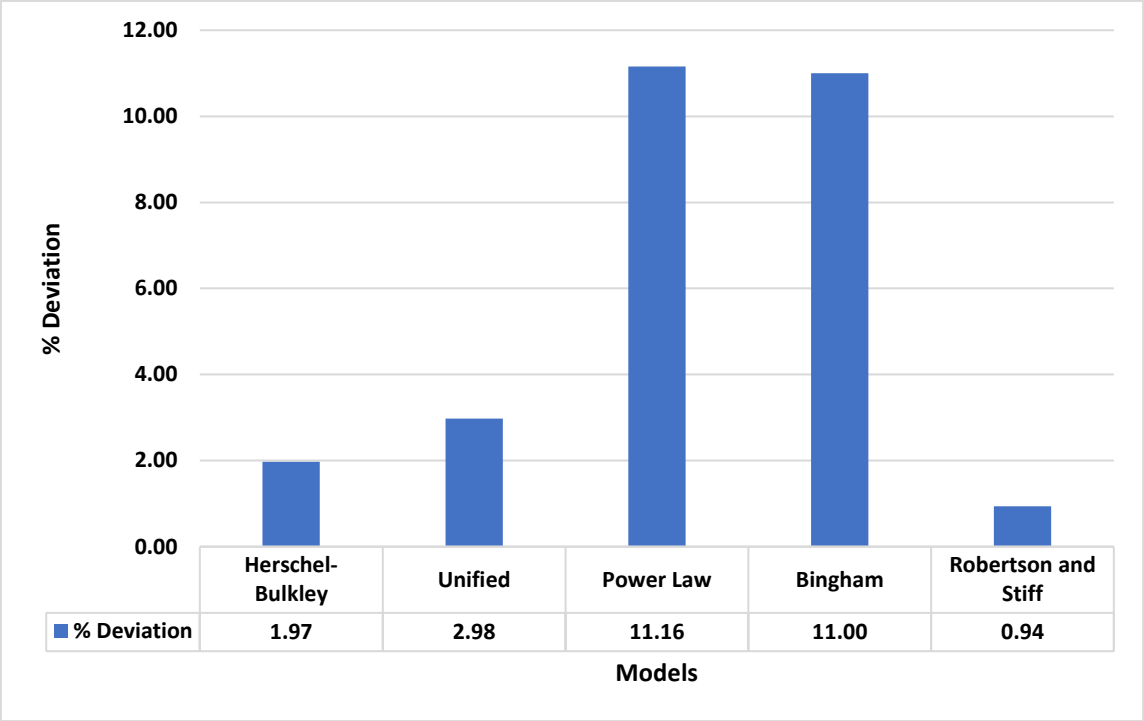

Figure C.9: Deviation of Models for Base Whole Bentonite Fluid at 20°C

Table C.10: Base whole Bentonite fluid at 50°C

Model	Equation
Herschel-Bulkley	7.388+ 0.079*γ^0.849
Unified	7.362+0.087*γ^0.834
Power Law	4.429*γ^0.265
Bingham	0.027*γ+8.359
Robertson and Stiff	0.395*(100.731+γ)^0.6356
Newtonian	

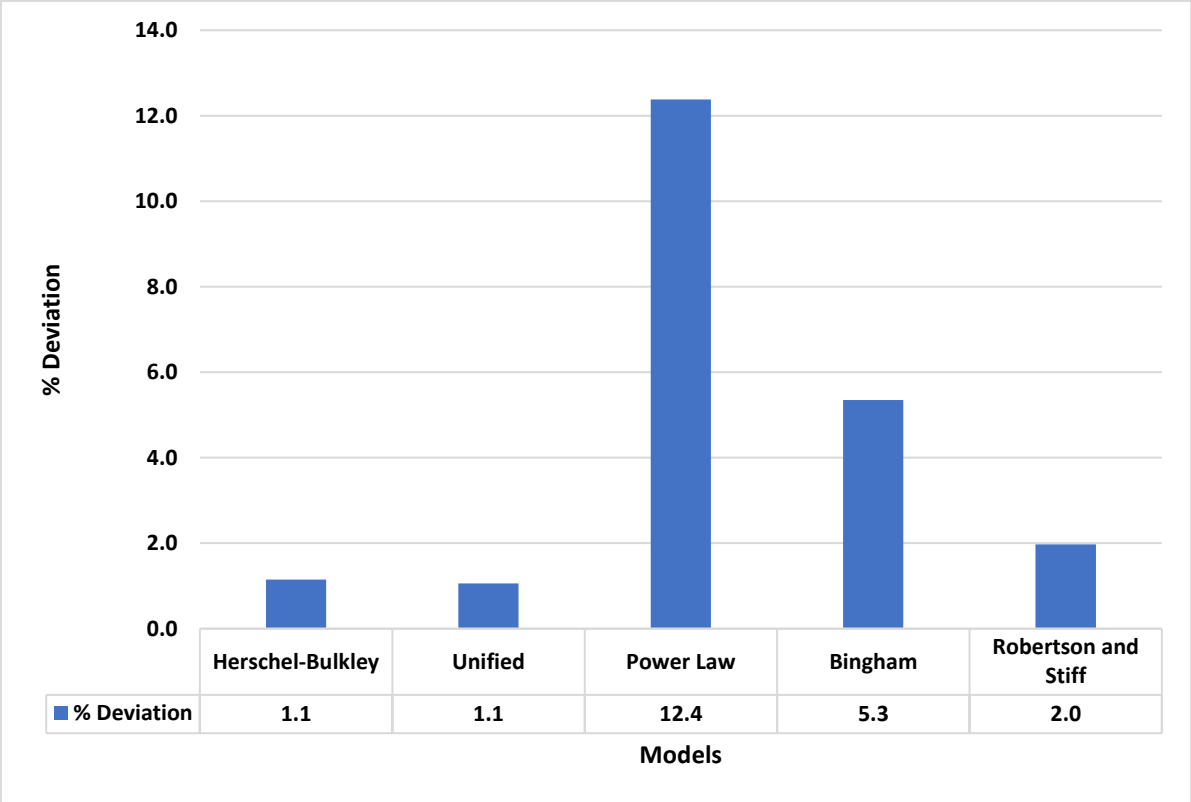

Figure C.10: Deviation of Models for Base Whole Bentonite Fluid at 50°C

Table C.11: Base whole Bentonite fluid at 80°C

Model	Equation	% Deviation	cP
Herschel Bulkley	7.609 + 0.136*γ^0.750	2.4	
Unified	7.469+0.187*γ^0.699	2.0	
Power Law	4.958*γ^0.239	9.6	
Bingham	0.022*γ+9.462	10.3	10.629
Robertson and Stiff	0.857*(75.69 +γ)^0.511	1.7	

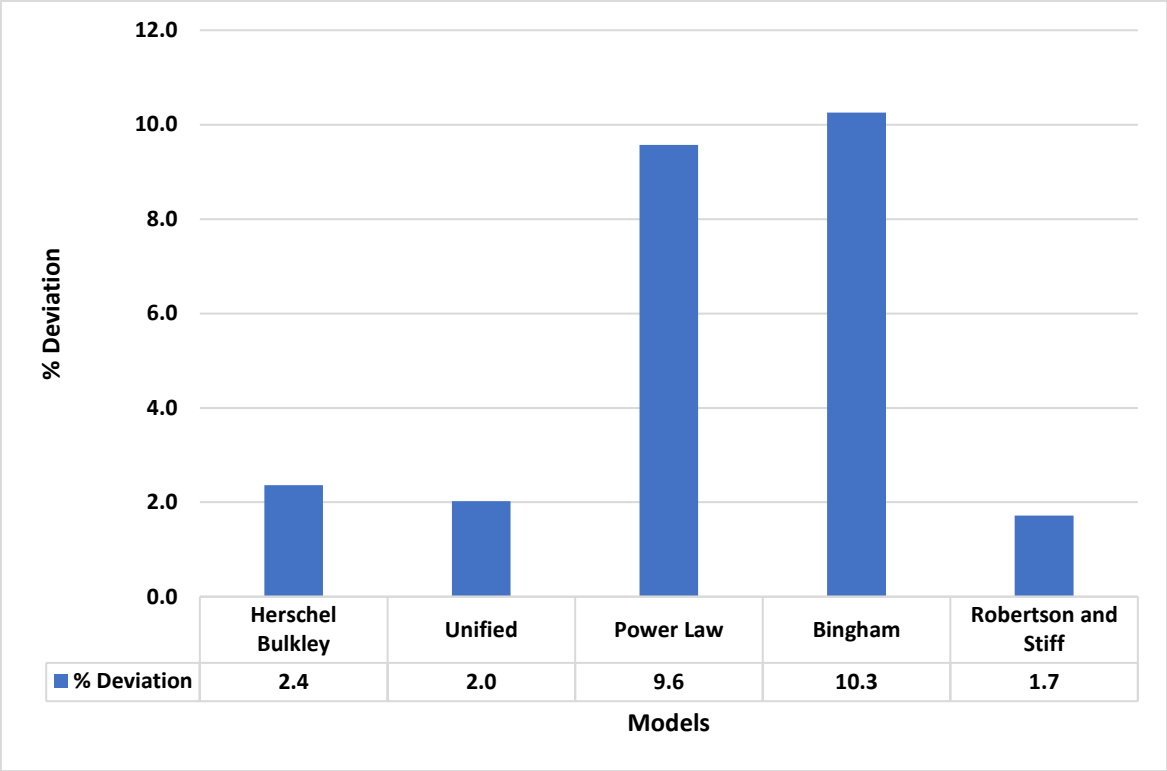

Figure C.11: Deviation of Models for Base Whole Bentonite Fluid at 80°C

Table C.12: Whole Bentonite fluid 2.2 at 20°C

Model	Equation	τo,τy, A	k, C	n, B	μp, μ	% Deviation	cP
Herschel-Bulkley	7.630 + 0.1159*γ^0.8092	7.630	0.1159	0.80920		1.05	
Unified	7.469+0.1687*γ^0.7493	7.469	0.1687	0.7493		1.13	
Power Law	4.577*γ^0.2751		4.577	0.2751		11.30	
Bingham	0.0298*γ+9.149	9.149			0.0298	7.82	14.26824
Robertson and Stiff	0.46*(89.9973+γ)^0.6291	0.4599	89.9973	0.6291		1.20	
Newtonian					0.0428	50.29	20.49264

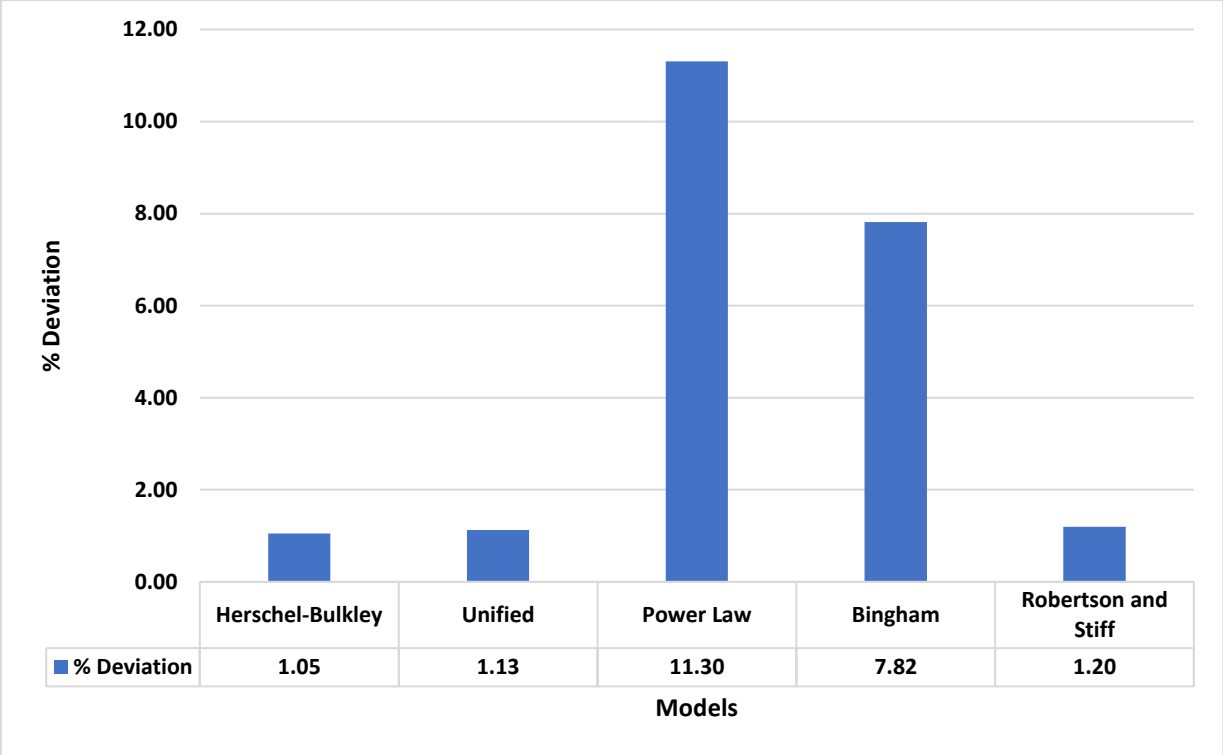

Figure C.12: Deviation of Models for Whole Bentonite fluid 2.2 at 20°C

Table C.13: Whole Bentonite fluid 2.2 at 50°C

Model	Equation	τo,τy, A	k, C	n, B	µp, µ	% Deviation	cP
Herschel-Bulkley	7.512 + 0.168*γ^0.727	7.512	0.168	0.727		1.4	
Unified	7.469+0.184*γ^0.713	7.469	0.184	0.713		1.2	
Power Law	4.886*γ^0.249		4.886	0.249		8.7	
Bingham	0.024*γ+9.502	9.502			0.024	10.2	11.443
Robertson and Stiff	1.138*(55.724+γ)^0.4762	1.138	55.724	0.4762		1.6	
Newtonian					0.0374	53.1	17.907

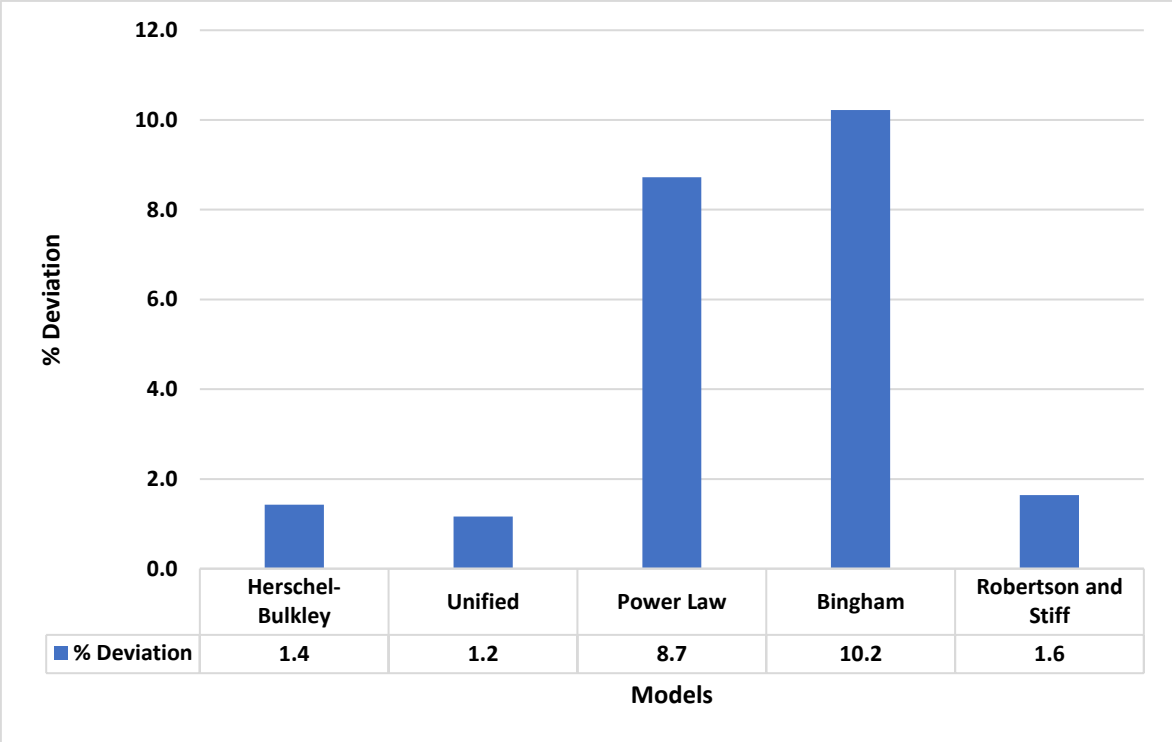

Figure C.13: Deviation of Models for Whole Bentonite fluid 2.2 at 50°C

Table C.14: Whole Bentonite fluid 2.2 at 80°C

Model	Equation	τo,τy, A	k, C	n, B	μp, μ	% Deviation	cP
Herschel Bulkley	8.722 + 0.132*γ^0.715	8.722	0.132	0.715		1.0	
Unified	8.536+0.206*γ^0.645	8.536	0.206	0.645		1.7	
Power Law	6.195*γ^0.189		6.195	0.189		8.4	
Bingham	0.018*γ+10.11	10.110			0.018	6.6	8.475
Robertson and Stiff	1.190*(94.835+γ)^0.443	1.190	94.835	0.443		1.7	
Newtonian					0.0321	55.2	15.369

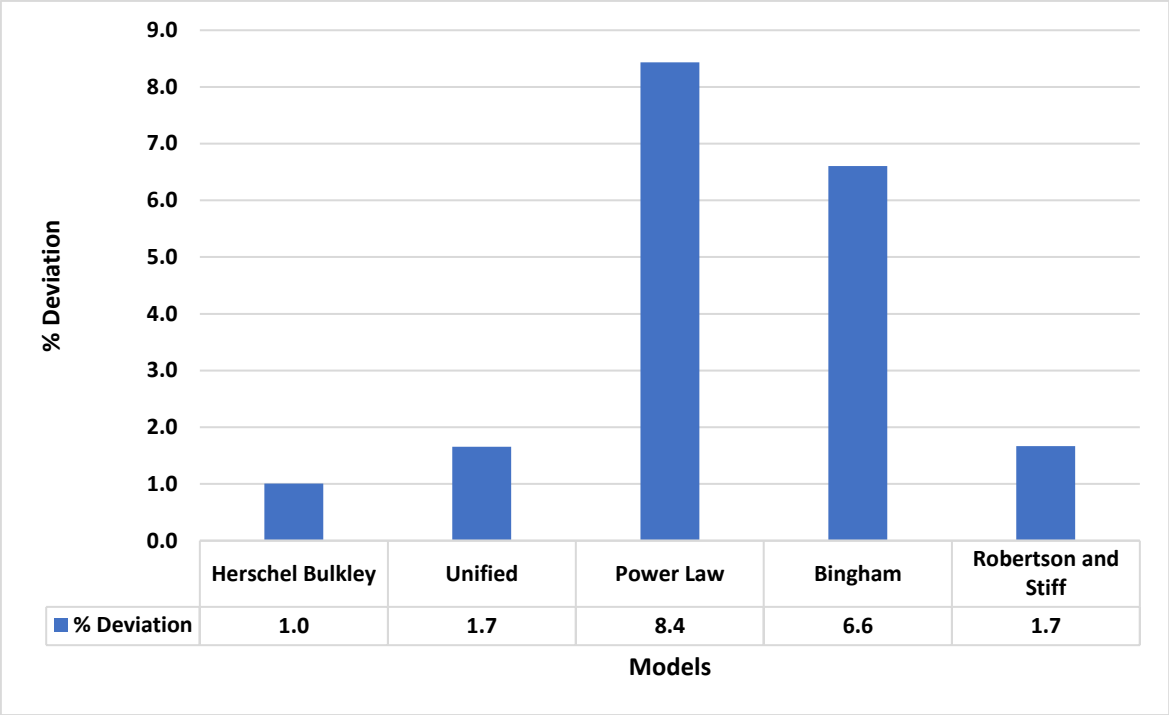

Figure C.14: Deviation of Models for Whole Bentonite fluid 2.2 at 80°C

Appendix D: More Hydraulics Simulations

D.1 Bentonite whole ECD and Pump Pressure figures

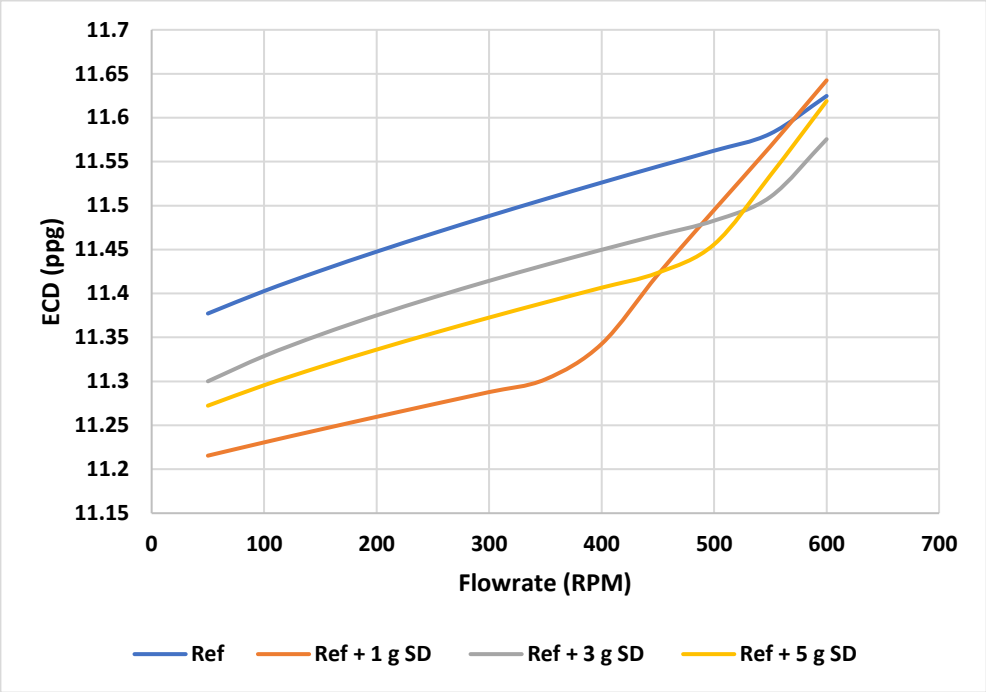

Figure D.1: ECD vs Flowrate <71µm SD 20°C

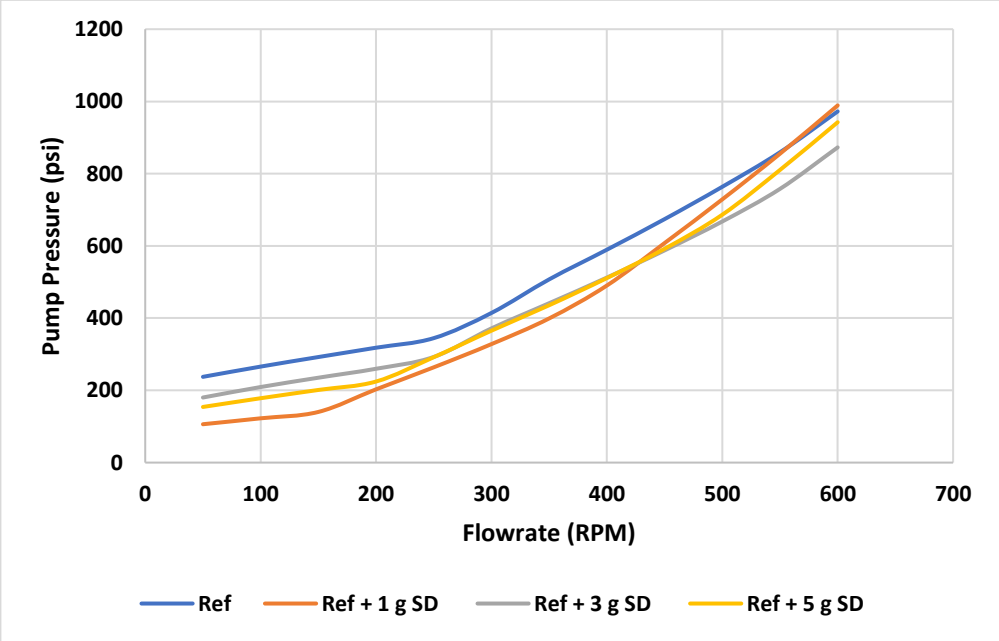

Figure D.2: Pump Pressure vs Flowrate <71µm 20°C

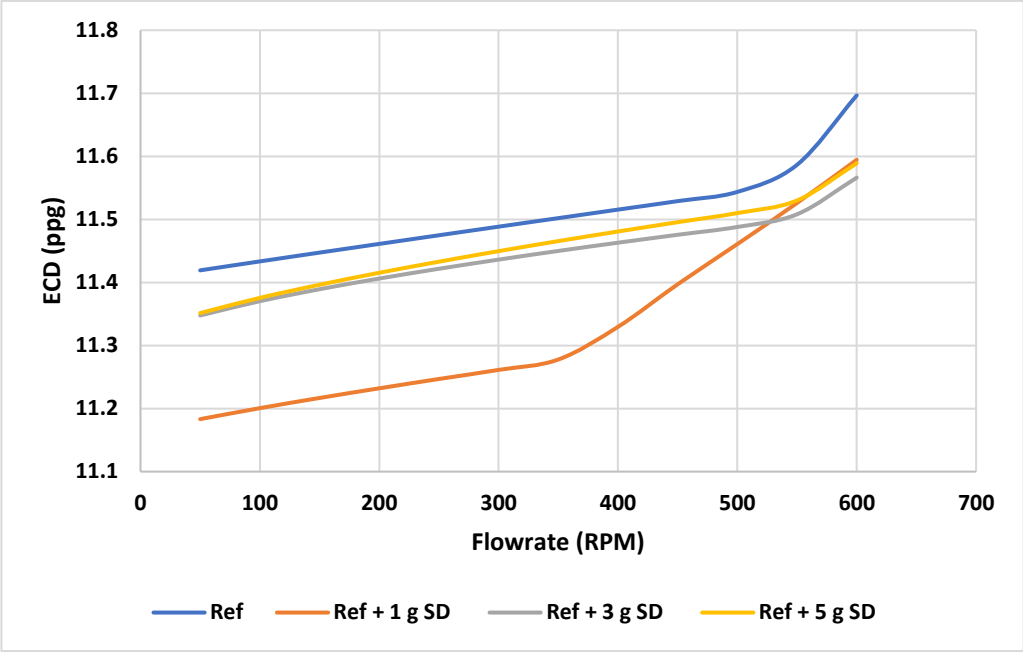

Figure D.3: ECD vs Flowrate <71µm SD 50°C

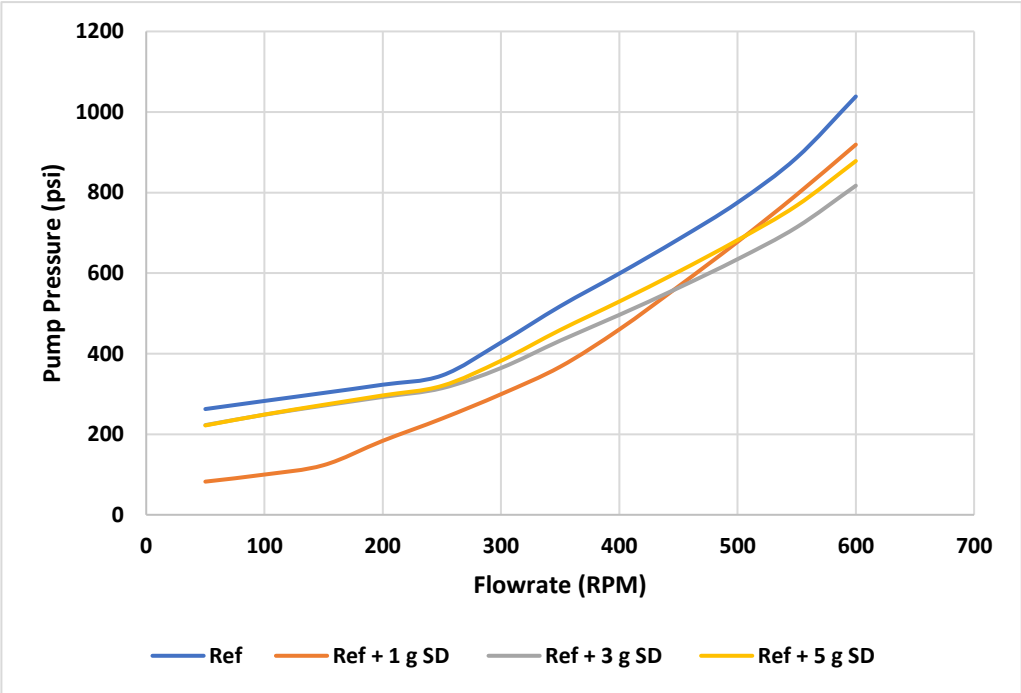

Figure D.4: Pump Pressure vs Flowrate <71µm 50°C

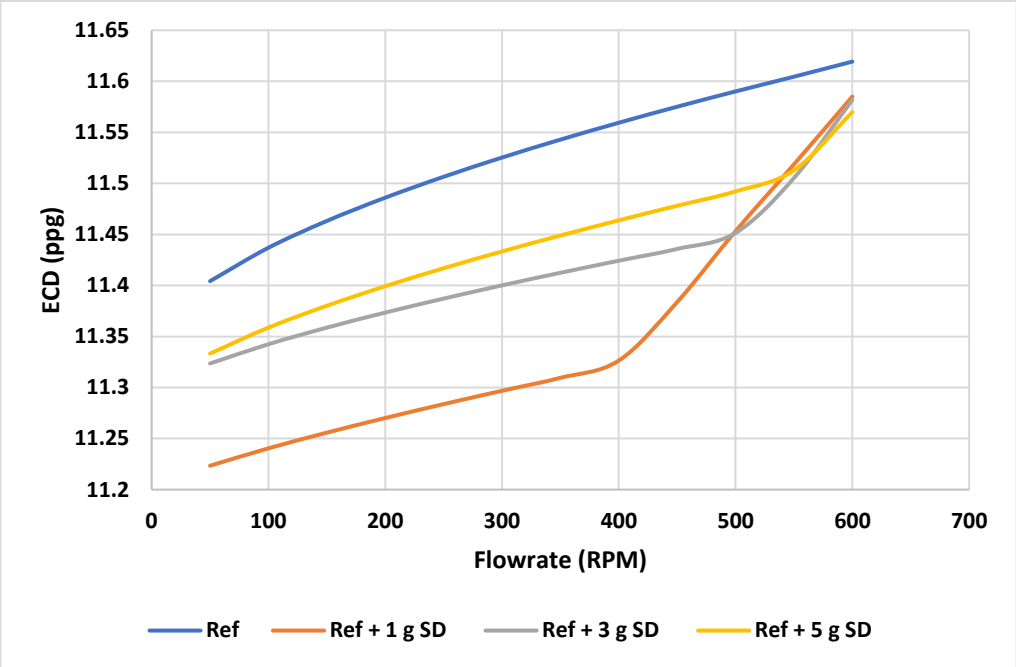

Figure D.5: ECD vs Flowrate <71µm SD 80°C

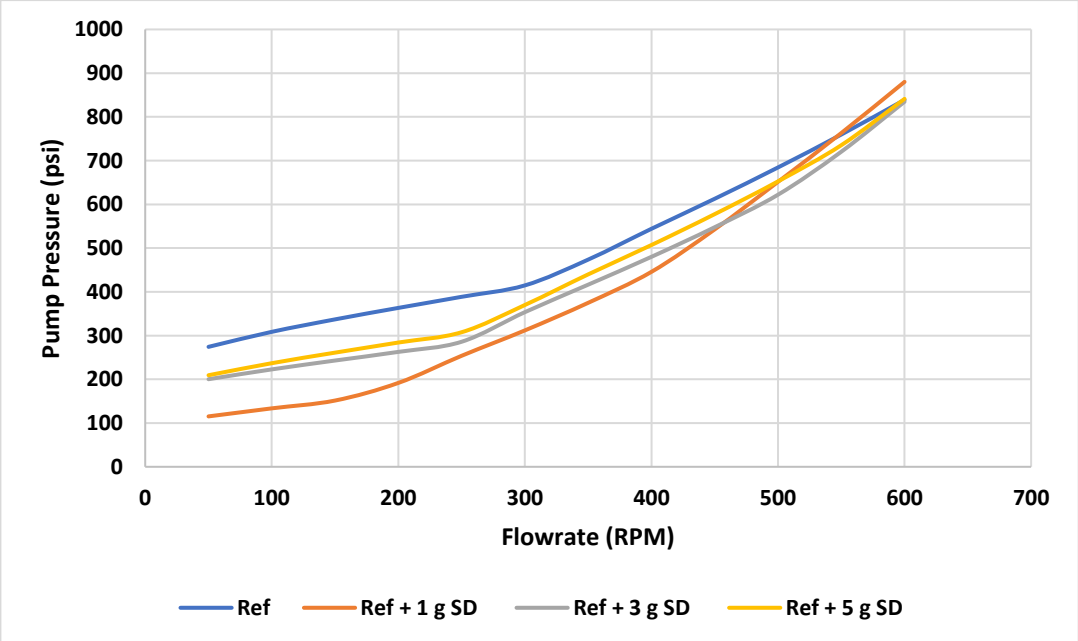

Figure D.6: Pump Pressure vs Flowrate <71µm 80°C

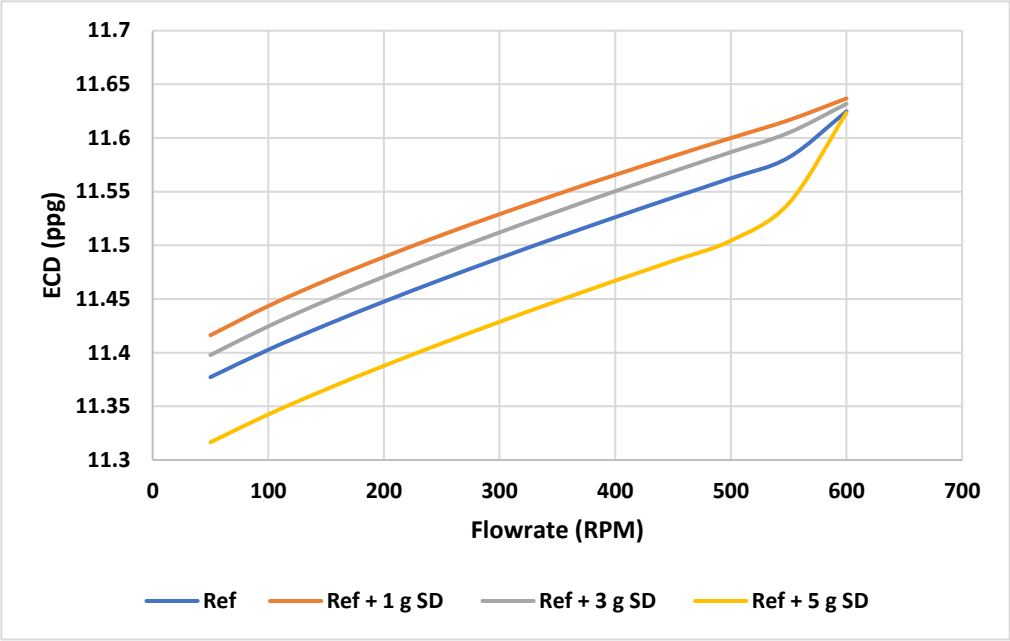

Figure D.7: ECD vs Flowrate 125-150 µm 20°C

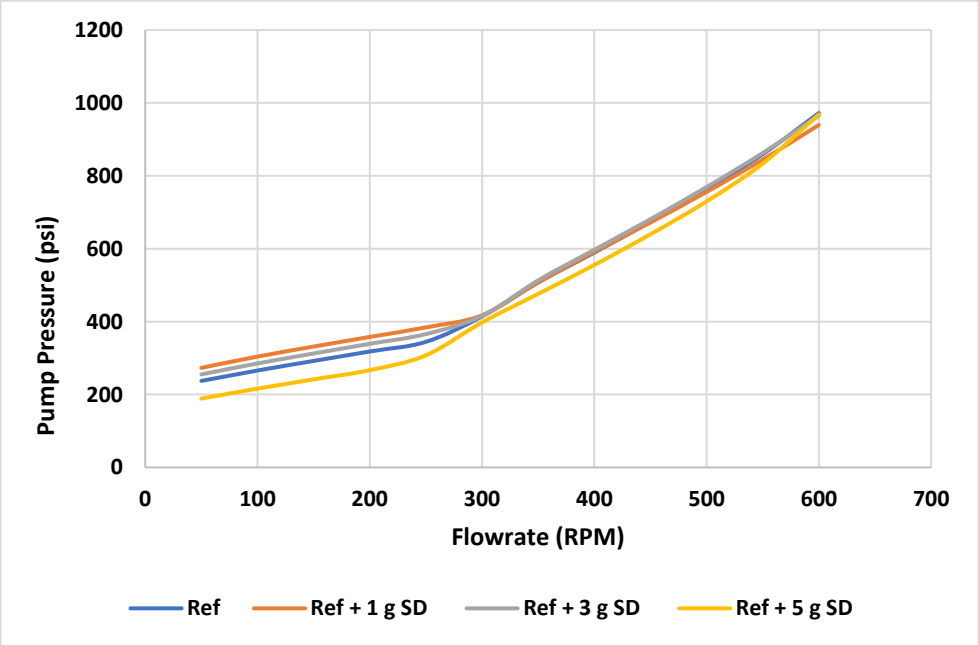

Figure D.8: Pump Pressure vs Flowrate 125-150 µm 20°C

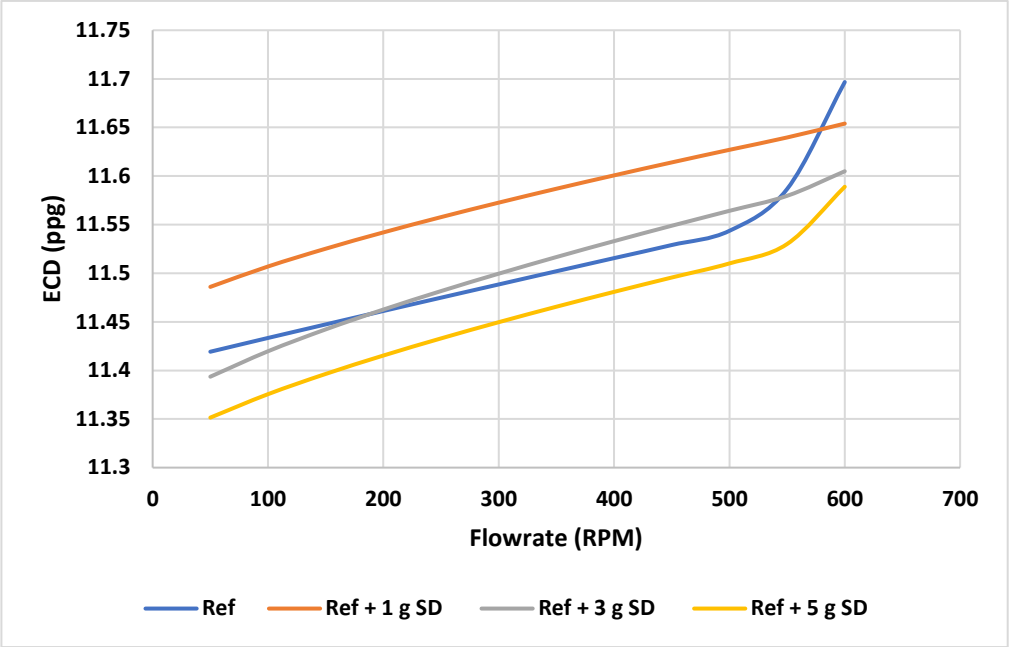

Figure D.9: ECD vs Flowrate 125-150 µm 50°C

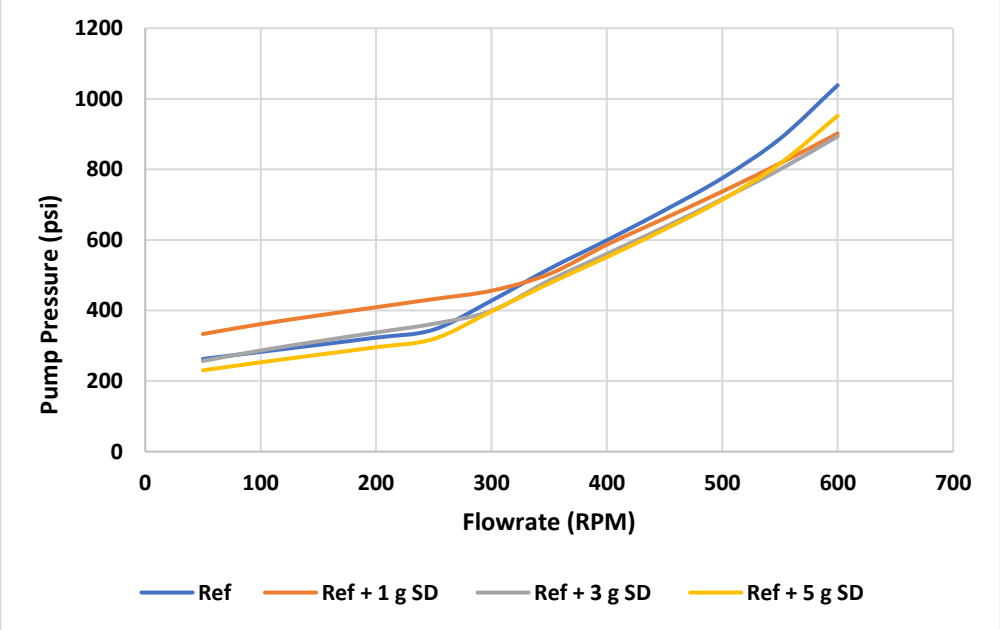

Figure D.10: Pump Pressure vs Flowrate 125-150 µm 50°C

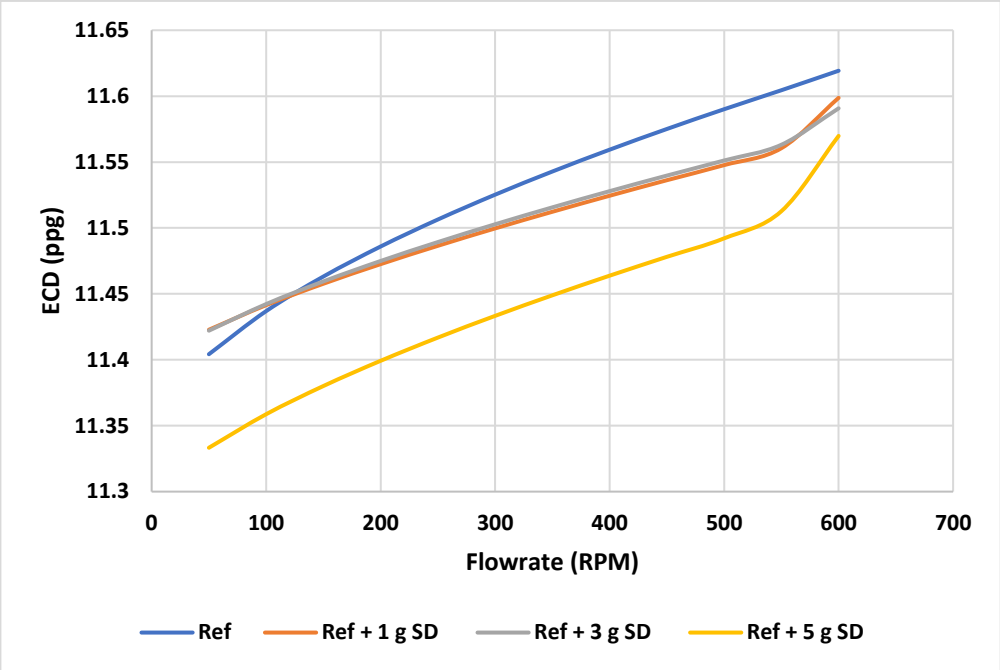

Figure D.11: ECD vs Flowrate 125-150 µm 80°C

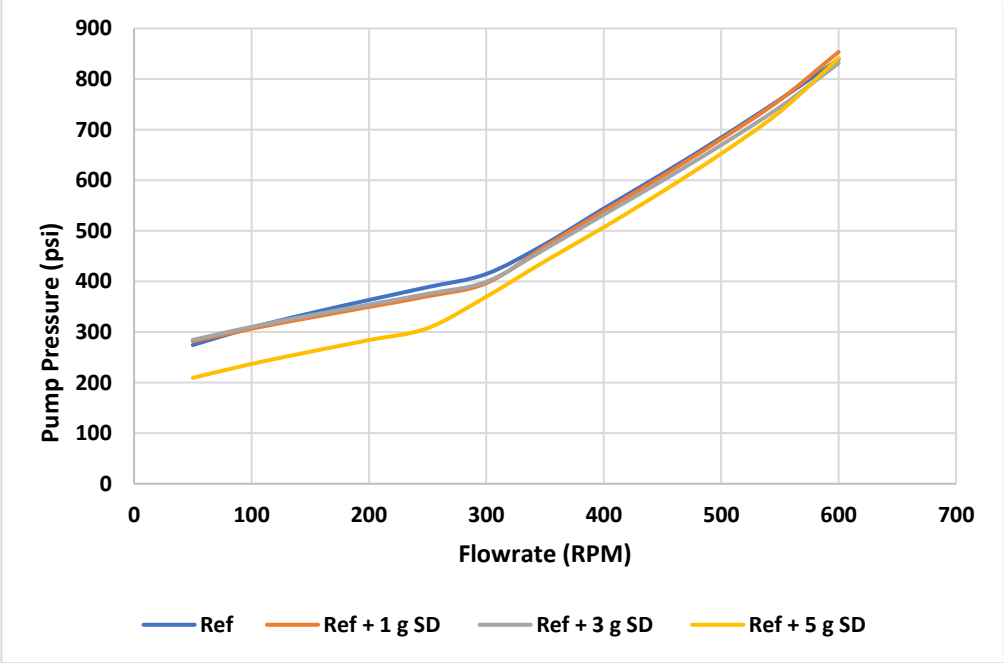

Figure D.12: Pump Pressure vs Flowrate 125-150 µm 80°C

D.2 Bentonite replacement ECD and Pump Pressure figures

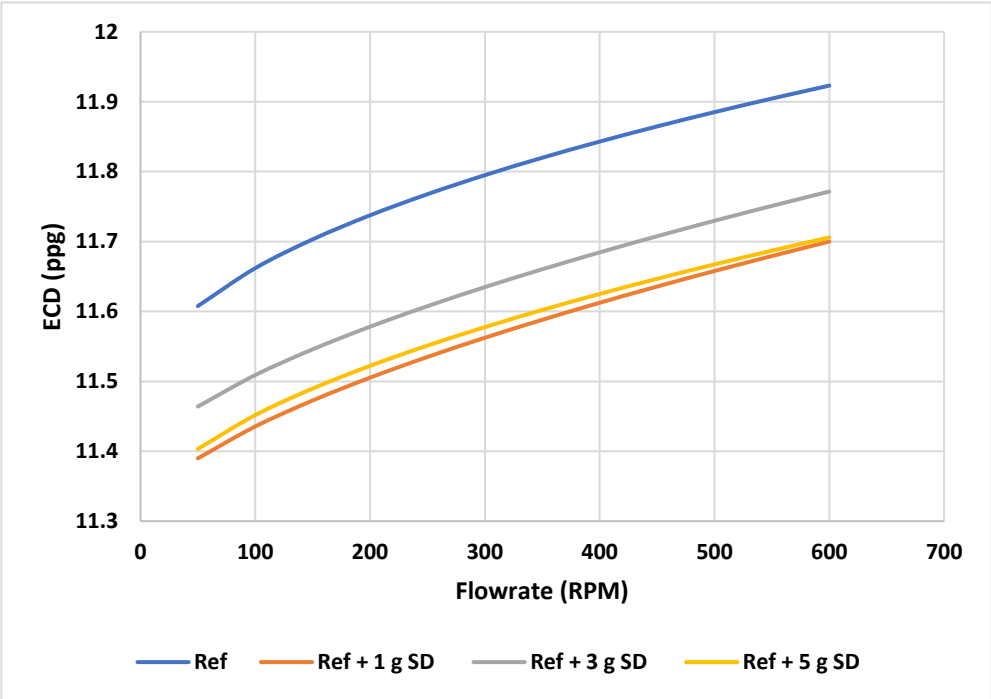

Figure D.13: ECD vs Flowrate <71µm SD 20°C

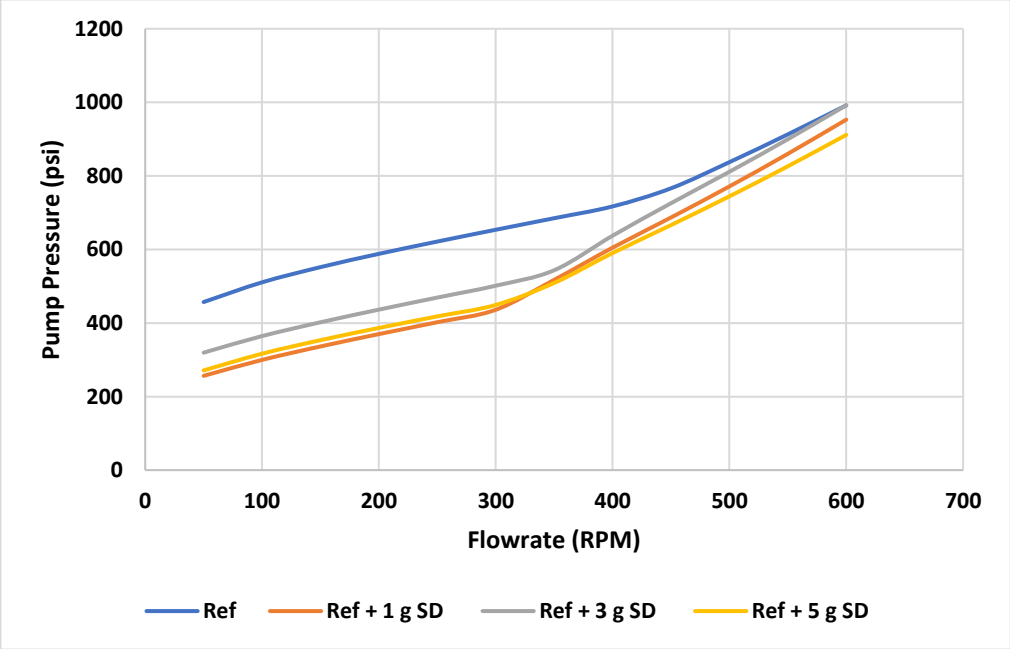

Figure D.14: Pump Pressure vs Flowrate <71µm SD 20°C

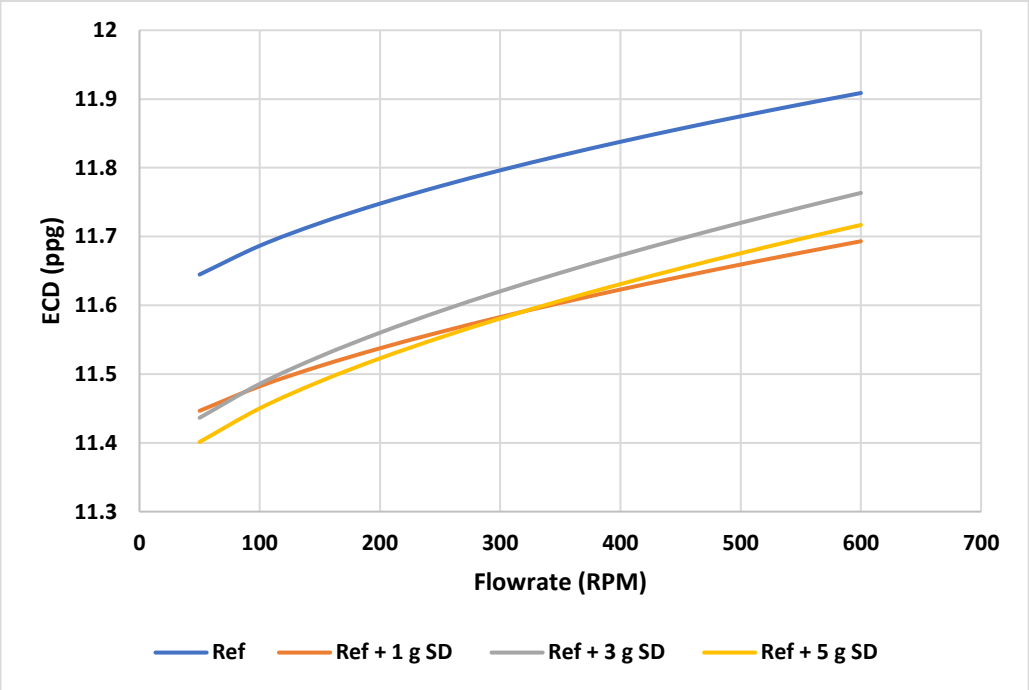

Figure D.15: ECD vs Flowrate <71µm SD 50°C

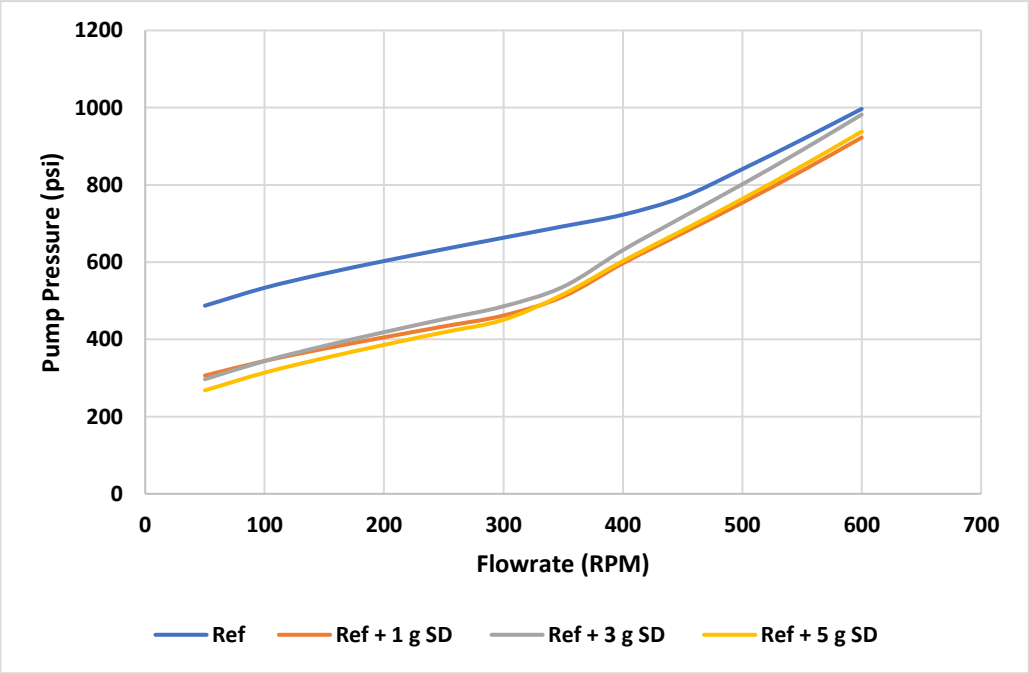

Figure D.16: Pump Pressure vs Flowrate <71µm SD 50°C

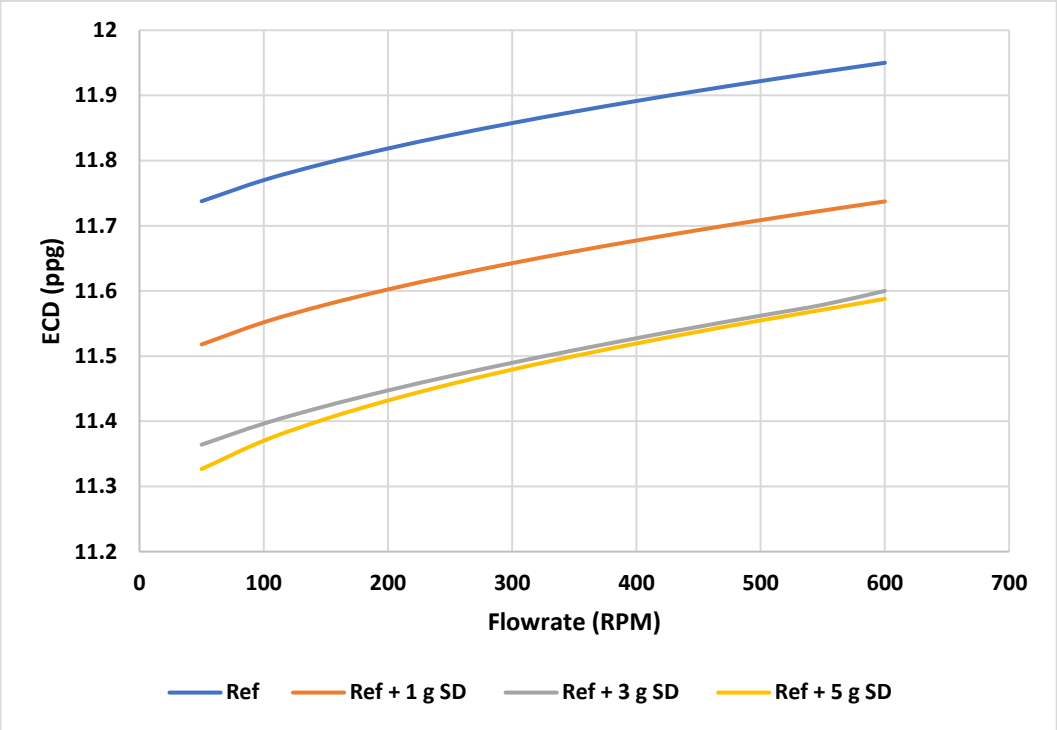

Figure D.17: ECD vs Flowrate <71µm SD 80°C

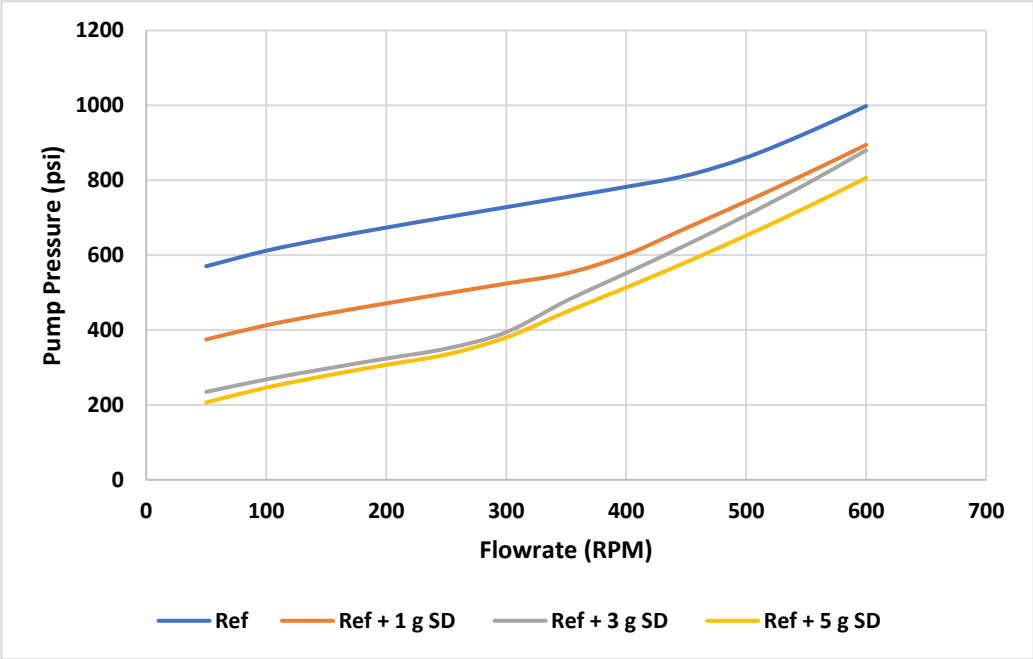

Figure D.18: Pump Pressure vs Flowrate <71µm SD 80°C